AD-A198 409

FILE COPY

(2)

REPORT DOCUMENTATION PAGE

1a. REPORT SECURITY CLASSIFICATION: UNCLASSIFIED	1b. RESTRICTIVE MARKINGS
2a. SECURITY CLASSIFICATION AUTHORITY	3. DISTRIBUTION/AVAILABILITY OF REPORT: Approved for public release; distribution unlimited.
2b. DECLASSIFICATION/DOWNGRADING SCHEDULE	
4. PERFORMING ORGANIZATION REPORT NUMBER(S)	5. MONITORING ORGANIZATION REPORT NUMBER(S): AFOSR-TR- 88-0917
6a. NAME OF PERFORMING ORGANIZATION: Electrical & Comp Eng, North Carolina State Univ	6b. OFFICE SYMBOL (If applicable)
7a. NAME OF MONITORING ORGANIZATION: AFOSR/NE, Bldg 410	
6c. ADDRESS (City, State and ZIP Code): Raleigh, NC 27695-7911	7b. ADDRESS (City, State and ZIP Code): Bolling AFB, DC 20332-6448
8a. NAME OF FUNDING/SPONSORING ORGANIZATION: AFOSR/NE	8b. OFFICE SYMBOL (If applicable)
9. PROCUREMENT INSTRUMENT IDENTIFICATION NUMBER: AFOSR-85-0201	
8c. ADDRESS (City, State and ZIP Code): Bldg 410, Bolling AFG, DC 20332-6448	10. SOURCE OF FUNDING NOS.

PROGRAM ELEMENT NO.	PROJECT NO.	TASK NO.	WORK UNIT NO.
61102F	2306	B1	

11. TITLE (Include Security Classification): DEFECT REDUCTION IN EPITAXIAL GROWTH USING SUPERLATTICE BUFFER LAYERS

12. PERSONAL AUTHOR(S): Professor Bedair

13a. TYPE OF REPORT	13b. TIME COVERED	14. DATE OF REPORT (Yr., Mo., Day)	15. PAGE COUNT
Final	FROM 01/04/85 TO 01/03/88		

16. SUPPLEMENTARY NOTATION

17. COSATI CODES			18. SUBJECT TERMS (Continue on reverse if necessary and identify by block number)
FIELD	GROUP	SUB. GR.	Aluminum, Gallium Arsenide, Indium Phosphide

19. ABSTRACT (Continue on reverse if necessary and identify by block number)

Superlattice (SL) structures are both fundamental and technical interest. Two classes of superlattices have been investigated. IN the first class, the superlattice layers have lattice parameters that closely match those of the substrate, such as in the case of the AlGaAs-GaAs and $InP_{0.53}Ga_{0.47}As$ systems. In the second class, the strained-layer superlattice (SLS) [1], the alternating layers have lattice parameters that are different by a significant amount, but the layers are thin enough to ensure that the lattice mismatch is entirely accommodated by elastically straining the layers without the generation of misfit dislocations.

DTIC ELECTE AUG 25 1988 S D

20. DISTRIBUTION/AVAILABILITY OF ABSTRACT	21. ABSTRACT SECURITY CLASSIFICATION
UNCLASSIFIED/UNLIMITED ☐ SAME AS RPT. ☐ DTIC USERS ☐	UNCLASSIFIED

22a. NAME OF RESPONSIBLE INDIVIDUAL	22b. TELEPHONE NUMBER (Include Area Code)	22c. OFFICE SYMBOL
MALLOY	(202) 767-4931	NE

DD FORM 1473, 83 APR EDITION OF 1 JAN 73 IS OBSOLETE.

SECURITY CLASSIFICATION OF THIS PAGE

88 8 25 074

DISCLAIMER NOTICE

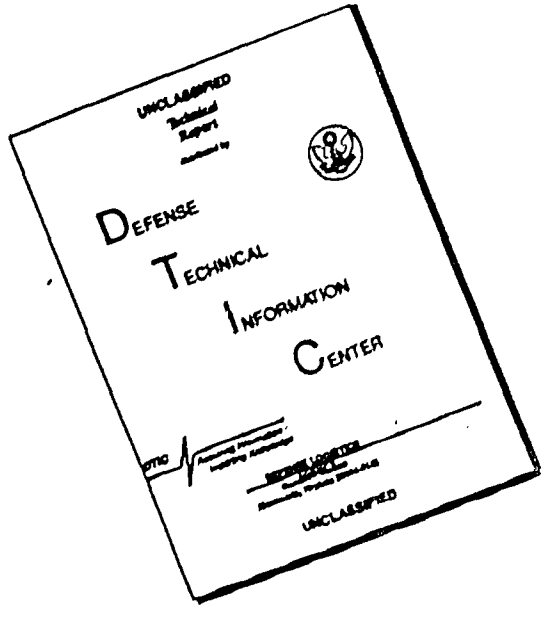

THIS DOCUMENT IS BEST QUALITY AVAILABLE. THE COPY FURNISHED TO DTIC CONTAINED A SIGNIFICANT NUMBER OF PAGES WHICH DO NOT REPRODUCE LEGIBLY.

Final Report

DEFECT REDUCTION IN EPITAXIAL GROWTH USING SUPERLATTICE BUFFER LAYERS

Submitted to

U.S. Air Force Office of Scientific Research

AFOSR-85-0201

By

S.M. Bedair, Professor
Electrical and Computer Engineering Department
North Carolina State University
Raleigh, North Carolina 27695-7911

July 1988

I. INTRODUCTION

Superlattice (SL) structures are of both fundamental and technical interest. Two classes of superlattices have been investigated. In the first class, the superlattice layers have lattice parameters that closely match those of the substrate, such as in the case of the AlGaAs-GaAs and InP−$In_{0.53}Ga_{0.47}As$ systems. In the second class, the strained-layer superlattice (SLS) [1], the alternating layers have lattice parameters that are different by a significant amount, but the layers are thin enough to ensure that the lattice mismatch is entirely accommodated by elastically straining the layers without the generation of misfit dislocations. Examples of these SLS are the GaAs-InGaAs, GaAsP-GaAs and GaAsP/InGaAs systems. These SLS's have several unique features since their electronic and optical properties can be modified over a wide range by the proper choice of material and geometrical parameters [1]. A number of applications using those SLS structures in lasers [2]-[6], light-emitting diodes (LED's) [7]-[9], photodetectors [10]-[12], and FET's [13] have been reported. Although these SLS's have great flexibility in device design, their reliability has been questioned. In particular, it has been observed that under conditions where constant high-level of excitation or rapid thermal cycling is required, the SLS devices are unstable [4]. It is believed that these instabilities are due to the lattice mismatch between the SLS and the substrate and, consequently, misfit dislocations are generated at the interface between the SLS and the substrate [14]. Such conditions are always present in binary/ternary SLS structures [14].

Ternary/Ternary SLS, such as GaAsP/InGaAs, can be grown lattice matched to the GaAs substrate and thus can avoid this problem, thus improving the lifetime of these SLS devices. We will review the methods of growth, properties of these SLS, their stability under levels of current injection and their use to reduce defects in epitaxial layers.

II. CURRENT LIMITATIONS IN BINARY-TERNARY STRAINED LAYER SUPERLATTICES

Strained layer superlattices such as GaAs-InGaAs [9] and GaAsP-GaAs [12] have been studied extensively. However, these superlattices and other binary-ternary structures suffer from major limitations. The average lattice parameter of these binary-ternary structures does lattice match that of the substrate such as GaAs. For example, $In_xGa_{1-x}As$−GaAs SLS will have a lattice parameter which corresponds to a bulk $In_{x/2}Ga_{(1-x)/2}As$ as shown in figure 1. Thus, when grown on GaAs substrate, defects in the form of misfit dislocations appear at the SLS/substrate interfaces [15]. Figure 2 shows a cross-section TEM micrographic of $In_{0.16}Ga_{0.84}As$/GaAs SLS grown on GaAs substrate. Dislocations are shown by arrows at the SLS/GaAs interfaces [15]. In this case the total thickness of the SLS exceeds the critical thickness for the generations of misfit dislocations for bulk grown $In_{0.08}Ga_{0.92}As$ on GaAs substrate. This problem can be avoided by reducing the number of SLS periods so that the total thickness of the SLS is less than the critical thickness for the generation of misfit dislocations [16]. However, this will impose limitations on the number of periods, specially for the case where high strain is present. For example, for $In_{0.3}Ga_{0.7}As$/GaAs SLS, only few periods will be allowed before

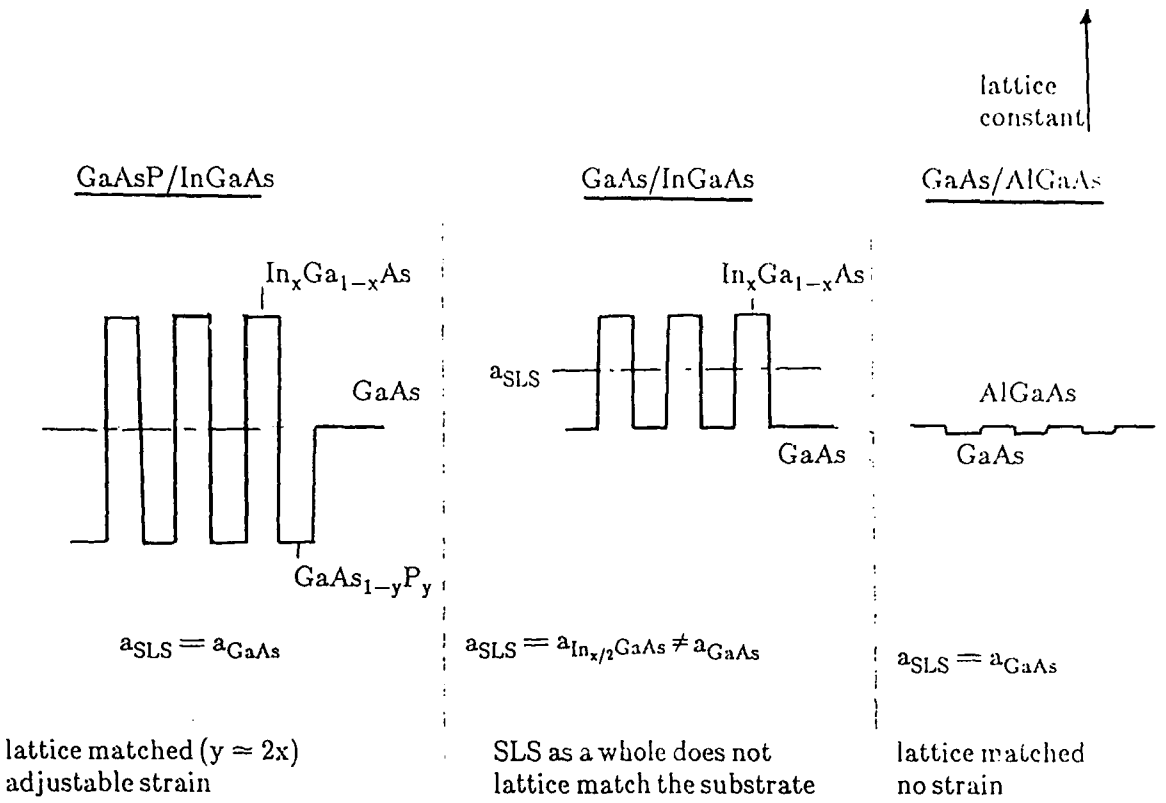

Figure 1 Schematic of the lattice constant of several superlattice structure (a) AlGaAs/GaAs (b) InGaAs/GaAs (c) GaAsP/InGaAs.

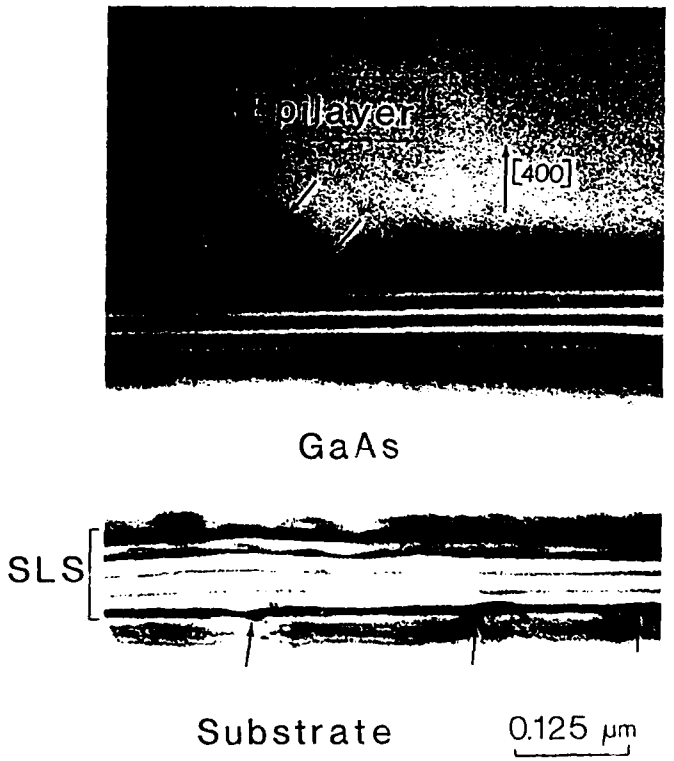

Figure 2. Cross-section TEM micrograph of $In_{0.1}Ga_{0.9}As$/GaAs SLS grown on GaAs substrate. Dislocations as shown by arrows at the SLS/GaAs interfaces.

dislocations are generated at the SLS/GaAs substrate interface. Another approach is to insert an $In_{x/2}Ga_{(1-x)/2}As$ buffer layer between the GaAs substrate and the $In_xGa_{1-x}As/GaAs$ SLS [17]. In this case defects are not generated at the interface between the SLS and the buffer layer. The presence of a buffer layer that does not lattice match the substrate can create several problems. For example, this buffer layer can be highly defective and cannot be obtained with high resistivity [17]. This will have impact on FET structures with the SLS as active layers. Also, if the lattice mismatch between the buffer and the substrate is large, high density of threading dislocation will be generated and will propagate to the SLS structure.

The above problems can be avoided if these binary-ternary SLS's are replaced by other material systems. What is needed is a superlattice composed of two materials having equal but opposite lattice mismatches such that the average lattice constant matches that of GaAs. For example, a SLS made of $GaAs_{1-y}P_y/In_xGa_{1-x}As$ ternary alloys can satisfy these requirements [8].

III. GaAsP-InGaAs STRAINED LAYER SUPERLATTICES

$GaAs_{1-y}P_y/In_xGa_{1-x}As$ SLS can be grown directly on GaAs substrate with an average lattice constant equal to that of GaAs. In such a structure, with $y \simeq 2x$, the InGaAs will be under compression, whereas the GaAsP layer will be under tension and the lattice parameter of the SLS as a whole will be equal to that of GaAs as shown in figure 1. In this case, no defects are generated between the SLS and the substrate and no limitations are imposed on the value of strain between the individual layers or the number of SLS periods. Such a structure will thus allow the use of GaAs or AlGaAs as buffer or confining layers since all layers including the SLS have the same lattice constants in the growth plane. Other material systems can satisfy these requirements; examples are: GaAsP – GaAsSb, GaAsP – InGaAsSb and $Ga_{0.52+x}In_{0.48-x}P - Ga_{0.52-x}In_{0.48+x}P$.

III-1. Epitaxial Growth of GaAsP/InGaAs SLS

GaAsP/InGaAs SLS contains both As and P compounds which makes it difficult to be synthesized by Molecular Beam Epitaxy (MBE). Two techniques were used for the growth of this SLS, mainly metalorganic chemical vapor deposition MOCVD [18], and molecular stream epitaxy MSE [19]. Gas source MBE can also be a potential technique for the synthesis of this SLS.

The MOCVD approach [18] uses TMG, TEI, AsH_3 and PH_3 as sources of Ga, In, As and P. Both AsH_3 and PH_3 are 5% in H_2. The growth temperature was 630°C, which is a compromise between ideal growth temperature for the two ternary alloys. For GaAsP a relatively high growth temperature is required to obtain a wide range of GaP composition since phosphorous incorporation is low at low temperature [20]. On the other hand, for InGaAs, a low growth temperature is preferable because InAs incorporation decreases as the growth temperature increases. Details of the growth process were previously described

[18]. A relatively low growth rate ranging from 100-150 Å/min was used to minimize the gas transient effect and to allow better control of layer thicknesses. The growth process proceeds by sequential injection of TEI and PH_3 while TMG and AsH_3 are flowing all the time. GaAsP-GaAsSb and GaAsP-GaInAsSb SLS's were also grown using this approach [8], where TMSb was used as the Sb source. SLS's with periods as thin as 50 Å were obtained using this injection approach. Thinner SLS's can be obtained by minimizing dead spaces and pressure transients in the gas manifold. To avoid some of the above mentioned problems this SLS was grown by a new process called molecular stream epitaxy [19], which is a modification of the atomic layer epitaxy [21] process previously developed by our group. In this technique the growth of the SLS proceeds by rotating the substrate between two gas streams, one containing TMG, TEI and AsH_3, and the other containing TMG, PH_3 and AsH_3. These two streams are on all the time, thus there is no flow transients or dead spaces resulting from the gas switching processes. SLS with layers as thin as 8 Å was obtained using MSE [19], which is difficult to achieve by conventional MOCVD, specially for material systems containing As and P compounds. MSE it was also possible to grow the SLS at temperatures as low as 520° due to the higher P incorporation [22] in MSE as compared with MOCVD. This will allow high strains between the individual SLS layers.

III-2. Characterization of GaAsP/InGaAs SLS

The GaAsP/InGaAs SLS's were characterized both structurally and optically. As mentioned earlier there is no restriction on the number of periods, and structures with several hundred periods was grown without the creation of defects at the SLS/GaAs interface. If the SLS is not balanced i.e., $y \simeq 2x$ or the thickness of the individual SLS layers exceeds the critical values for the generation of misfit dislocations [18], cross-hatched features are observed on the sample surface. We found that examination of the SLS surface by optical microscope is usually a rough and quick test to check that the SLS has balanced composition.

Epitaxial layers thickness and superlattice structures were examined using x-ray diffraction technique as shown in figure 3. Figure 3a shows the 400 diffraction pattern for 45 periods of $GaAs_{0.8}P_{0.2}$–$In_{0.1}Ga_{0.9}As$ SLS grown on GaAs substrate. The zero-order diffraction peak ($n = 0$) gives the lattice parameter of the SLS as a whole, with a lattice mismatch of less than 0.1% to the GaAs substrate. The extra satellite peaks are due to the periodicity of the SLS, giving a period of 350 Å. This value is consistent with that predicted from the growth rate and that obtained from the total thickness measurement of the SLS on a cleaved sample. Figure 3b shows the corresponding diffraction pattern of GaAsP-GaInAsSb SLS. When this ternary/quaternary SLS was disordered by Zn diffusion at 800°C a GaInPAsSb quinary alloy was obtained [8]. The peak, indicated by A, results from the homogeneous quinary alloy and corresponds to the average lattice constant of the SLS as a whole (peak indicated by $n = 0$ in figure 3b). Rough estimate of the lattice constant of this quinaryy alloy agrees with the position of the peak A [23]. Thus, from figure 3, these ternary/ternary or ternary/quaternary SLS's can be grown lattice matched to GaAs substrates under the proper growth conditions.

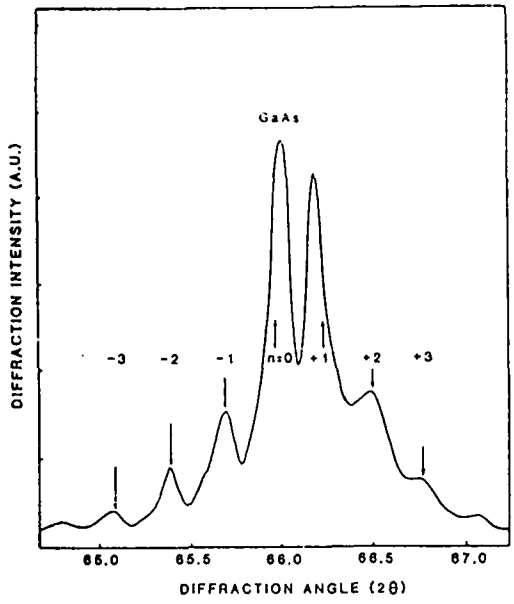

Figure 3 X-ray diffraction pattern in the vicinity of (400) reflection of SLS n's show the order of the satellite peaks originating from the periodicity of the SLS

a) $Ga_{0.8}AsP_{0.2} - In_{0.1}G_{0.9}As$

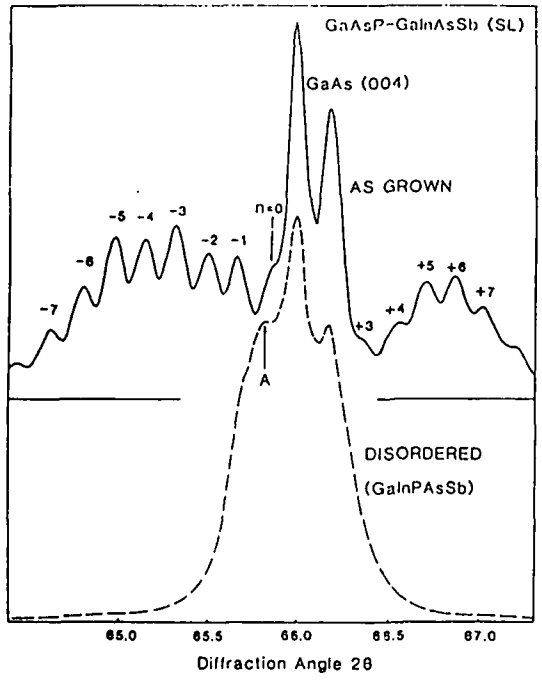

b) $Ga_{0.76}AsP_{0.24} - Ga_{0.92}In_{0.08}As_{0.95}Sb_{0.05}$
In this SLS Zn diffusion resulted in disordering and thus forming the GaInAsSbP quinary alloy. The arrow A shows the quinary diffraction peak.

The optical properties and interface quality of $GaAs_{0.3}P_{0.7}/In_{0.15}Ga_{0.85}As$ SLS were characterized by photoluminescence at 77 and 4.5°K, for a SLS with 5 periods, 130 Å thick each, as being determined from x-ray diffraction. The PL data is shown in figure 4 and the peak at 1.405 eV has a FWHM of 4 meV, indicating that this SLS structure can be grown with excellent interface quality. This peak at 1.405 eV corresponds to the transition between the first electron level (n = 1) and heavy-hole band. The biaxial compression in the InGaAs well breaks the degeneracy of light-hole and heavy-hole valence bands at k = 0 and increases the effective bandgap of InGaAs [24]. In addition, the quantum size effect increases the effective bandgap of the SLS. These two effects result in the energy shift of about 110 meV from the bulk InGaAs value.

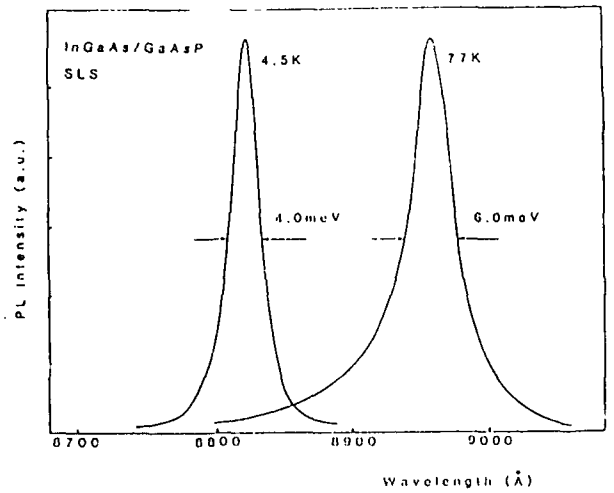

Figure 4 PL spectra of 5 periods $In_{0.15}Ga_{0.85}As/GaAs_{0.7}P_{0.3}$ SLS at 77°K and 4.5°K.

The optical quality of the SLSs versus depth, especially near the SLS/substrate interface, was investigated using PL. This was done by scanning the laser beam along a beveled section of the layers as shown in figure 5. Several samples were beveled on a Plexiglas plate using Ludox. The bevel angle was about 1/3 degrees, which resulted in a vertical magnification factor of 172x. The laser spot size used with PL measurement was about 50 μm and the penetration depth is estimated to be less than 2000 Å based on GaAs absorption data. Figure 5b shows the PL spectra (77°K) of different spots (A-E) which correspond to the positions shown in figure 5a. As the laser beam was moved from position (A) to (B), the PL intensity decreased by more than one order of magnitude. This is because of mechanical damage introduced by polishing. However, the spectral shape did not change. From (B) to (D) the intensity still decreased gradually, while the spectral peak shifted slightly toward the higher-energy side and a shoulder appeared at the lower-energy side. As the beam approached the SLS/substrate interface the shoulder grew, while the main peak decreased and finally disappeared. As shown in figure 5b, there are some variations (~ 10 meV) in the peak emission spectrum from the SLS. These fluctuations can be the result of compositional and periodicity fluctuation in the SLS. The

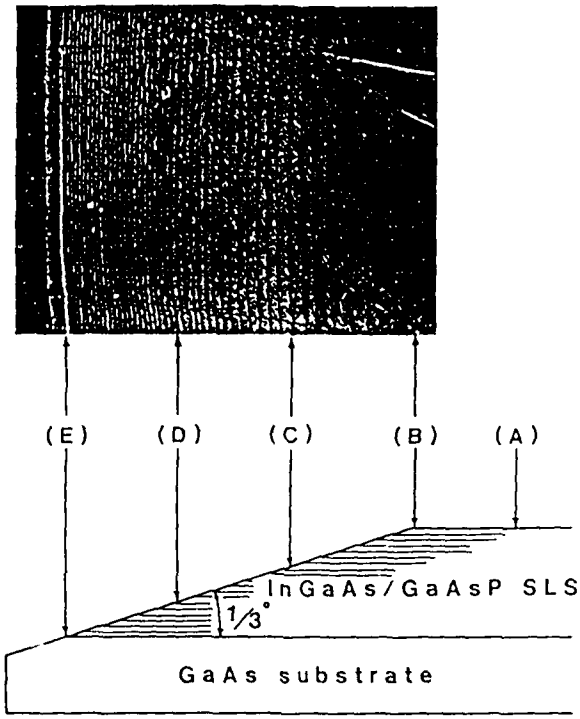

(a)

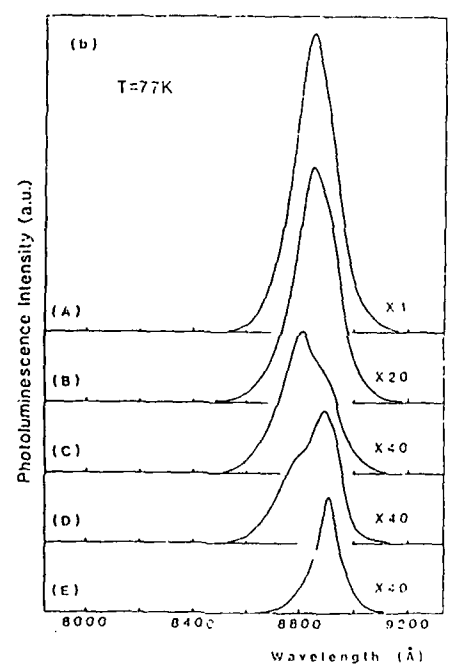

(b)

Figure 5 a) Schematic of the beveled SLS surface at about 1/3°
b) PL spectra at 77°K along the beveled surface.

variation of 10 meV corresponds to the compositional fluctuation of about 6.8% in the InGaAs well assuming no periodicity fluctuation. At the interface (E) the PL linewidth became 9 meV, whereas the PL intensity stayed almost the same as that of position (D). PL from the Si-doped GaAs substrate was very weak and almost undetectable, even at the position (E). This suggests that the photocarriers generated in the GaAs layer will be efficiently collected in the first SLS layer which is InGaAs. Most of the samples showed a tendency for the PL linewidth (FWHM) to decrease or remain unchanged as the SLS/substrate interface was approached. This feature is different from other SLS's whose average lattice constants are not matched to those of their substrates [25]. We have done a similar experiment on InGaAs/GaAs SLSs, which have similar geometrical and compositional parameters to those of InGaAs/GaAsP SLSs shown in figure 5. A significant decrease of PL intensity and spectral line broadening near the SLS/substrate interface was observed. This is probably due to the high density of misfit dislocations at the InGaAs/GaAs SLS and the substrate interface. This result indicates that the average lattice constant of the SLS must be matched to that of the substrate to obtain a high optical quality throughout the entire layer. This is very important, especially when SLSs are used in the active regions of devices.

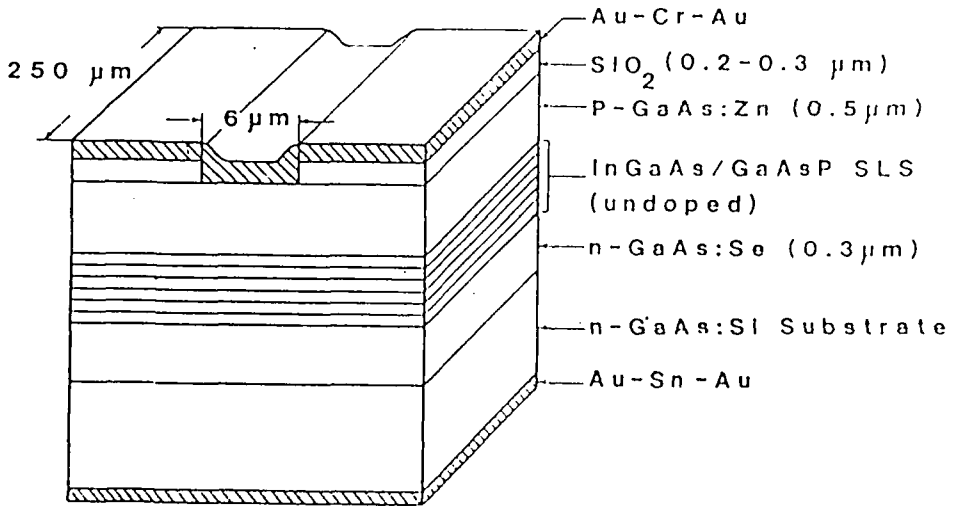

Figure 6 Schematic of SLS LED structure. The undoped active region consists of $GaAs_{0.8}P_{0.2}/In_{0.1}Ga_{0.9}As$ ten periods, each layer is 100 Å thick.

IV. STABILITY OF SLS AND LIFETIME TEST OF LIGHT EMITTING DIODES

A schematic cross-section of the LED [26] structure is shown in figure 6. First a Se-doped 0.3-μm GaAs ($n \sim 1 \times 10^{18} cm^{-3}$) was grown on a (100) Si-doped GaAs substrate. Then an undoped ten-periods $In_{0.1}Ga_{0.9}As/GaAs_{0.8}P_{0.2}$ SLS active region was grown by injecting TEI and PH_3 alternately during the growth of GaAs. The thickness of each layer is about 100 Å (total active region is about 2000 Å). The mismatch between GaAs and the two compounds in their bulk crystal form is ± 0.69 percent. Finally, a Zn-doped 0.5-μm GaAs layer ($p \sim 1 \times 10^{18} cm^{-3}$) was grown on the SLS. The growth temperature was 630°C for all these layers. A SiO_2 layer (2000 ~ 3000 Å) was deposited by plasma-assisted CVD to make a 6-μm-wide stripe structure. The wafer was thinned down to about 70 μm and polished, then ohmic contacts were made by depositing Au-Sn-Au (100, 2000, 1000 Å) followed by annealing at 300°C for 10 seconds for n-type and Au-Cr-Au (100, 200, 1000 Å) for p-type. Finally, the wafer was cleaved and sawed into individual diodes with typical dimensions of 250 x 300 μm^2. The ideality factor for these diodes ranged between 2 and 3 over three orders of magnitude on a current scale. Diodes were mounted to a gold-plated copper block with the p-type face down and held by a spring clip. The optical output was detected by a Si photocell. Three current injection levels, namely, 830, 3000, and 4000 A/cm^2, were used in the lifetime tests. Seven devices have been randomly selected and tested (one at 830, 3000, and 4000 A/cm^2, and five at 4000 A/cm^2). Since the junction of the diode is formed less than 1 μm below the p-type electrode, the current spreading effect is not significant. These SLS LEDs had operated at such high current densities for several thousands hours without any degradation in the optical characteristics as was previously reported [26].

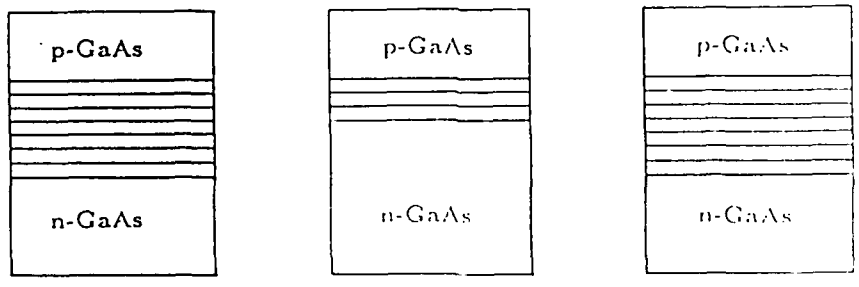

$In_{0.2}Ga_{0.8}As/GaAs_{0.6}P_{0.4}$ (100 Å, 7 periods) (a)

$In_{0.2}Ga_{0.8}As/GaAs$ (100 Å, 3 periods) (b)

$In_{0.2}Ga_{0.8}As/GaAs$ (100 Å, 7 periods) (c)

Figure 7 Schematics of different SLS structures used as the active regions in LED's.

LEDs with the same structure as shown in figure 6 were tried; however, GaAsP-InGaAs SLS active region is replaced by InGaAs/GaAs SLS's the structures are shown in figure 7. The SLS layer's thicknesses in the three structures (shown in figure 7) is 100 Å and number of periods is seven for the structures in figures 7a and 7c and three for the structure in figure 7b. Lifetime tests for these three LED structures at a current injection level of 4000 A/cm^2 were carried out and the results are shown in figure 8. Both structures in figure 7a and 7b have been operating for more than one year without any observed degradation in the optical output, where the structure in (figure 7c) died out in a few hours. These results can be explained based on the average lattice constant of the SLS and its lattice mismatch with the substrate. The ternary/ternary SLS is balanced and no defects are expected to be present between the SLS interfaces and the GaAs layers. For the structure in figure 7b there is lattice mismatch between the $In_{0.2}Ga_{0.8}As$/GaAs, SLS and with an average lattice constant corresponding to the $In_{0.1}Ga_{0.9}As$ bulk and the substrate. However, this mismatch can be accommodated elastically since the total thickness of the SLS (300 Å) is less than the critical thickness for an $In_{0.1}Ga_{0.9}As$ film required to generate defects at the GaAs interface [27]. The situation is quite different for the structure in figure 7c, where the thickness of the seven periods SLS exceeds the critical thickness for the generation of misfit dislocation at the SLS/GaAs interfaces [27]. This very high density of defects will result in the catastrophic failure of this LED structure as shown in figure 8. These preliminary observations suggest that a SLS which is lattice matched to the substrate is stable under high-current-injection conditions and can have potential applications in several devices.

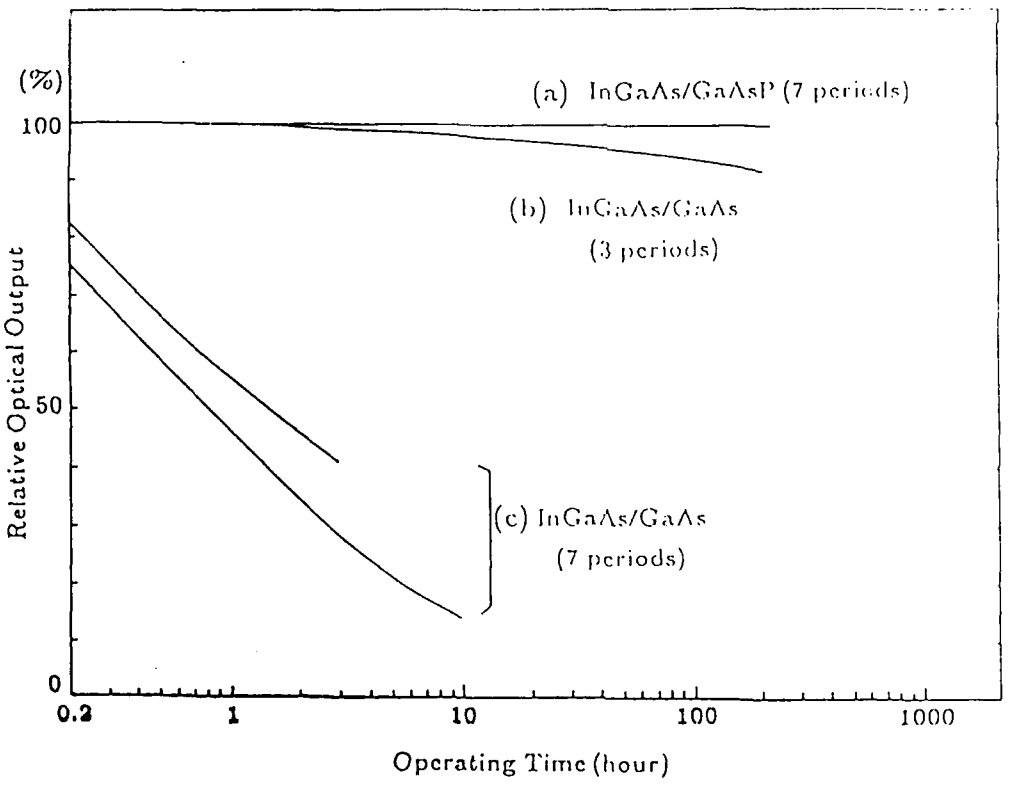

Figure 8 Lifetime test for LED structures shown in Figure 7.

V. DEFECT REDUCTION USING SLS

V-1. Characterization Techniques for Defects

X-ray topography (XRT) and electron beam induced current (EBIC) are non-destructive techniques for defect characterization. XRT is suited for studying large area samples but magnification is only possible by enlarging the micrographs. The defect density suitable for XRT is 10^6 cm^{-2} or less. Therefore, the effect strained layer structures grown on a GaAs substrate are ideal for an investigation by XRT. On the other hand, TEM gives the highest magnification but gives only a very limited observation area. Samples must have high density of defects (higher than 10^6 cm^{-2}) to be studied by TEM. EBIC bridges the two techniques concerning resolution of defects and the observation area. It is possible to decide whether a misfit dislocation is located at the GaAs/SLS interface or within the SLS by using both XRT and EBIC. Cross-sectional TEM was extensively used for direct observations of dislocations and to reveal how dislocations are bent or thread in the SLS. The $g \cdot b$ analysis on dislocations allowed us to identify the types of the dislocations.

V-2. Critical Layer Thickness (CLT) for a Single Strained Layer

In order to determine the value of CLT for a single strained layer of $GaAs_{1-y}P_y$ ($y \sim 0.15$), we employed XRT to examine the substrate prior to the growth of a $GaAs_{1-y}P_y$ film. The growth of the $GaAs_{1-y}P_y$ layer was performed in a stepwise fashion with each step resulting in the deposition of a controlled thickness added to previously existing film. The heterointerface between the ternary layer and the GaAs bulk was characterized at each step by transmission XRT. For a thin $GaAs_{1-y}P_y$ film, less than ~600Å, only substrate threading dislocations are observed. When a $GaAs_{1-y}P_y$ layer of ~900Å thickness was grown, a few generation sites for misfit dislocations appeared near the sample edge. The number of these generation sites of misfit dislocations increased as the thickness of the $GaAs_{1-y}P_y$ epilayer was increased to ~1200Å. When the thickness reached 1600Å, misfit dislocations were formed from these generation sites indicating the process of glide at the $GaAs_{1-y}P_y$/GaAs interface. From these observations we concluded that the value of CLT for the onset of misfit dislocations in a $GaAs_{1-y}P_y$ ($y \sim 0.15$) single layer is approximately 900Å. This value is a few times higher than the value of CLT predicted by Matthews and Blakeslee and about 1/5 of that by People and Bean. It seems that the generation of misfit dislocations is not critically dependent on the film thickness but rather of kinetic nature at the very early stage of generation.

V-3. Critical Layer Thickness in Multilayer

A SLS is constructed of $In_xGa_{1-x}As$ and $GaAs_{1-y}P_y$ epitaxial layers with equal thickness, $x \sim 0.08$, and $y \sim 0.16$. Alternate $GaAs_{1-y}P_y$ and $In_xGa_{1-x}As$ layers are under tension and compression such that the SLS as a whole is lattice matched to the GaAs substrate. EBIC was used to determine the value of CLT for the constituent layers of this SLS structure because XRT can reveal misfit dislocations located at the GaAs/SLS

interface and not those within the SLS. EBIC studies were carried out for SLS's whose period thickness was varied from 500Å to 800Å. For SLS period of ~500Å, even with the acceleration voltage of 25 keV which is sufficient to reach through the SLS, no misfit dislocations were observed indicating that the ternary layer thickness did not exceed the CLT. However, when the period thickness was increased to ~550Å misfit dislocations appeared in the SLS showing that the CLT thickness was exceeded. The density of misfit dislocations increased for the SLS with a period thickness of ~800Å. From these observations the value of CLT for the misfit of 0.6% is estimated to be approximately 280Å which is in reasonable agreement with the Matthews' and Blakeslee's model. We believe this EBIC technique gives an accurate information pertaining to the onset of misfit dislocation generation which is interpreted as the critical layer thickness.

V-4. Defect Reduction Using GaAsP-InGaAs SLS by MOCVD

Strained superlattice buffer layers have been grown with an average lattice constant equal to that of GaAs, as shown by the x-ray diffraction data. Epitaxial GaAs layers grown on these SLB's show significantly smaller dislocation densities than simultaneously grown layers directly on GaAs substrates. TEM studies show that threading dislocations which start in the GaAs substrate do not penetrate the SLS layer. It is expected that devices and circuits fabricated in epitaxial layers on top of SLB's will exhibit less variation in electrical parameters than those fabricated directly on a GaAs substrate (see attached papers).

V-5. Defect Reduction Using GaAs-InGaAs SLS by MBE

GaAsP/InGaAs SLS cannot be grown by MBE due to problems with phosphorous, thus, we used GaAs-InGaAs SLS structures. Results indicate that compared to epitaxial layers grown directly on GaAs substrates, a GaAs-$In_xGa_{1-x}As$ superlattice ($x<0.12$) reduces the dislocations by approximately two orders of magnitude. Transmission electron microscopy, electron beam induced current, and etch pit density have been used to characterize the effectiveness of using superlattice buffer layers for the reduction of defects in GaAs epilayers (see attached papers).

V-6. Defect Reduction of GaAs Grown on Si Substrates

As a result of the large lattice mismatch and the large difference in the thermal expansion coefficient a very high density of dislocations are present in a GaAs film grown directly on a Si substrate. Therefore, a SLS grown on the GaAs film on Si contains dislocations whose density is sufficient for an investigation by TEM. The GaAs film directly on top of a Si substrate are 1 ~ 3 μm thick and the defect density near the top of the layer was found to be 10^8 - 10^9 cm^{-2} range.

It has been shown that the $In_xGa_{1-x}As$–$GaAs_{1-y}P_y$ ($y\simeq 2x$) is an appropriate and highly effective buffer layer for reducing dislocations originating at the GaA-Si interface. The SLS structure also permits high values of strain to be employed without the SLS

generating dislocations of its own. However, the present results also indicate that the effectiveness of the SLS depends on the density of dislocations. For instance, when the dislocation density is low, the threading dislocations are confined to the SLS interfaces and do not propagate into the GaAs epilayer. In contrast, when the dislocation density is very high, it is apparent that the SLS is not as effective. Further work is required to optimize the SLS structure by varying the strain and the number of SLS layers in order to achieve high-quality GaAs on silicon with a very low dislocation density. It is also evident that much more work is needed to understand the interaction and movement of dislocations at the SLS interfaces (see attached papers).

REFERENCES

1) G. C. Osbourn, J. Appl. Phys., vol. 53, p. 1586, 1982.

2) M. J. Ludowise et al., Appl. Phys. Lett., vol. 42, p. 257, 1983.

3) P. L. Gourley, J. P. Hohimer, and R. M. Biefield, Appl. Phys. Lett., vol. 47, p. 552, 1985.

4) M. D. Camras et al., J. Appl. Phys., vol. 54, p. 6183, 1983.

5) W. D. Laidig, P. J. Caldwell, Y. F. Lin, and C. K. Peng, Appl. Phys. Lett., vol. 44, p. 653, 1984.

6) W. D. Laidig, Y. F. Lin, P. J. Caldwell, J. Appl. Phys., vol. 57, p. 33, 1985.

7) S. M. Bedair, T. Katsuyama, M. Timmons, and M. A. Tischler, IEEE Electron Device Lett., vol. EDL-5, p. 45, 1984.

8) S. M. Bedair, T. Katasuyama, P. K. Chiang, N. A. El-Masry, M. A. Tischler, and M. Timmons, J. Cryst. Growth, vol. 68, p. 477, 1984.

9) L. R. Dawson et al., J. Vac. Sci. Technol., vol. B2, p. 179, 1984.

10) G. E. Bulman, T. E. Zipperian, and L. R. Dawson, Appl. Phys. Lett., vol. 49, p. 212, 1986.

11) G. E. Bulman, D. R. Myers, T. E. Zipperian, and L. R. Dawson, Appl. Phys. Lett., vol. 48, p. 1015, 1986.

12) R. M. Biefield, J. Electron, Mater., vol. 15, p. 193, 1986.

13) J. J. Rosenberg, M. Benlamri, P. D. Kirchner, J. M. Woodull, and G. D. Pettit, IEEE Electron Device Lett., vol. EDL-6, p. 491, 1985.

14) J. M. Matthews and A. E. Blakelee, J. Cyst. Growth, vol. 27, p. 118, 1974.

15) S. M. Bedair, T. P. Humphreys, N. A. El-Masry, Y. Lo, N. Hamaguchi, C. Lamp, A. Tuttle, D. L. Dreifus and P. Russel, Appl. Phys. Lett., vol. 49, p. 942, 1986.

16) J. W. Matthews and A. E. Blakeslee, J. Cryst. Growth, vol. 27, p. 118, 1974.

17) T. E. Zipperian, L. R. Dawson, G. C. Osbourn and I. J. Fritz, Proc. 1983, IEDM, p. 696, 1983.

18) T. Katsuyama, S. M. Bedair, N. C. Giles, R. R. Burns and J. F. Schetzina, J. Appl. Physic., vol 62, p. 498, 1987.

19) T. Katsuyama, M. A. Tischler, N. H. Karam, N. El-Masry and S. M. Bedair, Appl. Phys. Lett., vol 51, p. 529 1987.

20) G. B. Stringfellow, J. Crystal Growth, vol. 62, p. 225, 1983.

21) S. M. Bedair, M. A. Tischler, T. Katsuyama and N. A. El-Masry, Appl. Phys. Lett., vol. 47, p. 51, 1985.

22) T. Katsuyama and S. M. Bedair, J. Appl. Physics, accepted.

23) S. M. Bedair (to be published).

24) G. C. Osbourn, P. L. Gourly, I. J. Fritz, R. M. Biefied, L. R. Dawson and T. E. Zipperian in Semiconductor and Semimetal, vol. 24, 1987.

25) N. G. Anderson, W. D. Laidig and Y. F. Lin, J. Electron Mat., vol. 14, p. 187, 1985.

26) T. Katsuyama, Y. J. Yang and S. M. Bedair, Electron Dev. Lett., vol. 8, p. 240, 1987.

Journal of Crystal Growth 77 (1986) 89–94
North-Holland, Amsterdam

GROWTH AND CHARACTERIZATION OF COMPOUND SEMICONDUCTORS BY ATOMIC LAYER EPITAXY

M.A. TISCHLER and S.M. BEDAIR

Department of Electrical and Computer Engineering, North Carolina State University, Raleigh, North Carolina 27695-7911, USA

The growth of GaAs, InAs and $In_xGa_{1-x}As$ ($0 < x < 0.43$) by atomic layer epitaxy (ALE) is described. The growth rate by ALE is found to be independent of the column III flux. ALE GaAs, grown between 450 and 630°C, has been characterized by photoluminescence and Hall measurements. Initial results indicate that ALE gives improved incorporation and uniformity in the growth of InGaAs compared to conventional MOCVD and can be a suitable technique for growing ternary and quaternary layers over large areas.

1. Introduction

Atomic layer epitaxy (ALE) is a relatively new growth technique which offers control of the growth process at the atomic level. Growth proceeds by the deposition of individual layers of atoms. GaAs, for example, is grown by first depositing an atomic layer of Ga and then an atomic layer of As. This cycle is repeated until the desired thickness is achieved. The total thickness is then determined only by the atomic spacing and the number of deposition cycles, and thus can be controlled very accurately. The thickness should also be very uniform across the substrate since the grown layer is built up by the deposition of a single column III or column V monolayer at a time. Atomically abrupt interfaces may be possible since the reactant species can be changed within one atomic layer. The growth of ternary and quaternary compounds by ALE should exhibit very good compositional uniformity because column III and column V species are deposited separately and gas phase reactions between them are eliminated. An example of such a reaction is one which occurs between triethylindium (TEI) and AsH_3. The amount of In available for incorporation in the solid is reduced by this reaction, leading to nonuniform lateral compositions. In ALE, the In and As are deposited separately, their gaseous sources never mix, and thus the gas phase reaction does not have a chance to occur. Additionally, ALE may be used as a tool to investigate growth mechanisms and impurity incorporation by MOCVD.

Atomic layer epitaxy was first reported for II–VI compounds by Suntola and Antson [1]. III–V compounds have also been grown using ALE by Nishizawa et al. [3] and our group [4,5]. In II–VI compounds, the high vapor pressure of these elements is reported to be the mechanism which results in only one monolayer being deposited on the surface per cycle [6]. The first deposited layer is chemically adsorbed on the surface and remains there while any following layers which deposit are weakly bonded and will re-evaporate. This results in a self-limiting mechanism which ensures that only one monolayer of atoms is deposited at a time. This mechanism was not expected to occur with the column III species used in the growth of III–V compounds because of their relatively low vapor pressures. Without a self-limiting mechanism, ALE would require very exact control of the fluxes to achieve monolayer deposition. Larger fluxes would result in higher deposition rates, eventually leading to balling and poor surface morphology. Smaller fluxes would give incomplete surface coverage. In either case, the growth rate would not be accurately known, and thickness and interface control would be compromised. Most column V species have higher vapor pressures and are not expected to be a problem.

This paper describes the conditions for the atomic layer epitaxy of GaAs, InAs and $In_xGa_{1-x}As$ ($0 < x < 0.43$) using metalorganic chemical vapor deposition (MOCVD). We have found that a self-limiting mechanism is present in the ALE of these compounds [5,7] which allows the deposition of only about one monolayer per cycle over a wide range of column III and V input fluxes. Additionally, the compositional uniformity of $In_xGa_{1-x}As$, for large x values, across the substrate is improved over that grown under identical conditions by bulk MOCVD in the same system.

2. Growth system

The growth system for ALE is shown in fig. 1a and has been described previously [4,5,7]. Basically, the substrate, located in the recess of part R of the susceptor, is continuously rotated and cuts through streams of gases containing the column III and V species. The column III and V gases are introduced through separate tubes and the gases impinge directly on the substrate only during the time that it is under the inlet tube. GaAs, for example, is grown by the deposition of a single layer of Ga, rotation to the other gas stream containing AsH_3, and deposition of a single layer of As. This cycle is repeated until the desired thickness is achieved. The depth of the substrate recess is adjusted to provide a few mils clearance between the top of the substrate and the fixed part F of the susceptor. This fixed part acts to shear off a portion of the gaseous boundary layer above the substrate. The susceptor is designed to allow the gas streams to flow unimpeded except when the substrate is directly under the stream as shown in Fig. 1b. This prevents the buildup of a gaseous boundary layer over the non-rotating part of the susceptor. The susceptor is made of graphite coated with silicon carbide and is RF heated. A graphite wedge, in conjunction with a large flow of H_2 (5000 SCCM) from the center tube, acts to prevent mixing of the column III and column V species.

The susceptor is rotated continuously by a stepping motor under computer control. One revolution, or cycle, consisting of the deposition of a single column III and a single column V layer, takes place in 2.6 s. The exposure time to each gas stream is about 0.3 s.

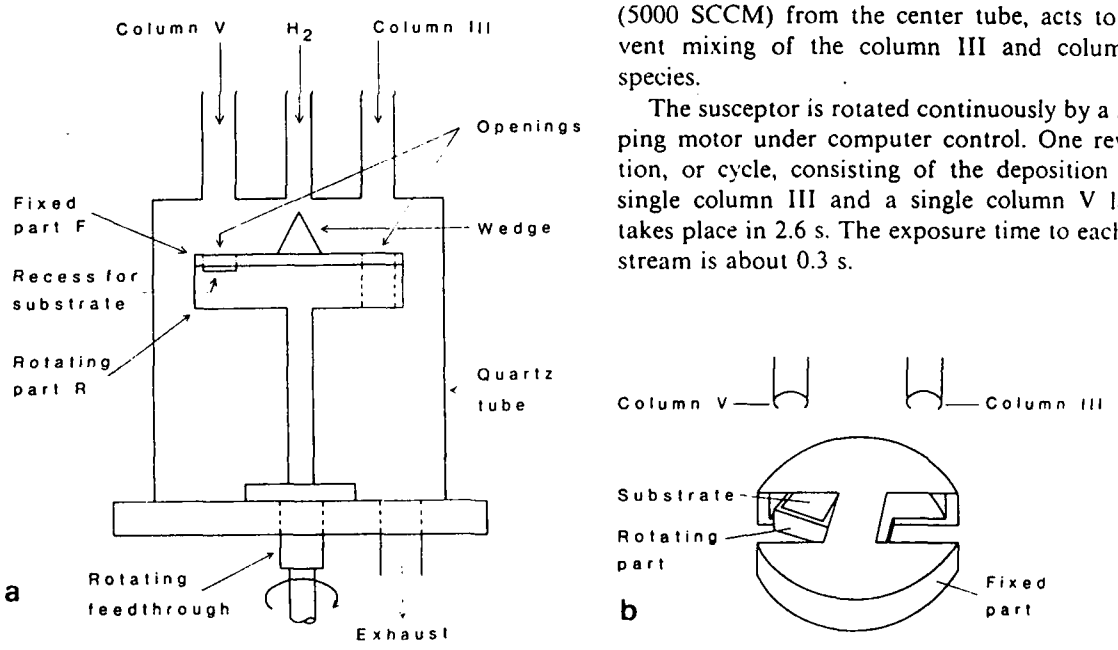

Fig. 1. (a) Schematic diagram of the susceptor and growth chamber for ALE. The substrate is located in a recess in the rotating part R. The column V and III gases enter through separate tubes. A graphite wedge, in conjunction with a large flow of H_2 from the center tube, minimizes mixing of the column III and column V species. (b) Schematic diagram of the susceptor showing the openings through which the gases flow. These gases only impinge on the wafer when the substrate is rotated to the opening.

3. Atomic layer growth

3.1. GaAs

The growth of GaAs by ALE was investigated over a wide range of conditions. The sources for Ga and As were trimethylgallium (TMG) (− 13°C) and AsH_3 (5% in H_2) respectively. The H_2 flow through the TMG bubbler was varied from 0.75 to 10 SCCM. The AsH_3 flow was 25 SCCM. The H_2 carrier gas flows for the TMG and AsH_3 were 500 SCCM each. A typical growth consisted of 1200 cycles.

GaAs grown by ALE is single crystal, as determined by transmission electron diffraction, and has a mirror-like surface. The thickness per cycle is found to be independent of the TMG flux, with only about one monolayer being deposited per cycle [7]. The range in the growth per cycle is shown in fig. 2. The thickness of these layers was determined from cleaved cross-sections using optical microscopy and transmission electron microscopy. Most growths were done at 630°C but this same growth rate per cycle was observed from 450 to 700°C. Two substrate orientations, (100), 2° towards ⟨110⟩ and ⟨111⟩ B, where used and both resulted in the deposition of about one monolayer per cycle. Additionally, increasing the AsH_3 flux by almost an order of magnitude resulted in this same growth rate.

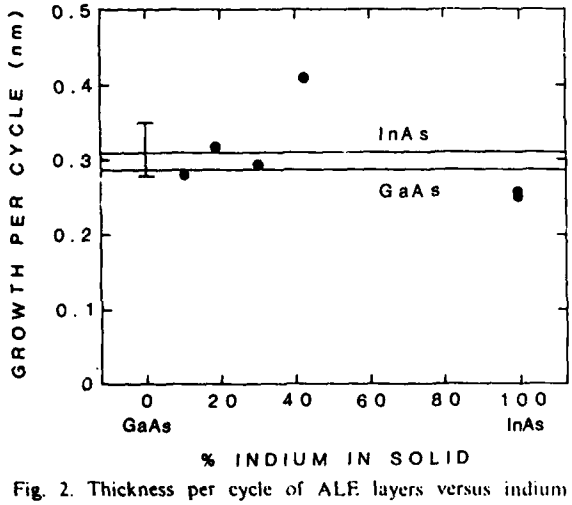

Fig. 2. Thickness per cycle of ALE layers versus indium compositon. The horizontal lines indicate the ideal ALE thickness per cycle of GaAs and InAs in the (100) direction.

Several experiments were performed to ensure that the constant growth per cycle was not arising from the experimental setup or growth conditions. One possibility was that the growth resulted from the gases which are trapped between the substrate and the fixed part of the susceptor. However, if this were true, increasing the TMG input flux would also increase the amount of TMG in the trapped volume, yielding a thicker layer. This did not occur, which also indicates that the trapped gases do not play a major role in growth by ALE.

A second possibility was that the growth could result from cross-diffusion of AsH_3, i.e. AsH_3 diffusing to the Ga side. Increasing the AsH_3 flux by almost an order of magnitude, which should also increase the amount of AsH_3 diffusing to the Ga side, resulted in this same growth rate. Additionally, GaAs was grown by ALE but with the AsH_3 being switched off and flushed from the growth chamber each time before the substrate was exposed to the TMG. The growth rate in this case was still about one monolayer per cycle. Thus, cross-diffusion does not play a significant role in growth by ALE.

A possible explanation for this self-limiting mechanism comes from the fact that the thermal boundary layer is quite thin and the TMG molecule may not decompose until it is very near to, or actually on the substrate surface. At this point, the TMG molecule may be partially or fully cracked or re-evaporate undissociated. The cracking efficiency of TMG on GaAs at 630°C can be quite high [3], and this will result in a monolayer of Ga, or perhaps some intermediate compound, being deposited on the substrate. The cracking efficiency or condensation coefficient of subsequent TMG molecules on this initial layer may be small, allowing these molecules to re-evaporate before they have a chance to crack. If the self-limiting mechanism is a result of the molecular origin of the column III species, one would not expect it to be present in ALE performed by conventional MBE. The exact nature of this process is not clear and requires further study.

The room temperature carrier concentrations and Hall mobilities for GaAs grown by ALE at 630°C are shown in table 1. There are two values listed. The first one (630a) is for GaAs grown

when the susceptor was quite new. The second (630b) is for GaAs grown after many other runs. These two layers were grown under identical conditions. The large difference in carrier concentrations may be a result of carbon incorporation. The graphite susceptor was coated with SiC, but after many runs, part of this coating was worn off, resulting in a larger background concentration of carbon. The low mobilities are partially a result of the thinness of the layers. Identical layers, grown by conventional MOCVD under the same conditions in the same system were semi-insulating and could not be contacted.

Growth of GaAs at low temperatures is interesting because it offers reduced impurity diffusion and incorporation and reduced diffusion of interfaces. We have examined the ALE of GaAs at 450 and 500°C. The growth conditions are the same as mentioned previously except that the H_2 flow through the TMG bubbler was 10 SCCM and the AsH_3 flow was 200 SCCM.

The 77 K photoluminescence (PL) of GaAs grown by ALE at 450°C is shown in fig. 3a. Fig. 3b shows the PL response of GaAs grown by conventional MOCVD under identical conditions in the same system. It can be seen that the PL intensity is greater for the ALE sample. The full width at half maximum (FWHM) for the ALE layer is about 7 meV, which is comparable to the best GaAs we have grown by conventional MOCVD. The large peak is due to the GaAs band to band transition and the smaller peak is probably from a carbon impurity. The peak in the bulk sample is probably from a shallow impurity and its FWHM is about 9 meV. The PL responses of GaAs grown at 500°C by ALE and conventional MOCVD were similar to each other in intensity and emission wavelength.

The room temperature carrier concentration and Hall mobilities for these layers are listed in table 1. It can be seen that all the layers are p-type. Again, layers grown by conventional MOCVD under identical conditions in the same system were semi-insulating and could not be contacted.

3.2. InAs and InGaAs

The experimental setup and rotation scheme for the growth of InAs was the same as that for GaAs except that the TMG was replaced by TEI InAs was successfully grown under the following conditions: Two flows of H_2 through the TE (20°C) bubbler were used, 350 and 450 SCCM The H_2 carrier gas flows for the AsH_3 and TE

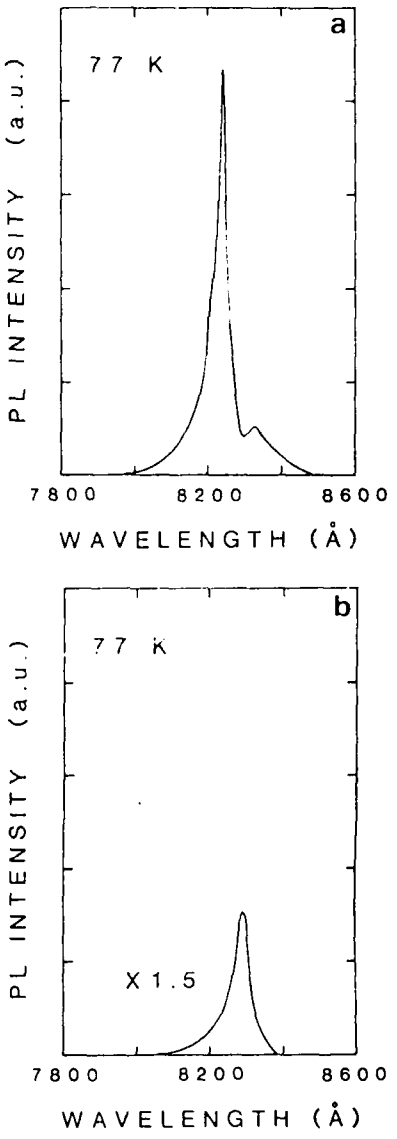

Fig. 3. (a) 77 K photoluminescence of GaAs grown by ALE at 450°C. (b) 77 K photoluminescence of GaAs grown by conventional MOCVD at 450°C in the same system under identical conditions.

were 800 SCCM each. The growth temperature was 480°C and the substrates used were GaAs, oriented (100), 2° towards ⟨110⟩. A typical growth consisted of 1200 cycles.

The thickness per cycle of InAs is shown in fig. 2 and corresponds to about one monolayer per cycle [8]. This result indicates that the TEI acts similarly to TMG in the ALE process. Cross diffusion tests, similar to those for GaAs [4], were performed to ensure that growth was occurring by ALE and not by gases diffusing from one side of the growth chamber to the other. The grown layers were single crystal as determined by X-ray diffraction. They had hazy surfaces partially because of the large lattice mismatch.

InGaAs was grown by ALE by combining the TEI and TMG gases in one inlet tube and keeping the AsH_3 separate in the other inlet tube. Again the experimental setup and rotation scheme was the same as that for the ALE of GaAs and InAs. However, in this case a cycle consisted of the deposition of a single layer of Ga + In, then rotation to the AsH_3 side and deposition of a single layer of As. The H_2 flow through the TMG (−13°C) bubbler was 4 SCCM. The H_2 flow through the TEI (20°C) bubbler was varied from 75 to 450 SCCM. The AsH_3 flow was 25 SCCM. The H_2 carrier gas flows for the column III and column V species were 800 SCCM each. The growth temperature was 630°C and the substrates were GaAs, oriented (100), 2° towards ⟨110⟩. A typical growth consisted of 1200 cycles.

The thickness per cycle for InGaAs is shown in fig. 2 and it can be seen that the self-limiting mechanism described for GaAs and InAs is also present in the growth of InGaAs. The deposited films are shiny for $x < 0.1$ and become hazy at larger In concentrations.

Preliminary results indicate that the incorporation of In in the solid is linear with TEI flux over a greater range in growth by ALE than by conventional MOCVD [8]. Additionally, growth by ALE results in improved uniformity of composition, across the substrate, for large x-values [8]. We believe that this is because, in ALE, the AsH_3 and TEI are separated and are unable to react. In the conventional MOCVD growth these gases mix and react, resulting in a depletion of In in the gas phase. This depletion then leads to a saturation in the gas versus solid composition curve as well as a non-uniform composition across the substrate. These results indicate that ALE may be a potential technique for growing uniform ternary and quaternary layers over large areas.

Table 1
Room temperature carrier concentration and Hall mobility for GaAs grown by atomic layer epitaxy

Growth temperature (°C)	Carrier concentration p (cm^{-3})	Hall mobility ($cm^2/V \cdot s$)
450	2×10^{16}	215
500	5×10^{17}	190
630a	1×10^{15}	280
630b	2×10^{17}	210

4. Conclusion

The growth of GaAs, InAs and $In_xGa_{1-x}As$ ($0 < x < .43$) by atomic layer epitaxy has been demonstrated. A self-limiting mechanism has been observed which limits the growth rate to about one monolayer per cycle independent of the column III flux. The improved incorporation of In in the solid and uniformity of composition suggests that ALE may be a suitable technique for growing compound semiconductors over large areas. Additionally, ALE has the potential to provide layers with uniform thickness and abrupt interfaces, and may also be used to explore growth mechanisms and impurity incorporation by MOCVD.

Acknowledgement

We would like to acknowledge the support of the Air Force Office of Scientific Research.

References

[1] T. Suntola and M.J. Antson, US Patent No. 4-058-430 (1977).

[2] M. Pessa, R. Mäkelä and T. Suntola, Appl. Phys. Letters 38 (1981) 131.

[3] J. Nishizawa, H. Abe and T. Kurabayashi, J. Electrochem. Soc. 132 (1985) 1197.
[4] S.M. Bedair, M.A. Tischler, T. Katsuyama and N.A. El-Masry, Appl. Phys. Letters 47 (1985) 51.
[5] M.A. Tischler, N.G. Anderson and S.M. Bedair, Electronic Materials Conf., Boulder, CO, June 1985.
[6] M. Pessa, O. Jylhä and M.A. Herman, J. Crystal Growth 67 (1984) 255.
[7] M.A. Tischler and S.M. Bedair, Appl. Phys. Letters, to be published (June 16, 1986).
[8] M.A. Tischler and S.M. Bedair, to be published.

Improved uniformity of epitaxial indium-based compounds by atomic layer epitaxy

M. A. Tischler and S. M. Bedair
Electrical and Computer Engineering Department, North Carolina State University, Raleigh, North Carolina 27695-7911

(Received 21 March 1986; accepted for publication 5 June 1986)

Atomic layer epitaxy (ALE) has been employed to grow InAs and $In_xGa_{1-x}As$ ($0 < x < 0.43$). The ALE of InAs, for example, proceeds by the deposition of a single layer of In followed by the deposition of a single layer of As. This cycle is repeated until the desired thickness is achieved. The column III and column V species are physically separated and thus the gas phase reaction between triethylindium and AsH_3 is greatly reduced. This leads to improved incorporation of indium in the solid and improved compositional uniformity across the substrate. A self-limiting mechanism has been found which controls the thickness deposited per cycle to about one monolayer independent of the column III flux.

In-based compounds can meet the material specifications for several important structures and devices such as long wavelength detectors, and emitters and detectors operating in the minimum attenuation regions of fiber optic cables. Also, when combined with lattice-mismatched materials, strained-layer structures composed of InGaAs-GaAs and InGaAs-GaAsP, for example, may be produced.[1,2] The growth of In-based compounds by metalorganic chemical vapor deposition (MOCVD) suffers from the occurrence of a gas phase reaction between triethylindium and AsH_3 and PH_3. This reaction results in a depletion of the amount of In available for incorporation in the solid as well as a nonuniform composition across the substrate.[3,4] Several techniques have been applied to reduce this problem. They include the use of trimethylindium (TMI)[5] and adduct forms of the metalorganic indium[6] which react less with the hydrides than triethlyindium (TEI), growth at low pressure[7] to reduce the amount of time that the species are mixed, and the addition of N_2 to the H_2 carrier gas[7,8] to reduce the thermal boundary layer thickness in which part of the reaction occurs.

The atomic layer epitaxy (ALE) of several II-VI[9] and III-V[10,11] compounds has been previously reported. In this letter we present our results for the ALE of In-based compounds and demonstrate that this technique has the potential to reduce the gas phase reaction between TEI and AsH_3 and produce layers with improved compositional uniformity. Since growth proceeds by the deposition of a single layer at a time, thickness control and uniformity are also expected to be very good.

The ALE of InAs was first investigated using TEI. The growth chamber and susceptor designs have been previously reported.[11,12] A schematic of the susceptor is shown in Fig. 1. The TEI and AsH_3 enter the growth chamber through two separate inlet tubes. These gases flow through holes in the susceptor and only impinge on the substrate when it is rotated directly under a gas stream. Thus, growth proceeds by the deposition of a layer of In, rotation to the AsH_3 side, and the deposition of a layer of As, and this cycle is repeated as many times as desired. A typical run consisted of 1200 cycles. The substrate makes one rotation (controlled by a stepping motor) in 2.6 s and the exposure time to each gas is 0.3 s. The H_2 flows through the TEI (20 °C) bubbler were 350 and 450 sccm. The AsH_3 (5% in H_2) flow was 200 sccm. The H_2 carrier gas flows for the TEI and AsH_3 were 800 sccm each. A center flow of H_2 (5 lpm), not shown in Fig. 1, helps prevent mixing of the TEI and AsH_3. The growth temperature was 480 °C and the substrates were GaAs, oriented (100), 2° towards ⟨110⟩.

The growth rate of InAs was approximately one monolayer per cycle, independent of the TEI flux. This indicates that a self-limiting mechanism, like one for the growth of GaAs,[12] is occurring. The grown layers were single crystal as determined by x-ray diffraction and had hazy surfaces because of the large lattice mismatch. A cross-diffusion test, similar to that for the ALE of GaAs,[11,12] was also performed to ensure that growth was occurring by ALE and not by gases diffusing from one side of the growth chamber to the other. This was done by positioning a substrate under the TEI input tube with both the TEI and AsH_3 flowing. This resulted in a rough, metallic deposit which could easily be scraped off. Additionally, no InAs could be detected by x-

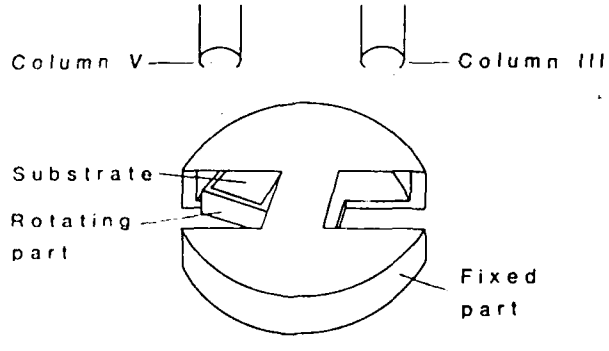

FIG. 1. Schematic diagram of the susceptor used for growth by ALE. The input gases flow unimpeded until the substrate is rotated directly under the inlet tube.

 0003-6951/86/310274-03$01.00

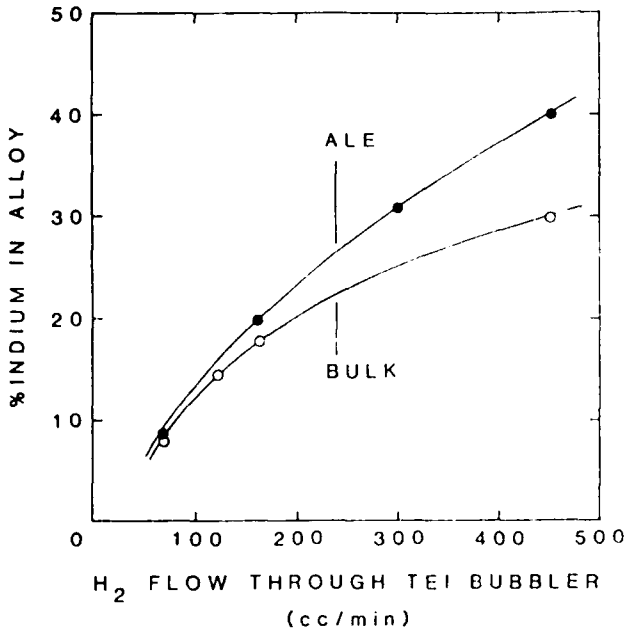

FIG. 2. Percent indium in the alloy vs the H_2 flow through the TEI bubbler. These values are taken from the center of the substrate. (●) ALE, (○) conventional bulk MOCVD.

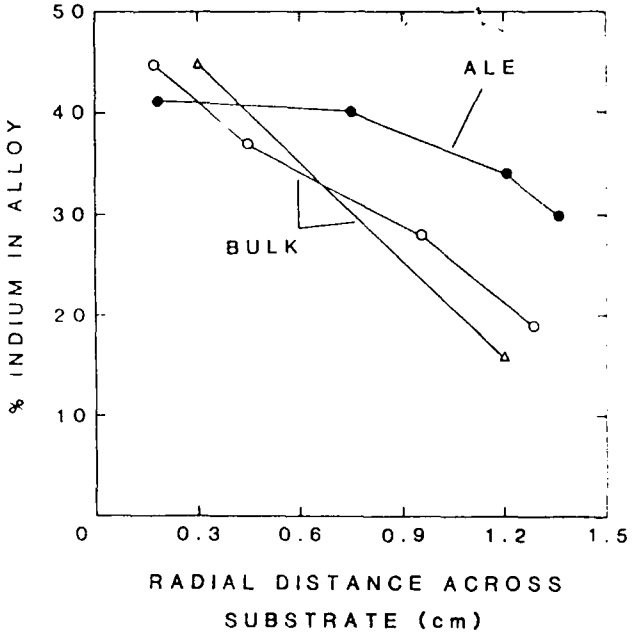

FIG. 3. Variation in the composition of InGaAs across the substrate in the radial direction. The H_2 flow through the TEI bubbler is 450 sccm. Uniform layers are produced by both methods when the amount of indium is less than 20%. (●) ALE, (○, △) conventional bulk MOCVD.

ray diffraction.

InGaAs was next grown by ALE. This was done by combining the TEI and trimethylgallium (TMG) gases in one inlet tube and keeping the AsH_3 separate in the other tube. The experimental setup and rotation scheme was the same as that for the ALE of InAs. However, in this case a cycle consisted of the deposition of a layer of Ga + In, rotation to the AsH_3 side and deposition of a layer of As. The H_2 flow through the TMG (− 13 °C) bubbler was 4 sccm. The H_2 flow through the TEI (20 °C) bubbler was varied from 75 to 450 sccm. The AsH_3 flow was 25 sccm. The H_2 carrier gas flows for the column III and column V species were 800 sccm each. The growth temperature was 630 °C and the substrates were GaAs. A typical growth consisted of 1200 cycles.

The growth rate of InGaAs was again about one monolayer per cycle independent of the column III flux. Thus the self-limiting mechanism described for GaAs and InAs is also present in the growth of InGaAs. The deposited films are shiny for $x < 0.1$, and start to become hazy at larger In compositions. The composition of the layers was determined by x-ray diffraction.

The incorporation of In in the solid by ALE is quite linear with the TEI flux, keeping the TMG flux constant. This is shown in Fig. 2, which also shows the composition of InGaAs layers grown under identical conditions by conventional MOCVD in the same system. In this case, the TMG, TEI, and AsH_3 flow together through one inlet tube directly onto a stationary substrate. The compositions plotted in Fig. 2 are taken from the center of the substrate. It is evident that the linear range is greater by ALE than conventional MOCVD. Larger In concentration in the solid may be achieved by ALE; however, we were limited by the mass flow controllers associated with the TEI and TMG bubblers.

The variation of the solid composition of InGaAs in the radial direction is shown in Fig. 3 for a H_2 flow through the TEI bubbler of 450 sccm. Also shown is the variation for InGaAs grown under identical conditions by conventional MOCVD in the same system. Uniform layers are produced by both methods when the amount of indium is less than 20%. It is evident that growth by ALE gives greater uniformity across the substrate for large In compositions.

The AsH_3 and TEI are separated during growth by ALE and thus any gas phase reaction between the two is

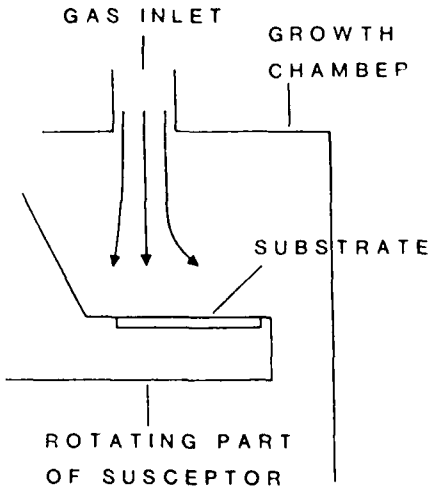

FIG. 4. Detail of the growth system showing the relationship between the position of the gas inlet tube and the substrate. Note that the inlet tube is shifted to the left of the center of the substrate.

prevented from occurring. The situation is quite different in the conventional bulk growth. In this case, the AsH_3 is mixed with the TEI and a gas phase reaction can take place in the inlet tube to the growth chamber, in the growth chamber itself, or within thermal boundary layer near the surface of the hot substrate. The inside of the inlet tube showed a yellowish discoloration after the bulk growth of InGaAs which indicates the possibility of a close to room-temperature reaction. This discoloration did not occur with the ALE of InGaAs. However, as shown in Fig. 3, the innermost portion of the bulk-grown layer (near zero cm) has an In composition similar to that of the ALE layer grown under identical conditions. This indicates that the room-temperature reaction in and directly below the input tube does not significantly reduce the TEI concentration in the gas phase.

The variation in the In composition by bulk growth may be explained by a reaction between AsH_3 and TEI in the thermal boundary layer above the substrate. The experimental setup is such that the column III gas stream is incident on the inside portion of the substrate as shown in Fig. 4. The gases must then flow outward to reach the other side of the wafer. As the gases flow outward over the hot substrate, the AsH_3 and TEI react, resulting in a reduction in the mole fraction of TEI in the gas phase and a corresponding reduction of In in the solid as shown in Fig. 3. This hypothesis is consistent with the results of adding N_2 to the H_2 carrier gas.[7,8] In this case, the higher thermal conductivity of N_2, with respect to H_2, acts to reduce the thermal boundary layer thickness resulting in a smaller volume in which the reaction can effectively occur. This approach has been used to improve the quality of $In_{0.53}Ga_{0.47}As$ grown on InP substrates.[7,8] The ability of ALE to produce layers with good compositional uniformity indicates that it may be a promising technique for producing ternary, and possibly quaternary, layers over large areas. This inherent control has been demonstrated by the production of large area ZnS electroluminescent displays by ALE.[1]

The growth of InAs and $In_xGa_{1-x}As$ $(0 < x < 0.43)$ by atomic layer epitaxy has been demonstrated. A self-limiting mechanism has been observed which controls the deposition to about one monolayer per cycle independent of the column III flux. The incorporation of In in the solid and the compositional uniformity are improved in the layers grown by ALE as compared to conventional MOCVD in the same system. These results indicate that ALE may be able to produce ternary, and possibly quarternary (such as InGaAsP and InGaAsSb), layers over large areas with uniform thickness and composition. ALE may also be used as a tool to investigate various aspects of growth mechanisms by MOCVD.

The authors would like to thank the Air Force Office of Scientific Research for supporting this work.

[1] G. C. Osburn, J. Appl. Phys. 35, 1586 (1982).
[2] S. M. Bedair, T. Katsuyama, M. Timmons, and M. Tischler, IEEE Electron Device Lett. EDL-5, 45 (1984).
[3] H. M. Manasevit and W. J. Simpson, J. Electrochem. Soc. 120, 135 (1973).
[4] B. J. Baliga and S. K. Ghandi, J. Electrochem. Soc. 122, 683 (1975).
[5] C. P. Kuo, J. S. Yuan, R. M. Cohen, J. Dunn, and G. B. Stringfellow, Appl. Phys. Lett. 44, 550 (1984).
[6] R. H. Moss, J. Cryst. Growth 68, 78 (1984).
[7] J. P. Duchemin, M. Bonnet, G. Beuchet, and F. Koelsch, Inst. Phys. Conf. Ser. No. 45, 10 (1978).
[8] M. Sacilotti, A. Mircea, and R. Azoulay, J. Cryst. Growth 63, 111 (1983).
[9] M. Pessa, R. Mäkelä, and T. Suntola, Appl. Phys. Lett. 38, 131 (1981).
[10] J. Nishizawa, H. Abe, and T. Kurabayashi, J. Electrochem. Soc. 132, 1197 (1985).
[11] S. M. Bedair, M. A. Tischler, T. Katsuyama, and N. A. El-Masry, Appl. Phys. Lett. 47, 51 (1985).
[12] M. A. Tischler and S. M. Bedair, Appl. Phys. Lett. 48, 1681 (1986).
[13] R. Antson, M. Grassebauer, M. Hamilo, L. Hiltunen, T. Koskinen, M. Leskelä, L. Niinistö, G. Stingeder, and M. Tammenmaa, Fresenius Z. Anal. Chem. 322, 175 (1985).

Ultrathin InAs/GaAs single quantum well structures grown by atomic layer epitaxy

M. A. Tischler, N. G. Anderson, and S. M. Bedair
Electrical and Computer Engineering Department, Box 7911, North Carolina State University, Raleigh, North Carolina 27695-7911

(Received 14 August 1986; accepted for publication 9 September 1986)

Extremely thin InAs/GaAs single quantum well structures have been grown by atomic layer epitaxy. The wells were 2 and 4 InAs monolayers thick. Photoluminescence spectra (19 K) from these structures are sharp, intense, and uniform across the sample with full widths at half-maximum for the 2 and 4 monolayer wells of 12 and 17 meV, respectively. These results indicate the high degree of control inherent in atomic layer epitaxy as well as its ability to grow high quality materials.

Quantum wells and superlattices, as well as devices incorporating these structures, such as modulation-doped field-effect transistors (MODFET's) and quantum well lasers, require the ability to produce thin layers with abrupt interfaces. The single quantum well (SQW), in particular, is of great interest because it can be used to investigate physics in the quantum regime as well as the ability of a growth system to produce these sophisticated structures. These demanding requirements have been achieved, with a large measure of success, by molecular beam epitaxy (MBE) and metalorganic chemical vapor deposition (MOCVD).[1-8] In this letter we report on very thin InAs single quantum wells grown by a different technique, atomic layer epitaxy (ALE).[9-15] We have previously reported on the atomic layer epitaxy of GaAs, InAs, and (InGa)As.[12-15] The photoluminescence (PL) data from these SQW structures indicate that ALE is capable of growing uniform, thin layers with extremely abrupt interfaces.

Atomic layer epitaxy is a relatively new technique for synthesizing compound semiconductors which has the potential for very precise control of the growth process.[9-15] Growth proceeds by the alternate deposition of the column III and column V species (for the growth of III-V semiconductors). This is in contrast to conventional growth where all of the species arrive at the substrate simultaneously. One very important feature of ALE is that only a single monolayer is deposited at a time,[10-15] thus giving excellent control of the layer thickness. GaAs, for example, is grown by the deposition of a layer of Ga or Ga species, followed by the deposition of a layer of As or As species. Since only one monolayer of GaAs ($\sim$2.83 Å) is deposited per cycle, the total thickness is determined only by the lattice constant of the material and the number of cycles and can be controlled very accurately. Additionally, very abrupt interfaces are possible simply by changing sources and continuing with the growth.

A schematic of the SQW structure is shown in Fig. 1. The substrates were silicon doped ($N_D = 3\times10^{18}$) GaAs, oriented (100), 2° towards (011). The growth takes place in a modified atmospheric pressure metalorganic chemical vapor deposition (MOCVD) system which has the capability to grow material by both conventional MOCVD and ALE. The 1-μm-thick GaAs buffer layer was grown by conventional MOCVD, that is, with the AsH_3 and trimethylgallium (TMG) arriving simultaneously at the substrate. The GaAs confining layers and the InAs wells were grown by ALE. The details of the ALE growth process have been reported previously.[12-15] To ensure that the InAs was deposited pseudomorphically (elastically strained), the well widths were kept below the critical thickness h_c for the onset of dislocation generation.[16] For this large lattice mismatch ($\sim$7.4%), h_c is about 20 Å.[16]

As shown in Fig. 1, the growth consisted of first 180 cycles of GaAs ($\sim$500 Å) for the bottom confining layer. The TMG source was then turned off and the triethylindium (TEI) source was turned on. The InAs wells were then grown using either two or four cycles, each cycle corresponding to one monolayer of InAs. Then the TEI source was turned off, the TMG source turned on, and the 180 cycle ($\sim$500 Å) GaAs top confining layer was grown. During the gas switching period between TEI and TMG ($\sim$1.5 min), the substrate sat under the AsH_3 flow. The growth temperature for the ALE layers was 480 °C. The surfaces of these layers were smooth and mirrorlike. Calculated widths of the quantum wells are approximately 6.6 and 13.1 Å, respectively, assuming a value of 3.28 Å per monolayer for pseudomorphic InAs strained to lattice match GaAs.

The single quantum wells were characterized by photoluminescence spectroscopy which is very sensitive to material and interface quality.[17-19] High quality SQW's typically exhibit sharp, intense peaks.[1-6,8] In preparation for PL, the samples were cleaved into squares 2–4 mm on a side, mounted in In on a copper sample holder, and cooled to 19 K in a

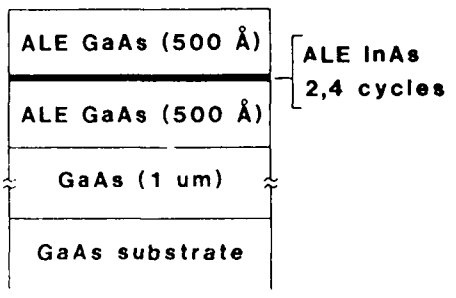

FIG. 1. Schematic of the InAs/GaAs single quantum well structure grown by atomic layer epitaxy. The buffer layer is grown by conventional bulk MOCVD.

 0003-6951/86/441199-02$01.00

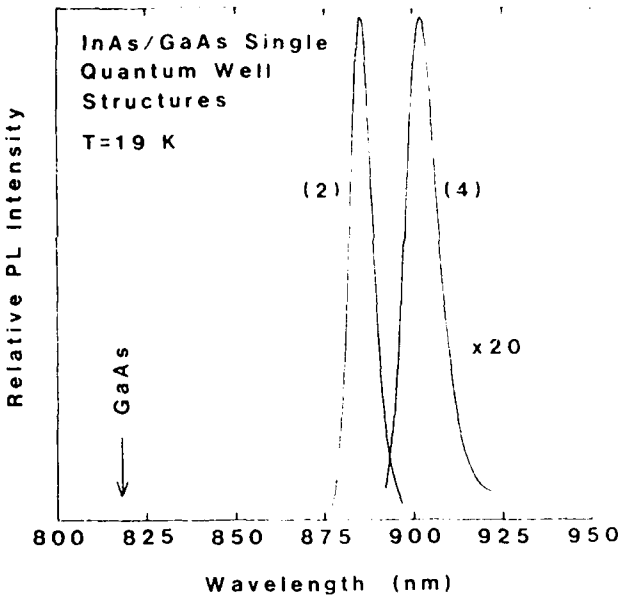

FIG. 2. Photoluminescence spectra for the 2 and 4 cycle single quantum wells. The integer next to each spectrum corresponds to the number of InAs monolayers in the well.

closed cycle He cryostat. A cw Ar^+ laser (λ = 5145 Å) was used as an excitation source with the beam focused to about a 30-μm spot on the sample surface. A relatively high power density of about 1.7×10^3 W/cm^2 was used for excitation. The PL spectra were obtained using a 0.64-m spectrometer and a cooled S 1 photomultiplier.

The spectra for the 2 and 4 cycle wells are shown in Fig. 2. The luminescence is strong with narrow spectral widths, indicating the high quality of the material and the interfaces. The FWHM of the spectra are 12 and 17 meV (for the 2 and 4 cycle wells, respectively) and are among the narrowest reported for such thin single quantum wells in this or other material systems.[1-6,20] An identical 2 cycle SQW structure, grown seven months after the first one, has almost identical spectral characteristics. Peak energies and full widths at half maximum (FWHM) for these 2 cycle structures are within 8 and 0.5 meV, respectively.

The potential of ALE to grow with a high degree of spatial thickness uniformity has also been studied for samples 1.5 cm on a side. The photoluminescence peak energy, FWHM, and photoluminescence peak energy variation ΔE across each sample are summarized in Table I. The peak energies, spectral widths, and line shapes across each sample are very uniform which indicates a high degree of control of layer thickness and interface quality. The peak energy variation ΔE across each sample is less than 1/4 of the energy difference between the 2 and 4 cycle structures suggesting that the layers are uniform to within one monolayer. The ability to produce uniform layers is very important in many applications. For example, in GaAs integrated circuits, variations in channel thickness translate into threshold voltage variations.

TABLE I. Spectral characteristics of 2 and, 4 cycle InAs/GaAs single quantum well structures. ΔE is the photoluminescence peak energy variation across a single sample. The samples are 1.5 × 1.5 cm.

Sample (cycles)	Peak energy (eV)	ΔE (meV)	FWHM (meV)
2a	1.401	7	12
2b	1.393		12.5
4	1.375	5	17

In conclusion, the growth of high quality InAs/GaAs single quantum well structures has been demonstrated by atomic layer epitaxy. Photoluminescence spectra from these wells show sharp intense peaks with FWHM for the 2 and 4 cycle wells (corresponding to ~ 6.6 and 13.1 Å) of 12 and 17 meV, respectively. These are among the narrowest reported for such thin wells in this or other material systems. The line shape and FWHM are also very uniform across each sample. In addition, 2 cycle structures grown seven months apart show almost identical spectral characteristics. These results indicate that ALE has the ability to grow uniform, high quality material with excellent control of layer thickness and interface abruptness. This control is inherent in ALE because growth proceeds one monolayer at a time.

The authors would like to acknowledge the assistance of R. M. Kolbas and the support of the Air Force Office of Scientific Research and the National Science Foundation.

[1] W. T. Tsang and E. F. Schubert, Appl. Phys. Lett. **49**, 220 (1986).
[2] C. E. Schaus, J. R. Shealy, L. F. Eastman, B. C. Cooman, and C. B. Carter, J. Appl. Phys. **59**, 678 (1986).
[3] H. Kawai, K. Kaneko, and N. Watanabe, J. Appl. Phys. **56**, 463 (1984).
[4] C. P. Kuo, K. L. Fry, and G. B. Stringfellow, Appl. Phys. Lett. **47**, 888 (1985).
[5] R. C. Miller, R. D. Dupuis, and P. M. Petroff, Appl. Phys. Lett. **44**, 51 (1984).
[6] D. E. Welch, G. W. Wicks, and L. F. Eastman, Appl. Phys. Lett. **43**, 762 (1983); **46**, 991 (1985).
[7] F. J. Grunthaner, M. Y. Yen, R. Fernandez, T. C. Lee, A. Madhukar, and B. F. Lewis, Appl. Phys. Lett. **46**, 983 (1985).
[8] N. G. Anderson, W. D. Laidig, R. M. Kolbas, and Y. C. Lo, J. Appl. Phys. **60**, 2361 (1986).
[9] T. Suntola and M. J. Antson, U.S. Patent Number 4,058,430 (1977).
[10] M. Pessa, O. Jylha, and M. A. Herman, J. Cryst. Growth **67**, 255 (1984).
[11] J. Nishizawa, H. Abe, and T. Kurabayashi, J. Electrochem. Soc. **132**, 1197 (1985).
[12] M. A. Tischler and S. M. Bedair, Appl. Phys. Lett. **48**, 1681 (1986).
[13] M. A. Tischler and S. M. Bedair, Appl. Phys. Lett. **49**, 274 (1986).
[14] M. A. Tischler and S. M. Bedair, J. Cryst. Growth (to be published).
[15] M. A. Tischler, Ph.D. thesis, North Carolina State University 1986.
[16] J. W. Matthews and A. E. Blakeslee, J. Cryst. Growth **27**, 118 (1974).
[17] B. Deveaud, A. Regreny, J-Y. Emery, and A. Chomette, J. Appl. Phys. **59**, 1633 (1986).
[18] J. H. Marsh, J. S. Roberts, and P. A. Claxton, Appl. Phys. Lett. **46**, 1161 (1985).
[19] J. Singh, K. K. Bajaj, and S. Chaudhuri, Appl. Phys. Lett. **44**, 805 (1984).
[20] I. Goldstein, F. Glas, J. Y. Marzin, M. N. Charasse, and G. LeRoux, Appl. Phys. Lett. **47**, 1099 (1985).

Lifetime Test for High-Current-Injection Strained-Layer Superlattice Light-Emitting Diode

T. Katsuyama
Y.J. Yang
S.M. Bedair

Reprinted from
IEEE ELECTRON DEVICE LETTERS
Vol. EDL-8, No. 5, May 1987

Lifetime Test for High-Current-Injection Strained-Layer Superlattice Light-Emitting Diode

T. KATSUYAMA, Y. J. YANG, AND SALAH M. BEDAIR, MEMBER, IEEE

Abstract—**Successful long-term room-temperature operation of InGaAs/GaAsP strained-layer superlattice (SLS) light-emitting diodes (LED's) under high constant current injection is reported. The devices have been tested up to 1000 h with 830 A/cm², 2000 h with 3000 A/cm², and 2000 h with 4000 A/cm² with no observed degradation in the optical outputs. These results indicate that an SLS with lattice constant well matched to that of the substrate is stable under high-level current injection.**

RECENTLY, strained-layer superlattices (SLS's) which consist of alternating thin layers of two semiconductors having different lattice constants in bulk crystal form have received considerable attention in electronic and optical device applications. The basic electronic and optical properties of the SLS's can be modified over a wide range by a proper choice of material and geometrical parameters [1]. A number of applications using those SLS structures in lasers [2]–[6], light-emitting diodes (LED's) [7]–[9], photodetectors [10]–[12], and FET's [13] have been reported. Although these SLS's have great flexibility in device design, their reliability has been questioned. In particular, it has been observed that under conditions where constant high-level excitation or rapid thermal cycling is required, the SLS devices are unstable [4]. It is noted, however, that many of SLS structures are not lattice matched to the substrate. Consequently, misfit dislocations are always generated at the interface between the SLS and the substrate when a total thickness of the SLS exceeds a strain-dependent critical thickness [14]. In order to avoid the generation of these misfit dislocations, device structures normally incorporate with a buffer layer whose lattice constant is equal to the average lattice constant of the SLS. However, misfit dislocations are still generated between the buffer layer and the substrate and propagate toward the SLS. This probably explains why SLS devices such as photopumped lasers are unstable especially under high-level excitation.

In this letter, we report a series of lifetime tests for InGaAs/GaAsP SLS LED's to investigate the reliability of these structures. Since the InGaAs/GaAsP SLS structure consists of alternating InGaAs and GaAsP layers with equal and opposite lattice mismatch with respect to the GaAs substrate, the average lattice constant can be matched to that of GaAs. Therefore this SLS can be incorporated with GaAs and AlGaAs device structures without the formation of misfit dislocations at the heterointerface. Several potential applications of this SLS including LED's [7], defect reduction [15], and solar cell [16] have been reported.

The LED structure was grown by metalorganic chemical vapor deposition (MOCVD) at atmospheric pressure. Trimethylgallium (TMG), triethylindium (TEI), AsH_3, and PH_3 were used in Ga, In, As, and P sources, respectively. H_2Se and dimethylzinc (DMZ) were used as the n-type and p-type dopant, respectively. A schematic cross section of the device is shown in Fig. 1. First, a Se-doped 0.3-μm GaAs ($n \sim 1 \times 10^{18}$ cm^{-3}) was grown on a (100) Si-doped GaAs substrate. Then an undoped ten-period $In_{0.1}Ga_{0.9}As/GaAs_{0.8}P_{0.2}$ SLS active region was grown by injecting TEI and PH_3 alternately during the growth of GaAs. The thickness of each layer is about 100 Å (total active region is about 2000 Å). The mismatch between GaAs and the two compounds in bulk crystal form is ± 0.79 percent. Finally, a Zn-doped 0.5-μm GaAs layer ($p \sim 1 \times 10^{18}$ cm^{-3}) was grown on the SLS. The growth temperature was 630°C for all these layers. A SiO_2 layer (2000 ~ 3000 Å) was deposited by plasma-assisted CVD to make a 6-μm-wide stripe structure. The wafer was thinned down to about 70 μm and polished; then ohmic contacts were made by depositing Au–Sn–Au (100, 200, 1000 Å) followed by annealing at 300°C for 10 s for n-type and Au–Cr–Au (100, 200, 1000 Å) for p-type. Finally, the wafer was cleaved and sawed into individual diodes with typical dimensions of 250 × 300 μm². The ideality factor for these diodes ranged between 2 and 3 over three orders of magnitude on a current scale.

Diodes were mounted to a gold-plated copper block with the p-type face down and held by a spring clip. The optical output was detected by a Si photocell. Three current injection levels, namely, 830, 3000, and 4000 A/cm², were used in our lifetime tests. Seven devices have been randomly selected and tested (one at 830 A/cm², one at 3000 A/cm², and five at 4000 A/cm²). Since the junction of the diode is formed less than 1 μm below the p-type electrode, the current spreading effect is not significant. Current–voltage measurements performed on several samples which had no direct connection between the metal contact and p-type GaAs layer (i.e., the SiO_2 layer has no stripe cut through it) showed a current three orders of magnitude less than the current through the tested devices. All

Manuscript received January 7, 1987; revised February 26, 1987. This work was supported by the National Science Foundation and the Air Force Office of Scientific Research.

The authors are with the Department of Electrical and Computer Engineering, North Carolina State University, Raleigh, NC 27695-7911.

IEEE Log Number 8714672.

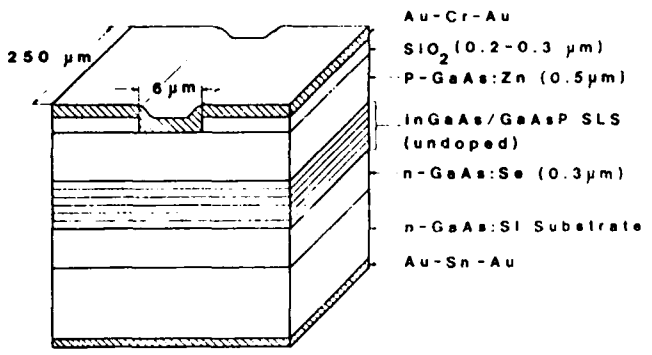

Fig. 1. Schematic drawing of SLS LED structure. The undoped active region consists of ten-period $In_{0.1}Ga_{0.9}As/GaAs_{0.8}P_{0.2}$ SLS (each layer ~100 Å) with lattice constant equal to that of GaAs.

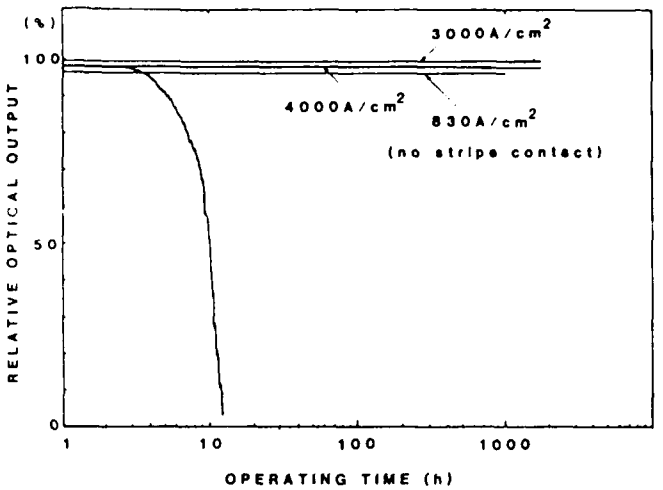

Fig. 2. Optical outputs as a function of operating time. After the initial reduction (less than a few percent) no degradation has been observed.

devices, including the ones without the metal contact stripe, were the same size (250 × 300 μm^2), and were tested at the same operating forward bias (1.45 V). Therefore the leakage current across the edges of the diode and through the SiO_2 insulation layer will be less than a fraction of a percent of the total current flowing through the junction. Moreover, the optical output for a given input current was found to be independent of the size of the diode for the same 6-μm-wide stripe structure. Consequently, the current density is determined by assuming the effective current injection area of 10 × 250 μm^2 for a stripe structure whose contact area is 6 × 250 μm^2.

Fig. 2 shows the optical outputs as a function of operating time with constant current injection at room temperature. No degradation in the optical outputs has been observed. For instance, for a 830-A/cm^2 current injection, the diode (no stripe structure, full-surface metallization 125 × 125 μm^2) has operated for more than 1000 h without degradation). The device tested at 830 A/cm^2 has no stripe structure, but all the other devices have the stripe structure shown in Fig. 1. It has also been observed that there is no degradation up to 2000 h at a current density of 3000 A/cm^2. By comparison, at 4000 A/cm^2, one of the five devices has operated for more than 2000 h without degradation. Lifetime testing at 4000 A/cm^2 on two of the five devices was suspended at 100 h with no observed degradation. Two of five devices tested at 4000 A/cm^2 failed after 6–10-h operation. Under such a high injection level, the device performance seems strongly dependent upon the method of device processing and mounting. We think that the catastrophic degradation of two samples at 4000 A/cm^2 is not directly related to the device structure, since other devices showed long-performance lifetimes. Although not shown in Fig. 2, there are slight reductions (less than a few percent) in the optical outputs within the first hour. This reduction is somewhat larger for the diode which has no stripe structure than it is for a stripe-structure diode. This is probably because of a larger surface leakage current due to the structure which has no SiO_2 insulation layer. For a stripe-structure diode, such an initial reduction in the optical output is very small. Under a high-level-injection condition at which the optical output almost saturates, a slight reduction in the optical output has been observed. This is mainly because of junction heating caused by the high current injection. In fact, above 4000 A/cm^2 the optical output decreases gradually as the current density increases because of the heating effect at the junction.

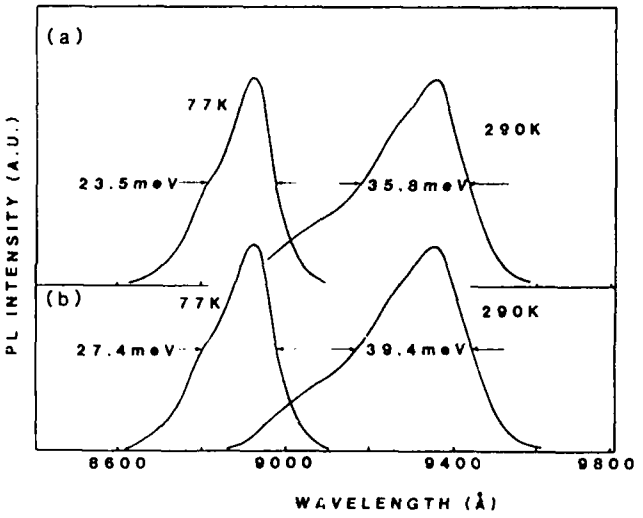

Fig. 3. Typical emission spectra of LED at 77 K and 290 K (*a*) before and (*b*) after 500-h operation with 3000-A/cm^2 current injection. The spectral peak positions remained unchanged, while the spectral widths were slightly broadened.

The lifetime test was interrupted after 500-h operation for the spectral measurements. Fig. 3 shows typical emission spectra at 77 K and 290 K both before and after 500-h operation with 3000-A/cm^2 current injection. The spectral measurements were done with the current density of 200 A/cm^2 both before and after the aging test. After 500-h operation, the spectral peak positions remained unchanged, while the spectral line widths increased slightly (3.6 meV at 290 K, 3.9 meV at 77 K) as illustrated in Fig. 3. After 2000-h operation (not shown in Fig. 3), the spectral peak positions still remained unchanged, while the spectral line widths increased (2.1 meV at 290 K, 3.5 meV at 77 K). The mechanism responsible for this broadening is not clear. However, this broadening may be attributed to the impurity diffusion into quantum wells. The interdiffusion at the SLS

interfaces, which will result in both spectral broadening and shift of the peak position, may be insignificant, since no spectral peak shift was observed. These preliminary observations suggest that an SLS which is lattice matched to the substrate is stable under high-current-injection conditions and has a great potential for practical device applications.

In conclusion, we have presented the lifetime test of InGaAs/GaAsP SLS LED's to investigate the reliability of the SLS structure. No degradation in the optical outputs has been observed up to 1000, 2000, and 2000 h with 830-, 3000-, and 4000-A/cm^2 injection current density, respectively. Although there is a slight spectral line with broadening reflecting some changes in the active region of the device, the important features of the LED, emission wavelength and output intensity, remain unchanged. These results indicate that the SLS which has a lattice constant equal to that of the substrate is stable under high current injection and has a great potential for practical SLS device applications.

Acknowledgment

The authors would like to acknowledge Dr. R. M. Kolbas, Dr. M. A. Tischler, and Dr. M. Timmons for their assistance.

References

[1] G. C. Osbourn, *J. Appl. Phys.*, vol. 53, p. 1586, 1982.
[2] M. J. Ludowise *et al.*, *Appl. Phys. Lett.*, vol. 42, p. 257, 1983.
[3] P. L. Gourley, J. P. Hohimer, and R. M. Biefeld, *Appl. Phys. Lett.*, vol. 47, p. 552, 1985.
[4] M. D. Camras *et al.*, *J. Appl. Phys.*, vol. 54, p. 6183, 1983.
[5] W. D. Laidig, P. J. Caldwell, Y. F. Lin, and C. K. Peng, *Appl. Phys. Lett.*, vol. 44, p. 653, 1984.
[6] W. D. Laidig, Y. F. Lin, and P. J. Caldwell, *J. Appl. Phys.*, vol. 57, p. 33, 1985.
[7] S. M. Bedair, T. Katsuyama, M. Timmons, and M. A. Tischler, *IEEE Electron Device Lett.*, vol. EDL-5, p. 45, 1984.
[8] S. M. Bedair, T. Katsuyama, P. K. Chiang, N. A. El-Masry, M. A. Tischler, and M. Timmons, *J. Cryst. Growth*, vol. 68, p. 477, 1984.
[9] L. R. Dawson *et al.*, *J. Vac. Sci. Technol.*, vol. B2, p. 179, 1984.
[10] G. E. Bulman, T. E. Zipperian, and L. R. Dawson, *Appl. Phys. Lett.*, vol. 49, p. 212, 1986.
[11] G. E. Bulman, D. R. Myers, T. E. Zipperian, and L. R. Dawson, *Appl. Phys. Lett.*, vol. 48, p. 1015, 1986.
[12] R. M. Biefeld, *J. Electron. Mater.*, vol. 15, p. 193, 1986.
[13] J. J. Rosenberg, M. Benlamri, P. D. Kirchner, J. M. Woodull, and G. D. Pettit, *IEEE Electron Device Lett.*, vol. EDL-6, p. 491, 1985.
[14] J. M. Matthews and A. E. Blakelee, *J. Cyst. Growth*, vol. 27, p. 118, 1974.
[15] M. A. Tischler, T. Katsuyama, N. A. El-Masry, and S. M. Bedair, *Appl. Phys. Lett.*, vol. 46, p. 294, 1985.
[16] T. Katsuyama, M. A. Tischler, D. J. Moore, N. Hamaguchi, N. A. El-Masry, and S. M. Bedair, to be published in *Solar Cell*.

Growth and characterization of InGaAs/GaAsP strained layer superlattices

T. Katsuyama and S. M. Bedair
Department of Electrical and Computer Engineering, North Carolina State University, Raleigh, North Carolina 27695-7911

N. C. Giles, R. P. Burns, and J. F. Schetzina
Department of Physics, North Carolina State University, Raleigh, North Carolina 27695-8202

(Received 20 October 1986; accepted for publication 24 February 1987)

InGaAs/GaAsP strained layer superlattices have been grown by metalorganic chemical vapor deposition on (100) GaAs at 630 °C. The superlattices consist of 5–45 periods of alternate InGaAs and GaAsP layers with equal and opposite lattice mismatch up to 1.1% with respect to the GaAs substrate. Thus, their lattice constant as a whole will be matched to that of GaAs. Cross-sectional transmission electron microscopy and x-ray diffraction measurements indicate that the superlattices have high structural quality with no misfit dislocations at the interface between the superlattice and the substrate. A very intense and sharp photoluminescence spectrum (linewidth = 4 meV) at 4.5 K suggests that the interface abruptness is less than two monolayers. Photoluminescence measurements along the beveled surface of the superlattice also indicate a high optical quality within the superlattice as well as at the superlattice/substrate interface.

I. INTRODUCTION

Semiconductor superlattices (SL) have been developed recently and have provided both fundamental and technical interest. Their properties, in principle, can be tailored by a proper choice of the materials and geometrical parameters. Most of the superlattice structures widely investigated are usually grown using lattice matched material systems such as GaAs/AlGaAs. However, superlattices can also be grown from lattice mismatched material systems which offer more degrees of freedom.[1] In such a structure the lattice mismatch between the two compounds is accommodated by elastic strain rather than by misfit dislocations at the interface as long as the thickness of each layer is less than a strain-dependent critical thickness.[2,3] The first strained layer superlattices (SLSs) were grown by vapor phase epitaxy using the GaAsP/GaAs system.[4] Recent developments of crystal growth techniques, such as molecular-beam epitaxy (MBE) and metalorganic chemical vapor deposition (MOCVD), allow the growth of high quality SLSs such as InGaAs/GaAs and GaAsP/GaP.[5–8] Although these SLSs show flexibility in device designs and have good optical and electrical properties, their average lattice constants are usually different from those of their substrates. Therefore, the total thickness of the SLS must be below a certain critical value, or a buffer layer whose lattice constant is equal to the average lattice constant of the SLS is required to avoid the generation of misfit dislocations at the interface between the substrate and the SLS. This requirement restricts the use of SLSs as a part of a device structure. Several material systems can be thought of to overcome this limitation, allowing the SLS as a whole to be lattice matched to a given substrate. Examples are InGaAs/GaAsP, GaAsP/GaAsSb, and GaAsP/InGaAsSb on GaAs substrate[9] and GaAs/InAs,[10] AlInAs/InGaAs,[11,12] and $In_xGa_{1-x}As/In_yGa_{1-y}As$[13] on InP substrate.

We have recently demonstrated several potential applications of $In_xGa_{1-x}As/GaAs_{1-y}P_y$ SLSs grown on GaAs substrates, such as light emitting diodes (LEDs),[14] defect reduction,[15] and solar cells.[16] In this structure, with $y = 2x$ and equal layer thickness, the InGaAs layers will be under biaxial compression, whereas the GaAsP layers will be under biaxial tension and the average lattice constant of the SLS will be equal to that of the GaAs substrate. The uniqueness of this SLS is that it allows the use of GaAs and AlGaAs for a device structure without the formation of a high density of misfit dislocations at the heterointerface. They may also provide enhanced carrier collection due to strain,[17] as well as a larger band-gap discontinuity. In this paper, we report the growth and characterization of InGaAs/GaAsP SLSs grown by MOCVD on (100) GaAs substrates. Structural and optical quality as well as interface quality of the heterojunction was examined by x-ray diffraction, transmission electron microscopy (TEM), optical microscopy, and photoluminescence.

II. MOCVD GROWTH OF InGaAs/GaAsP SLS

The InGaAs/GaAsP SLSs were grown by MOCVD at atmospheric pressure in a vertical reactor. Trimethylgallium (TMG) kept at 0 °C and triethylindium (TEI) kept at 20 °C were used as sources for Ga and In, respectively. AsH_3 and PH_3, both 5% in H_2, were used as As and P sources. Palladium diffused H_2 flowing at a rate of 3.6 l/min served as a carrier gas. The growth temperature was 630 °C, which is a compromise between ideal growth temperature for the two ternary alloys. For GaAsP, a relatively high growth temperature is required to obtain a wide range of GaP composition because phosphorous incorporation is low at low temperature.[18] This is explained by the low PH_3/AsH_3 pyrolysis ratio at low growth temperature. On the other hand, for InGaAs, a lower growth temperature is preferable, because InAs incorporation decreases as the growth temperature increases. A relatively low growth rate ranging from 100–150

 0021-8979/87/140498-05$02.40

TABLE I. Typical growth conditions for several $In_xGa_{1-x}As/GaAs_{1-y}P_y$ SLSs.

Run	Gas phase composition (μmol/min)				Solid composition (%)		Thickness of period (Å)	Number of period	Misfit with respect to GaAs (%)
	TMG	TEI	AsH_3	PH_3	x	y			
227	12.3	8.8	81	81	11	20	230	45	± 0.79
239	12.3	13.1	81	122	15	30	130	5	± 1.08

Å/min was used for both ternaries to minimize the gas transition effect and to obtain better control of the layer thickness. The substrates were (100) GaAs oriented 2° toward the ⟨110⟩ direction. They were prepared by a standard solvent cleaning and etching in a H_2SO_4:H_2O:H_2O_2 (7:1:1) solution for 5 min. A series of calibration runs were made to determine compositions and layer thicknesses which will give a equal and opposite lattice mismatch with respect to the GaAs substrate.

The SLSs were grown on top of a thin ($\sim 0.2\,\mu$m) GaAs buffer layer grown at 630 °C. The growth of the first InGaAs layer was initiated by turning on the TEI flow. After a period of time giving a desired thickness of InGaAs, the TEI was turned off and the PH_3 was immediately turned on. Then the PH_3 was turned off after a certain period of time, giving a GaAsP layer of the same thickness as the InGaAs layer, and the TEI was immediately turned back on. In other words, TEI and PH_3 were alternately injected into the growth chamber during the growth of GaAs. This gas switching procedure was controlled by a computer and continued until a desired superlattice thickness was obtained. Individual superlattice layers of different thicknesses and compositions were grown by keeping the flow rate of TMG and AsH_3 constant and changing the growth time and flow rate of TEI and PH_3. Table I shows typical growth conditions for several $In_xGa_{1-x}As/GaAs_{1-y}P_y$ SLSs. The solid compositions of each ternary layer were determined by photoluminescence and x-ray diffraction of bulk epitaxial layers (thickness $>0.5\,\mu$m) applying Vegard's law. The superlattice thicknesses were measured by optical microscope x-ray diffraction, and cross-sectional TEM.

III. CHARACTERIZATION

A. Structural properties

$In_xGa_{1-x}As/GaAs_{1-y}P_y$ SLSs have been grown with compositions of $0.05 < x < 0.15$ and $0.1 < y < 0.3$ and periods ranging from 130 to 400 Å. Figures 1(a) and 1(b) show Nomarski interference contrast micrographs of InGaAs/GaAsP SLSs. The total thickness of each SLS is about 1 μm. The SLS shown in Fig. 1(a) was grown under the lattice matched condition $y = 2x$ with equal layer thickness ($x = 0.1$). For this value ($x = 0.1$), the critical thickness below which the strain is relieved elastically is about 200 Å.[2] A mirrorlike surface indicates that the SLS is closely lattice matched to the GaAs substrate. However, the SLS shown in Fig. 1(b) ($x = 0.16$, $y = 0.17$) has slight crosshatching which is an indication of dislocation networks. This suggests that the average lattice constant of the SLS is not matched to the GaAs substrate. This feature is also frequently seen in other SLSs, such as InGaAs/GaAs[19] and GaAsP/GaAs, when the total thickness of the SLS exceeds a strain-dependent critical value that corresponds to the average composition of the SLSs.

Cross-sectional samples for the TEM were prepared by lapping and ion milling two pieces bonded together face to face. Figure 2 shows a bright-field TEM image of a 25-period SLS. InGaAs layers appear as dark bands while GaAsP layers appear as bright bands. The image shows a periodic layered structure with equal and uniform thickness for the two ternary alloys and no misfit dislocations at the SLS/substrate interface. The period of the superlattice in Fig. 2 is

(a)

(b)

FIG. 1. Nomarski interference contrast micrographs of the SLSs. (a) A mirrorlike surface indicates that the SLS is closely lattice matched to the GaAs substrate. (b) Slight crosshatching feature indicates misfit dislocations at the SLS/substrate interface.

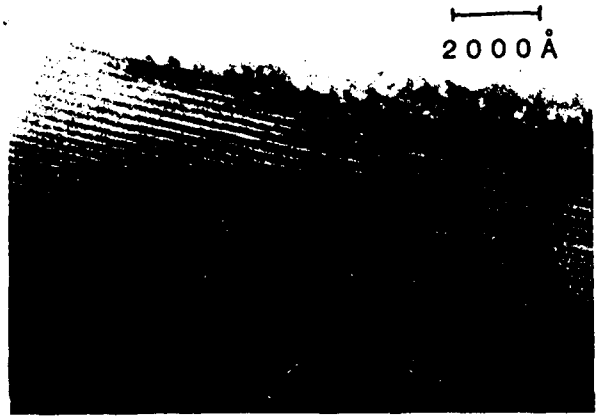

FIG. 2. Cross-sectional TEM image (bright field). Coherently strained and dislocation-free layered structures (200-Å period) have been observed.

about 200 Å, which is consistent with the growth rate calibration of the bulk ternary layers.

A conventional x-ray double diffraction measurement has been done using GaAs as a first crystal and Cu$K\alpha_1$ radiation as an x-ray source. Figure 3 shows the x-ray diffraction pattern of a 40-period $In_{0.1}Ga_{0.9}As/GaAs_{0.8}P_{0.2}$ SLS in the vicinity of the (004) reflection. The diffraction pattern consists of the (004) GaAs substrate reflection peak and several weaker satellite peaks due to the periodicity of the SLS. The number shown above each peak is the order of the satellite. The peak linewidths (FWHM) are in the range 30–70 arcsec, indicating a highly uniform layered structure. The average lattice mismatch of the SLS to the GaAs substrate can be calculated from the angular separation between the substrate peak and zero order peak ($n = 0$). Also, the thickness of each period can be deduced from the separation of the satellite peaks. The sample shown in Fig. 3 has a 0.187% average lattice mismatch and a 222-Å period. The thickness measurement by x-ray diffraction was in good agreement with results from TEM, optical microscope, and growth rate calibration.

B. Optical properties

The optical properties and interface quality of InGaAs/GaAsP SLSs were characterized by photoluminescence (PL). PL measurement was carried out at 77 and 4.5 K with an ordinary grating monochromater and S1 photomultiplier. An Ar-ion laser beam (5145 Å) was focused on a sample with a spot size of 100 μm. The excitation power density was about 500 W/cm^2. Figure 4 shows the PL spectra for a 5-period $In_{0.15}Ga_{0.85}As/GaAs_{0.7}P_{0.3}$ SLS (1 period = 130 Å) at 77 and 4.5 K. A very intense and sharp peak located at 1.405 eV with a full width at half maximum (FWHM) of 4 meV has been observed at 4.5 K. To the best of our knowledge, this is the narrowest value ever observed in any ternary-ternary SLS structures and indicates a very sharp interface and the high optical quality of the grown layers. There are several factors that affect the PL linewidths of the InGaAs/GaAsP SLSs. These factors include (1) periodicity fluctuation of the SLS, (2) interface roughness (i.e., the height and size of islands), and (3) band-gap fluctuation due to a random variation of the composition of InGaAs and GaAsP. Recently, several experimental results of quantum-well structures (AlGaAs/GaAs,[20] AlInAs/InGaAs[21,22]), as well as theoretical studies[23] of PL linewidth, have been reported. Based on reported data and analyses, we estimate that the interface roughness of our sample is less than two monolayers. The peak energy variation across the sample (~ 1.5 cm) is about 2 meV, suggesting excellent uniformity of composition and layer thickness. The peak energy 1.405 eV corresponds to the transition between the first electron ($n = 1$) and heavy-hole band. The biaxial compression in the InGaAs well breaks the degeneracy of light-hole and heavy-hole valence band at $k = 0$ and increases the effective band gap of InGaAs. In addition, the quantum size effect increases the effective band gap of the SLS. These two effects result in the energy shift of about 110 meV from the bulk InGaAs value.

The optical quality of the SLSs versus depth, especially near the SLS/substrate interface, was investigated using PL. This was done by scanning the laser beam along a beveled section of the layers. Several samples were beveled on a Plexiglas plate using Ludox. The bevel angle was about 1/3 degrees, which resulted in a vertical magnification factor of

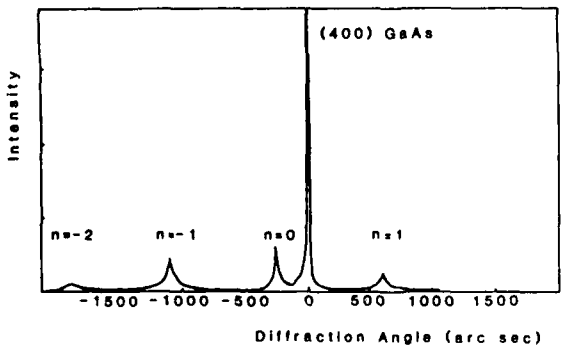

FIG. 3. X-ray diffraction pattern (400) of $In_{0.1}Ga_{0.9}As/GaAs_{0.8}P_{0.2}$ SLS. The number shown for each peak is the order of the satellite peaks.

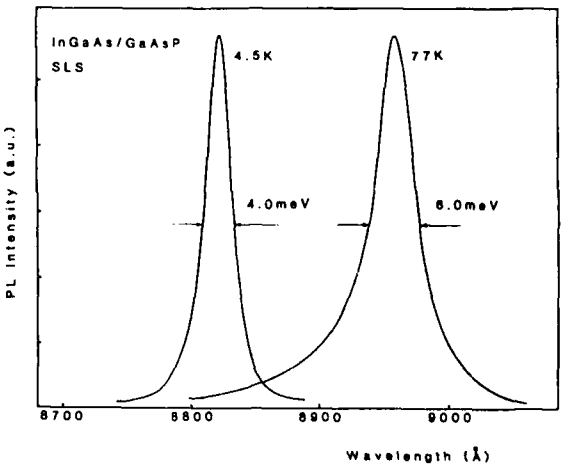

FIG. 4. PL spectra of 5-period $In_{0.15}Ga_{0.85}As/GaAs_{0.7}P_{0.3}$ SLS at 77 and 4.5 K. A very narrow peak (FWHM = 4 meV) indicates the excellent interface quality (less than two monolayers).

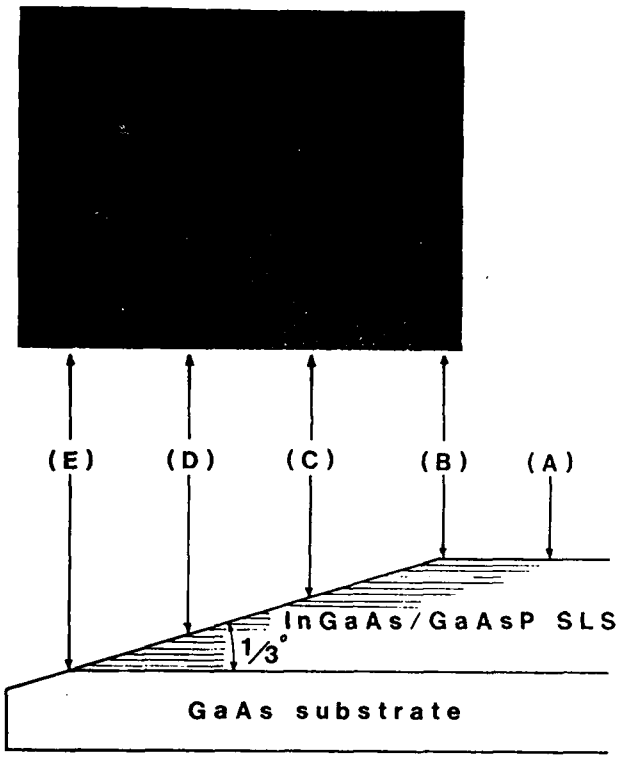

(a)

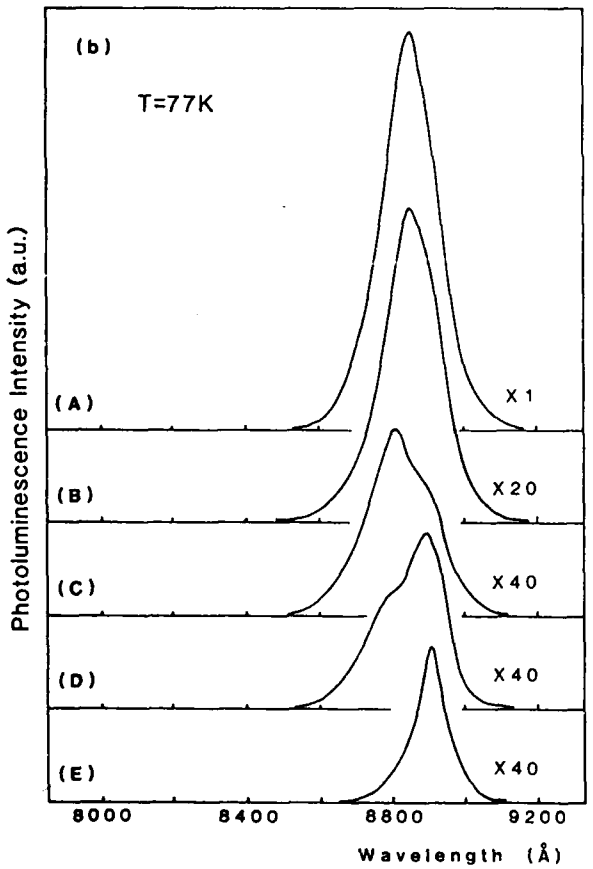

FIG. 5. (a) Optical micrograph of beveled surface and a schematic of the sample in cross section. The bevel angle is about 1/3 degrees, which results in a vertical magnification factor of 172×. (b) PL spectra (77 K) along the beveled surface. Spectra (A)–(E) correspond to the position shown in part (a). The variation of PL spectrum is probably due to compositional and periodicity fluctuations of the SLS.

172×. Figure 5(a) shows an optical micrograph of the beveled surface of an InGaAs/GaAsP SLS with 45 periods and a schematic of the sample in cross section. The wider separations of layers near the surface are due to a rounded edge from polishing. The laser spot size was about 50 μm and the penetration depth is estimated to be less than 2000 Å based on GaAs absorption data. Figure 5(b) shows the PL spectra (77 K) of different spots (A–E) which correspond to the position shown in Fig. 5(a). As the laser beam was moved from position (A) to (B), the PL intensity decreased by more than one order of magnitude. This is because of mechanical damage introduced by polishing. However, the spectral shape did not change. From (B) to (D), the intensity still decreased gradually, while the spectral peak shifted slightly toward the higher-energy side and a shoulder appeared at the lower-energy side. As the beam approached the SLS/substrate interface, the shoulder grew, while the main peak decreased and finally disappeared. As is shown in Fig. 5(b), there are some variations ($\sim$10 meV) in the peak emission spectrum from the SLS. These fluctuations can be the result of compositional and periodicity fluctuation in the SLS. The variation of 10 meV corresponds to the compositional fluctuation of about 6.8% in the InGaAs well assuming no periodicity fluctuation. At the interface (E), the PL linewidth became 9 meV, whereas the PL intensity stayed almost the same as that of position (D). PL from the Si-doped GaAs substrate was very weak and almost undetectable, even at the position (E). This suggests that the photocarriers generated in the GaAs layer will be efficiently collected in the first SLS layer which is InGaAs. Most of the samples showed a tendency for the PL linewidth (FWHM) to decrease or remain unchanged as the SLS/substrate interface was approached. This feature is different from other SLSs whose average lattice constants are not matched to those of their substrates.[24] We have done a similar experiment on InGaAs/GaAs SLSs, which have similar geometrical and compositional parameters to those of InGaAs/GaAsP SLSs. A significant decrease of PL intensity and spectral line broadening near the SLS/substrate interface was observed. This is probably due to a high density of misfit dislocations at the SLS/substrate interface. This result indicates that the average lattice constant of the SLS must be matched to that of the substrate to obtain a high optical quality throughout the entire layer. This is very important, especially when SLSs are used in the active regions of devices.

IV. CONCLUSION

Metalorganic chemical vapor deposition has been used for the growth of InGaAs/GaAsP strained layer superlattices (SLSs). The SLSs consist of alternate InGaAs and GaAsP layers with equal and opposite lattice mismatch up to 1.1% with respect to the GaAs substrate. Thus, the average lattice constant of the SLSs was closely matched to that of GaAs. The structural quality was examined by a combination of x-ray diffraction, TEM, and optical microscopy. These results showed coherently strained and dislocation free layered structures. Optical quality was evaluated by conventional PL measurement. A very intense and sharp

spectrum (FWHM = 4 meV) at 4.5 K indicates the excellent interface quality (less than two monolayers). In addition, PL spectra at different depths in the SLS suggest a high optical quality throughout the entire layer as well as at the SLS/substrate interface. This SLS structure can be used with GaAs and AlGaAs without the formation of a high density of misfit dislocations at the heterointerface, thus having a great potential for the application of a variety of novel device structures.

ACKNOWLEDGMENTS

This work has been supported by The National Science Foundation, The Air Force Office of Scientific Research, and The Solar Energy Research Institute.

[1]G. C. Osbourn, J. Appl. Phys. **53**, 1586 (1982).
[2]J. W. Matthews and A. E. Blakelee, J. Cryst. Growth **27**, 118 (1974)
[3]J. W. Matthews and A. E. Blakeslee, J. Cryst. Growth **32**, 265 (1976).
[4]A. E. Blakeslee, J. Electrochem. Soc. **118**, 1459 (1971).
[5]M. Quillec, L. Goldstein, G. Le Roux, J. Burgeat, and J. Primot, J. Appl. Phys. **55**, 2904 (1984)
[6]W. D. Laidig, J. W. Lee, P. K. Chiang, L. Simpson, and S. M. Bedair, J. Appl. Phys. **54**, 5382 (1983).
[7]R. M. Biefeld, G. C. Osbourn, P. L. Gourley, and I. J. Fritz, J. Electron. Mater. **12**, 903 (1983).
[8]R. M. Biefeld, J. Electron. Mater. **15**, 193 (1986).
[9]S. M. Bedair, T. Katsuyama, P. K. Chiang, N. A. El-Masry, M. A. Tischler, and M. Timmons, J. Cryst. Growth **68**, 477 (1984).
[10]T. Fukui and H. Saito, Jpn. J. Appl. Phys. **24**, L521 (1984).
[11]J. M. Kuo, B. Lalevic, A. Ourmard, T. Y. Chang, J. L. Zyskind, and J. W. Solhoff, *Semiconductor-Based Heterostructure; Interfacial Structure and Stability*, Proceedings of the 1986 Northeast Regional Meeting, edited by M. L. Green (Metallurgical Society, Warrendal, PA, 1986), p. 175.
[12]K. Nishi, K. Hirose, and T. Mizutani, Appl. Phys. Lett. **49**, 749 (1986).
[13]M. Quillec, J. Y. Marzin, J. Primot, G. Le Roux, J. L. Benchimol, and J. Burgeat, J. Appl. Phys. **59**, 2447 (1986).
[14]S. M. Bedair, T. Katsuyama, M. Timmons, and M. A. Tischler, IEEE Electron Lett. **EDL-5**, 45 (1984).
[15]M. A. Tischler, T. Katsuyama, N. A. El-Masry, and S. M. Bedair, Appl. Phys. Lett. **46**, 294 (1985).
[16]T. Katsuyama, M. A. Tischler, D. J. Moore, N, Hamaguchi, N. A. El-Masry, and S. M. Bedair (to be published).
[17]N. G. Anderson, Y. C. Lo, and R. M. Kolbas, Appl. Phys. Lett. **49**, 758 (1986).
[18]G. B. Stringfellow, J. Cryst. Growth **62**, 225 (1983).
[19]S. M. Bedair, T. P. Humphreys, N. A. El-Masry, Y. Lo, N. Hamaguchi, C. D. Lamp, A. A. Tuttle, D. L. Dreifus, and P. Russell, Appl. Phys. Lett. **49**, 942 (1986).
[20]D. C. Reynolds, K. K. Bajaj, C. W. Litton, P. K. Yu, J. Singh, T. Masselik, R. Fischer, and H. Morkoc, Appl. Phys. Lett. **46**, 51 (1985).
[21]D. F. Welch, G. W. Wicks, and L. F. Eastman, Appl. Phys. Lett. **46**, 991 (1985).
[22]F. Y. Juang, P. K. Bhattacharya, and J. Singh, Appl. Phys. Lett. **48**, 290 (1986).
[23]J. Singh, K. K. Bajaj, and S. Chaudhuri, Appl. Phys. Lett. **44**, 805 (1984).
[24]N. G. Anderson, W. D. Laidig, and Y. F. Lin, J. Electron. Mater. **14**, 187 (1985).

Molecular stream epitaxy of ultrathin InGaAs/GaAsP superlattices

T. Katsuyama, M. A. Tischler, N. H. Karam, N. El-Masry, and S. M. Bedair
North Carolina State University, Department of Electrical and Computer Engineering, Raleigh, North Carolina 27695-7911

(Received 26 May 1987; accepted for publication 18 June 1987)

Molecular stream epitaxy allows several molecular beam epitaxy (MBE) concepts to take place in a metalorganic chemical vapor deposition reactor. In this technique, the growth of InGaAs/GaAsP superlattices proceeds by rotating the substrate between two gas streams, one containing trimethylgallium (TMG), triethylindium, and AsH_3 and the other containing TMG, PH_3, and AsH_3. This technique eliminates gas flow transients and provides a method to mechanically shear off the gaseous boundary layer between successive exposures. Ultrathin strained-layer superlattices (SLS's) with 8-Å-thick films have been obtained. The optical properties of these SLS's are comparable to those obtained for equivalent superlattices by gas source MBE.

Molecular beam epitaxy (MBE) and metalorganic chemical vapor deposition (MOCVD) have been established as two major deposition techniques for the growth of semiconductor thin films. Each technique has its own limitations and advantages. Recently, several efforts have been directed to combine the advantages of both techniques. Examples are the recent impressive results obtained by gas source MBE (GSMBE)[1] and chemical beam epitaxy (CBE).[2] These efforts have been based on modifying the MBE growth chamber to allow the use of organometallic and hydride sources. On the other hand, a multichamber MOCVD system has improved interface quality.[3] We report here a new technique based on modifying the nature of the MOCVD deposition process to take advantages of MBE growth concepts. The MBE process allows direct incidence of atoms or molecules in a direct line of sight onto a heated substrate surface. Also there is no diffusion boundary layer through which the reactant species have to diffuse to reach the substrate surface. Moreover, the initiation and the termination of the growth process occur by opening and closing shutters that result in extremely abrupt interfaces. Molecular stream epitaxy (MSE)[4] allows the incorporation of these MBE concepts in a MOCVD reactor.

Figure 1 shows a schematic of the growth chamber and susceptor designed to allow some of the MBE features to be utilized during the MOCVD growth process. The system has been tested for the growth of InGaAs/GaAsP strained-layer superlattices (SLS's). Trimethylgallium (TMG), triethylindium (TEI), and AsH_3 are continuously flowing through tube A for the growth of the InGaAs film, whereas TMG, AsH_3, and PH_3 are continuously flowing through tube B for the growth of GaAsP films. The rf-heated susceptor consists of several parts. The fixed part F has two windows, facing the inlet tubes A and B. The substrate sits in a recess in the rotating part R of the susceptor. This part of the susceptor is driven by a computer-controlled stepping motor. Gases from the input tubes A and B flow unimpeded through the susceptor except when the substrate cuts through the gas streams. The fixed top part of the susceptor also acts to shear off most of the gaseous boundary layer between successive exposures. The clearance between the surface of the substrate and the top piece of the susceptor is several mils to avoid scratching of the substrate while minimizing the dead volume.

The growth process for the SLS proceeds as follows: The substrate is rotated to face tube A for a given time to grow an InGaAs film of a desired thickness. The substrate is then rotated away from this gas stream and simultaneously shears off any residual gas film that contains TMG and TEI. This will allow the sudden termination of the InGaAs growth. This action simulates the closing of In and Ga shutters in the MBE process. The substrate is now rotated to face tube B, thus cutting into the TMG, AsH_3, and PH_3 stream. Since the diffusion boundary layer is almost absent, the growth of GaAsP starts suddenly when the substrate is in the line of sight of this second stream, initiating an abrupt interface.

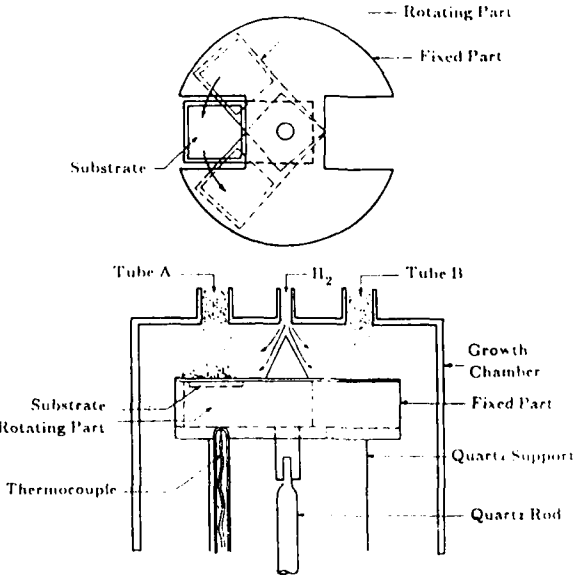

FIG. 1. Schematic of the growth chamber and susceptor of molecular stream epitaxy (MSE). The gaseous boundary layer above the substrate is sheared off mechanically between successive exposures.

 0003-6951/87/330529-03$01.00

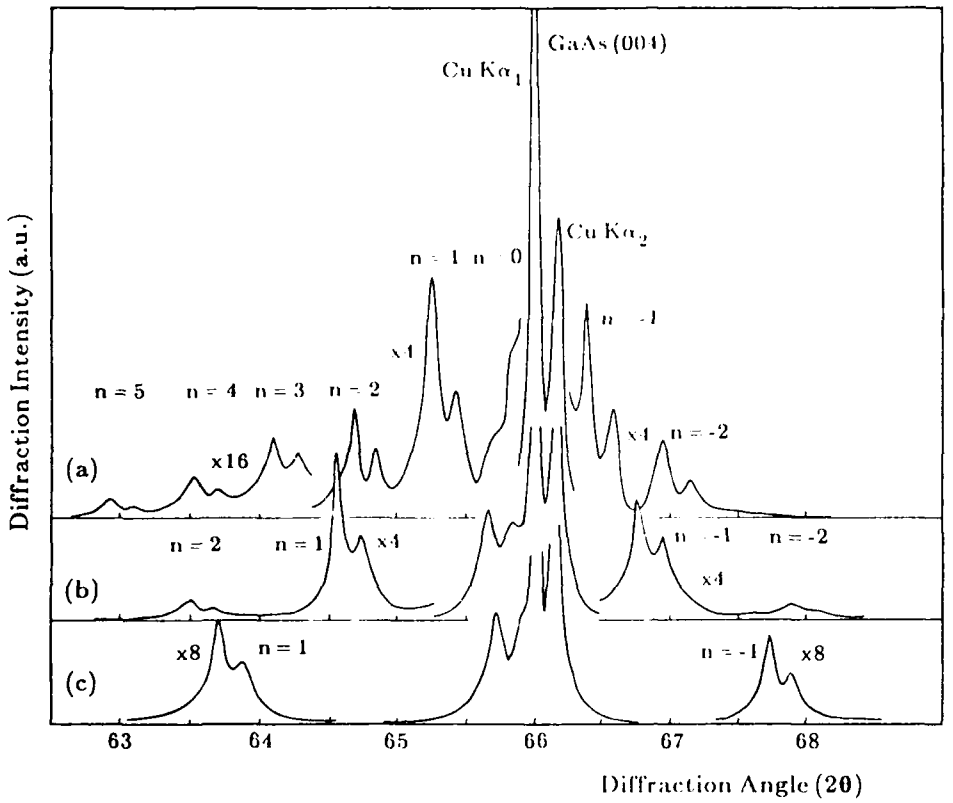

FIG. 2. Series of x-ray diffraction patterns of the strained-layer superlattices (SLS's) in the vicinity of the (004) reflection. Numbers shown above each peak are the order of the satellite peaks. (a) 183 Å period (10.3 s exposure); (b) 96 Å period (5.3 s exposure); (c) 52 Å period (2.8 s exposure).

This action will simulate the opening of shutters which initiates the MBE growth process. It should also be mentioned that the growth of this SLS is taking place without any switching of gases as in the conventional MOCVD process. Thus, problems such as dead volume and flow transients are avoided. Also, since the flow of gas streams is unimpeded most of the time, buoyancy effects can be reduced. The very initial stage of growth in MSE takes place with the near absence of diffusion and thermal boundary layers, thus assuring interface abruptness. When the growth proceeds for more than a second or so, this boundary layer will develop and will control the deposition mechanism of layers beyond the first few monolayers. The development of this diffusion boundary layer will not interfere with the generation of abrupt interfaces in MSE. It should also be mentioned that there is a finite volume of trapped gas, a few mils thick, that is present during the process of rotating the substrate between the two streams. The amount of TMG trapped in this volume will allow an additional growth of less than one hundredth of a monolayer of the ternary alloy to take place before the exposure to the second stream. It might also be possible that some minor cross contamination from the PH_3 side will take place, for example, during the deposition of InGaAs film. However, a graphite wedge in conjunction with large H_2 flow from the center tube helps in preventing this cross-diffusion effect.

$In_xGa_{1-x}As/GaAs_{1-y}P_y$ SLS's were grown by MSE on Cr-doped (100)GaAs substrates at 630 °C in a vertical MOCVD system operating at atmospheric pressure. The exposure time to each gas stream varied from 0.5 to 10.3 s. Equal exposure times were allowed for the two gas streams. The transition time from one stream to the other is about 1.5 s. The amount of the cross diffusion was estimated by growing GaAs at one side while flowing PH_3 at the other side. The results indicate that approximately 2% of a total flow of PH_3 will be incorporated with GaAs (or cross diffused). The mole fraction of TEI and PH_3 was adjusted to allow the growth of SLS with $x = 12\%$ and $y = 23\%$. These values of x and y allow the SLS to be grown with an average lattice constant that is closely lattice matched to the GaAs substrate.

Figure 2 shows the x-ray diffraction patterns obtained from the $In_{0.12}Ga_{0.87}As/GaAs_{0.77}P_{0.23}$ SLS's using Cu $K\alpha$ radiation. The period of these SLS's obtained for different exposure times was deduced from the separation of the satellite peaks shown in Fig. 2 and the results are summarized in Table I. Although not shown in Fig. 2, sample *d*, which was grown for an exposure time of 1.3 s, showed weak and broad x-ray satellite peaks whose separation corresponds to a 25-Å period. For sample *e* the exposure time was reduced to 0.5 s. However, we were not able to determine the period from the separation of the satellite peaks probably due to limitations

TABLE I. Growth conditions and structures of SLS's.

Run	Exposure time (s)	Number of periods	Period (Å)
a	10.3	30	183
b	5.3	120	96
c	2.8	200	52
d	1.3	400	25
e	0.5	800	16

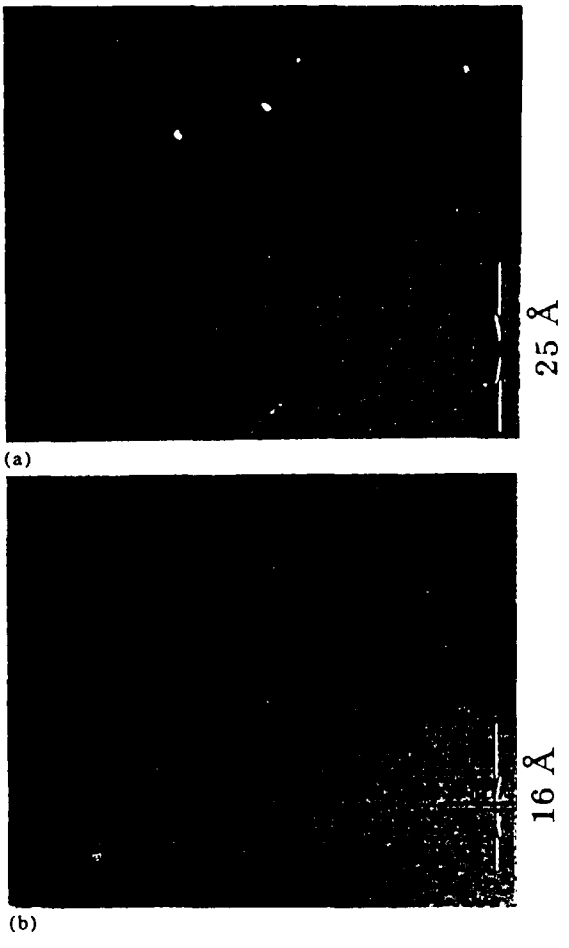

FIG. 3. High-resolution transmission electron microscope images of the MSE grown ultrathin InGaAs/GaAsP SLS's. (a) 25 Å period (1.3 s exposure); (b) 16 Å period (0.5 s exposure).

of our x-ray diffraction setup.

The high-resolution transmission electron microscope (TEM) technique was used to characterize these ultrathin SLS's. Figures 3(a) and 3(b) show cross-section TEM images of samples *d* and *e*, respectively. For exposure times of 1.3 and 0.5 s the SLS's are made of layers 13 and 8 Å thick, respectively. These SLS's were also characterized by photoluminescence (PL) measurements performed at 77 K using an Ar-ion laser. The PL results are shown in Fig. 4. As the well width (InGaAs layer thickness) was decreased, the PL peaks shifted toward the higher energy side due to the quantum size effect. The full width at half-maximum (FWHM) of the PL spectra ranged from 12 to 16 meV as shown in Fig. 4.

The above results obtained by x-ray diffraction, TEM, and PL show that MSE can be a very useful technique for the synthesis of ultrathin films with excellent optical and structural properties. Moreover, the layer thickness can be controlled precisely by changing exposure times. The InGaAs/GaAsP SLS was chosen to test the potential of this new deposition technique for two reasons. First, this SLS has several applications in optical devices such as light-emitting diodes[5,6] and as buffer layers for the reduction of defects in epitaxial GaAs films.[7] The second reason is to test the MSE

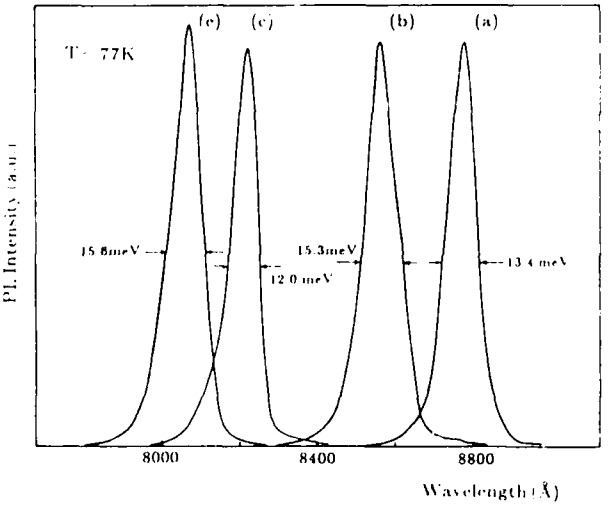

FIG. 4. Photoluminescence spectra of the SLS's at 77 K. Single sharp peaks corresponding to the transition between the first electron ($n = 1$) and heavy-hole band have been observed.

approach in the growth of SLS's that contain both As and P, which are difficult structures to synthesize with abrupt interfaces.[8] The 8-Å InGaAs well and GaAsP barrier shown in Fig. 3(b), demonstrated the ability of MSE to grow ultrathin films without gas switching. To the best of our knowledge, this is one of the thinnest films ever synthesized in a superlattice with alternating layers having As and P compounds.[9] Also the PL data showed that SLS's grown by MSE have comparable optical properties to those obtained by GSMBE[1] and CBE.[10] For example, the FWHM of InGaAs/GaAsP SLS at 77 K is about the same as that obtained by GSMBE at 6 K for InGaAsP/InP superlattice structure with 80-Å wells.[1] Also the 8-Å InGaAs quantum well in the InGaAs/GaAsP SLS has comparable PL properties to that obtained by CBE and low pressure MOCVD[9] at 2 K for an InP-InGaAs single quantum well.

In conclusion, MSE is a potential technique that allows some of the MBE growth features to take place during the MOCVD growth process. This has resulted in structures with abrupt interfaces that are comparable to those obtained by GSMBE and CBE.

This work has been supported by The National Science Foundation and the Air Force Office of Scientific Research.

[1] H. Temkin, M. B. Panish, P. M. Petroff, K. A. Hamm, J. M. Vandenberg, and S. Sumski, Appl. Phys. Lett. **47**, 394 (1985).
[2] W. T. Tsang, Appl. Phys. Lett. **45**, 1234 (1984).
[3] J. R. Shealy, Appl. Phys. Lett. **48**, 925 (1986).
[4] T. Katsuyama, M. A. Tischler, T. P. Humphreys, and S. M. Bedair, Electronic Material Conference, June 1986, Amherst, MA.
[5] S. M. Bedair, T. Katsuyama, M. Timmons, and M. A. Tischler, IEEE Electron Device Lett. **EDL-5**, 45 (1984).
[6] T. Katsuyama, J. Y. Yang, and S. M. Bedair, IEEE Electron Device Lett. **EDL-8**, 240 (1987).
[7] M. A. Tischler, T. Katsuyama, N. El-Masry, and S. M. Bedair, Appl. Phys. Lett. **46**, 294 (1985).
[8] J. P. André, E. P. Menu, M. Erman, M. H. Meynadier, and T. Ngo, J. Electron. Mater. **15**, 71 (1986).
[9] M. Razeghi and J. P. Duchemin, J. Cryst. Growth **70**, 145 (1984).
[10] W. T. Tsang and E. F. Schubert, Appl. Phys. Lett. **49**, 220 (1986).

Effectiveness of strained-layer superlattices in reducing defects in GaAs epilayers grown on silicon substrates

N. El-Masry and J. C. L. Tarn
Material Science and Engineering Department, North Carolina State University, Raleigh, North Carolina 27695

T. P. Humphreys, N. Hamaguchi, N. H. Karam, and S. M. Bedair
Electrical and Computer Engineering Department, North Carolina State University, Raleigh, North Carolina 27695-7911

(Received 20 July 1987; accepted for publication 15 September 1987)

In GaAs-GaAsP strained-layer superlattices grown lattice matched to GaAs are effective buffer layers in reducing dislocations in epitaxial GaAs films grown on Si substrates. The strained-layer superlattice structure permits high values of strain to be employed without the strained-layer superlattice generating dislocations of its own. We find that the strained-layer superlattice buffer is extremely effective in blocking threading dislocations of low density and is less effective when the dislocation density is high. It appears that for a given strained-layer superlattice there is a finite capacity for blocking dislocations. Transmission electron microscopy has been used to investigate the role of the superlattice buffer layer.

The growth of GaAs on silicon substrates provides a convenient method of integrating III-V compound-based devices and silicon electronic circuits. However, as a result of the large lattice mismatch that exists between the two materials, a high density of defects ($\sim 10^8$–10^9 cm^{-2}) is present in the GaAs epilayer. Furthermore, it is evident that the presence of these defects restricts the widespread applications of the GaAs-Si heteroepitaxial technology. To date, several approaches have been successfully employed to reduce the density of dislocations. These methods inlcude the application of strained-layer superlattices (SLS's),[1,2] thermal annealing,[3] and rapid thermal annealing.[4] Indeed, several SLS structures based on the $In_xGa_{1-x}As$-$GaAs$[5] and $GaAs_{1-y}P_y$-$GaAs$[6] systems have been reported. Utilizing these SLS buffer layers a reduction in the dislocation density has been observed. However, despite these results, it is evident that the ternary-binary (GaAs) SLS system cannot be grown lattice matched to the GaAs substrate. Moreover, these SLS structures, which as a whole have a lattice constant that corresponds to the ternary material with composition of $x/2$ (or $y/2$), have several inherent shortcomings. In particular, the total thickness of the SLS must be less than the critical thickness h_c, in order to circumvent the generation of misfit dislocations at the GaAs epilayer interface.[7] Consequently, this will limit the number of periods and, therefore, the number of *strained* interfaces that are available to suppress the propagation of threading dislocations. It follows, therefore, that in order to alleviate these problems in the ternary-binary SLS system, we require a superlattice composed of two materials having equal, but opposite, lattice mismatches, such that the average lattice constant matches that of the GaAs substrate. An exceptional material candidate is an $In_xGa_{1-x}As$-$GaAs_{1-y}P_y$ ($y \simeq 2x$) SLS which can be grown lattice matched to GaAs. A further advantage of utilizing this particular SLS structure is that high values of strain can be accommodated without the SLS generating dislocations of its own. Moreover, we have previously reported that the ternary-ternary SLS buffer was very effective in blocking dislocations originating at the GaAs substrate.[8] Indeed, it was apparent that a very low density of threading dislocations in the GaAs epilayer was achieved.

In this letter we investigate the effectiveness of utilizing a highly strained $In_xGa_{1-x}As$-$GaAs_{1-y}P_y$ SLS in reducing the density of threading dislocations that propagate from the GaAs-Si interface. The GaAs on silicon samples used in this study were provided by the University of Illinois, Spire Corporation, and the Kopin Corporation. Samples have also been grown in our laboratory. The strained-layer superlattices and GaAs epitaxial layers were grown by metalorganic chemical vapor deposition (MOCVD) at North Carolina State University. Several $In_xGa_{1-x}As$-$GaAs_{1-y}P_y$ SLS structures with $y \simeq 2x$ have been investigated. A schematic diagram of the SLS structure is shown in Fig. 1. The corresponding values of x and y were varied in the ranges of 8–25% and 16–40%, respectively. Individual layer thicknesses were varied from 80 to 300 Å, depending on the ternary alloy

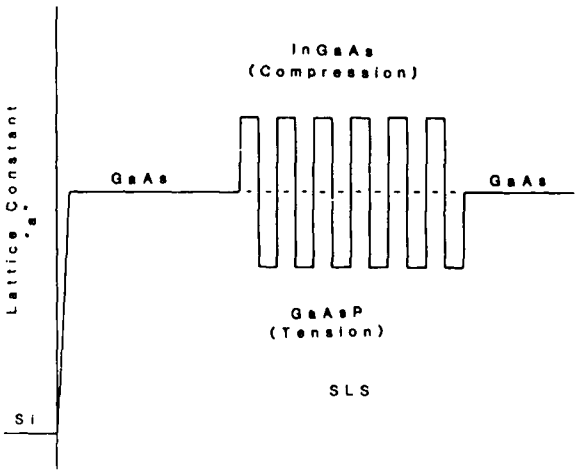

FIG. 1. Schematic diagram of the InGaAs-GaAsP strained-layer superlattice (SLS) structure.

 0003-6951/87/461608-03$01.00

FIG. 2. Cross-sectional bright-field image illustrating the effectiveness of the SLS in bending dislocations. Regions X and Y denote areas of low and high dislocation densities, respectively.

composition. The intrinsic strain was maintained in the 0–2% range. Transmission electron microscopy (TEM) samples for both cross-sectional and plan view were prepared by mechanical thinning followed by ion milling.

The effectiveness of utilizing the $In_xGa_{1-x}As$-$GaAs_{1-y}P_y$ SLS structure as a buffer layer is

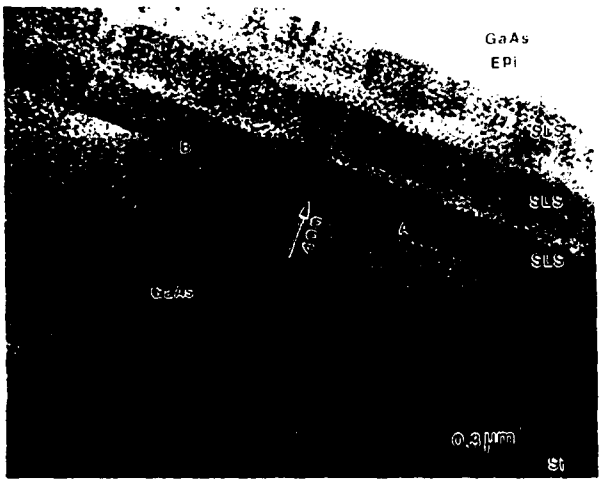

FIG. 3. Cross-sectional bright-field micrograph illustrating bending and the interaction of two dislocations, namely, A and B, along the interfacial planes of the SLS. A relatively low dislocation density has been achieved by rapid thermal annealing.

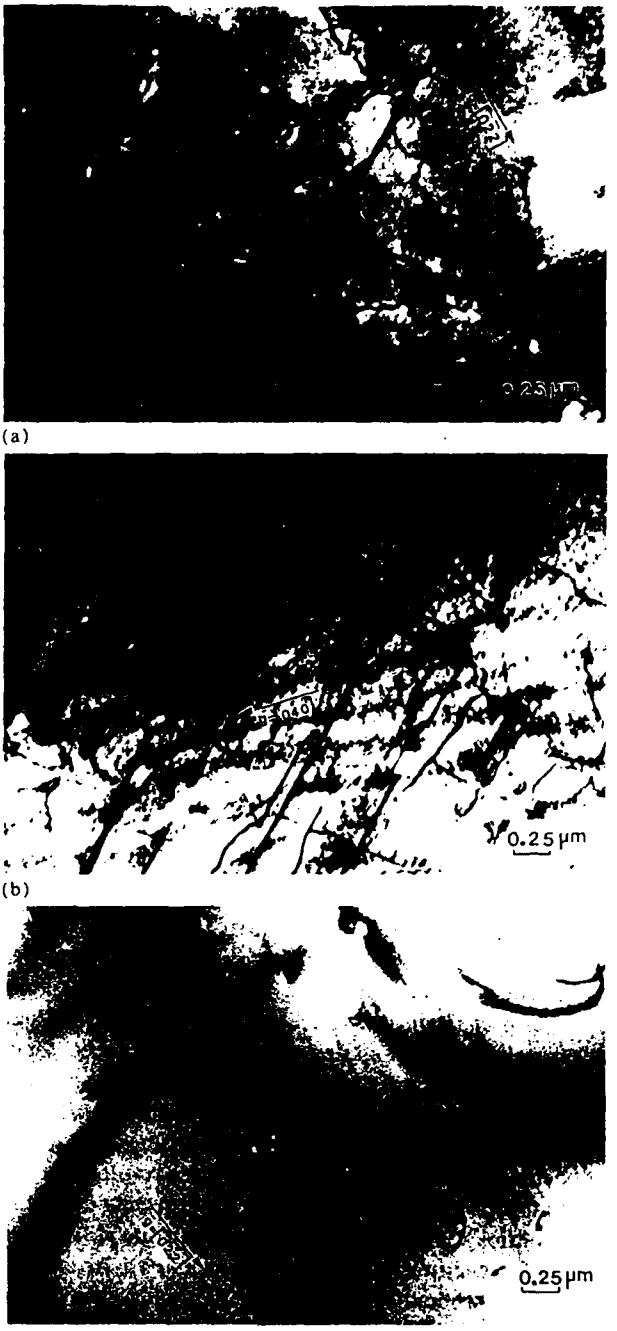

FIG. 4. [100] Plan-view transmission electron micrograph: (a) of as-grown GaAs/Si samples; (b) illustrating the bending and propagation of dislocations along the ⟨110⟩ directions within the InGaAs-GaAsP SLS; (c) epitaxial GaAs grown on top of the SLS.

shown in the bright-field micrograph of Fig. 2. In this image, regions denoted by X and Y are areas of low and high dislocation densities, respectively. It is clear that the impinging dislocations on the SLS in region X are confined by the strained field and bent along the SLS interface planes. Consequently, almost all the dislocations impinging on the SLS are blocked and do not thread to the GaAs top layer. Indeed, it is evident that the SLS is most effective in confining and bending the dislocations in the absence of a perturbing strain field generated by another dislocation. However, the interaction and a merger of a high density of dislocations in region

Y results in an upward threading of dislocations into the GaAs epilayer. Moreover, the higher the dislocation density, the greater the likelihood of dislocation-dislocation interactions and, consequently, the greater the probability that some of the dislocations will thread into the GaAs epilayer. Clearly, the SLS has only a finite capacity for bending the dislocations in the interfacial planes of the SLS.

It is apparent from the above results that in order for the SLS to be made more effective, the density of impinging threading dislocations on the SLS must be reduced. This reduction in dislocation density may be achieved by rapid thermal annealing the GaAs/Si samples at a temperature of 900 °C for 10 s prior to the growth of the SLS.[4] The effectiveness of the SLS in blocking dislocations in this low-density region is clearly shown in Fig. 3. Two dislocations labeled A and B on the micrograph are bent at the SLS buffer layer. In particular, dislocation A is bent at the second SLS period interface and proceeds undisturbed along this interfacial plane. However, when dislocation A encounters a strain field generated by dislocation B, which is confined at the first SLS interface, the propagation direction of A is changed. It is also possible that when the dislocations are in close proximity, one or more of the dislocations can thread into the GaAs epilayer.

Plan-view bright-field TEM has also been performed on nonannealed samples to assess the effectiveness of the SLS. Figure 4(a) shows a plan-view micrograph of the as-grown GaAs/Si interface prior to the growth of the SLS. The bending and propagation of dislocations along the ⟨110⟩ directions within this SLS are illustrated in Fig. 4(b). Also shown is the interaction between neighboring dislocations. In a plan-view TEM of the GaAs epilayer grown on top of the SLS, two distinct dislocation density regions are discernible. In an area of approximately $100\,\mu m^2$, no threading dislocations were observed. We believe that this area corresponds to region X in Fig. 2, where the SLS is highly effective in bending the dislocations. In contrast, we have also identified a region where the dislocation density is fairly high as shown in Fig. 4(c). This area may be compared to region Y in Fig. 2, where we have observed a small fraction of dislocations threading through the SLS.

In conclusion, it has been shown that the $In_xGa_{1-x}As$-$GaAs_{1-y}P_y$ ($y \simeq 2x$) is an appropriate and highly effective buffer layer for reducing dislocations originating at the GaAs-Si interface. The SLS structure also permits high values of strain to be employed without the SLS generating dislocations of its own. However, the present results also indicate that the effectiveness of the SLS depends on the density of dislocations. For instance, when the dislocation density is low, the threading dislocations are confined to the SLS interfaces and do not propagate into the GaAs epilayer. In contrast, when the dislocation density is very high, it is apparent that the SLS is not as effective. Further work is required to optimize the SLS structure by varying the strain and the number of SLS layers in order to achieve high-quality GaAs on silicon with a very low dislocation density. It is also evident that much more work is needed to understand the interaction and movement of dislocations at the SLS interfaces.

We acknowledge H. Morkoç (University of Illinois), J. Fan (Kopin Corporation), and S. Vernon (Spire Corporation) for providing a few of the samples used in this study. The work is supported by the Air Force Office of Scientific Research and by the Solar Energy Research Institute.

[1] S. M. Bedair, T. P. Humphreys, N. El-Masry, Y. Lo, N. Hamaguchi, C. D. Lamp, D. Dreifus, and P. Russel, Appl. Phys. Lett. **49**, 942 (1986).
[2] N. El-Masry, N. Hamaguchi, J. C. L. Tarn, N. Karam, T. P. Humphreys, D. Moore, S. M. Bedair, J. W. Lee, and J. Salermo, in Proceedings of the Spring Meeting of the Materials Research Society Conference, Anaheim, California, 1987 (in press).
[3] J. W. Lee, H. Shichijo, H. L. Tsai, and R. J. Matyi, Appl. Phys. Lett. **50**, 31 (1987).
[4] N. Chand, R. People, F. A. Baiocchi, K. W. Wecht, and A. Y. Cho, Appl. Phys. Lett. **49**, 815 (1986).
[5] R. Fisher, H. Morkoç, D. A. Neumann, H. Zabel, C. Choi, N. Otsuka, M. Longerbone, and L. P. Erickson, J. Appl. Phys. **60**, 1640 (1986).
[6] T. Soga, S. Hattori, S. Sakai, M. Takeyasu, and M. Umeno, J. Appl. Phys. **57**, 4578 (1985).
[7] J. W. Matthews, A. E. Blakeslee, and S. Mader, Thin Solid Films **33**, 253 (1976).
[8] M. A. Tischler, T. Katsuyama, N. El-Masry, and S. M. Bedair, Appl. Phys. Lett. **46**, 294 (1985).

Defect Reduction in GaAs Epilayers on Si Substrates Using Strained Layer Superlattices

by

N. El-Masry, N. Hamaguchi, J.C.L. Tarn, N. Karam, T.P. Humphreys, D. Moore and S.M. Bedair

Electrical and Computer Engineering Department
North Carolina State University
Raleigh, North Carolina 27695

J. W. Lee and J. Salerno

Kopin Corporation
Taunton, Massachusetts

ABSTRACT

$In_xGa_{1-x}As-GaAs_{1-y}P_y$ strained layer superlattice buffer layers have been used to reduce threading dislocations in GaAs grown on Si substrates. However, for an initially high density of dislocations, the strained layer superlattice is not an effective filtering system. Consequently, the emergence of dislocations from the SLS propagate upwards into the GaAs epilayer. However, by employing thermal annealing or rapid thermal annealing, the number of dislocation impinging on the SLS can be significantly reduced. Indeed, this treatment greatly enhances the efficiency and usefulness of the SLS in reducing the number of threading dislocations.

Transmission electron microscopy techniques have been used to characterize the dislocation behavior.

The growth of GaAs on Si substrates enables the integration of III-V compound based devices and Si electronic circuits. To date, several approaches have been investigated for the deposition of GaAs III-V compounds on Si substrates. These methods include, the use of a Ge intermediate layer,[1] direct deposition using molecular beam epitaxy,[2] metalorganic chemical vapor deposition[3] and laser stimulated deposition[4]. However, one of the major difficulties in this technology is the generation of a high density of defects in the GaAs epitaxial layers. Recently, several schemes have been successfully employed to reduce the density of defects. These approaches include thermal annealing,[5] rapid thermal annealing[6] and the use of strained layer superlattices (SLS).[7] The corresponding SLS structures that have been studied include, $In_xGa_{1-x}As-GaAs$[2] and $GaAs_{1-x}P_x-GaAs$[1]. As a consequence of using these SLS buffers layers, a significant reduction in the dislocation density has been obtained. However, despite these results the SLS composed of ternary-binary (GaAs) systems cannot be grown lattice matched to the GaAs substrate. Indeed, this SLS structure which as a whole has a lattice constant which corresponds to the ternary material with composition of x/2, has several inherent shortcomings. In particular, the total thickness of the SLS should be less than the critical thickness, h_c, in order to prevent the generation of misfit dislocations at the GaAs substrate/SLS interface[8]. Consequently, this will limit the number of periods and

Mat. Res. Soc. Symp. Proc. Vol. 91 1987 Materials Research Society

therefore, the number of interfaces capable of suppressing the propagation of threading dislocations. Furthermore, the binary-ternary SLS will also limit the amount of strain that can be present between successive layers in the SLS. Indeed, it has been previously reported[5] that when the $In_xGa_{1-x}As$–GaAs SLS has a total thickness greater than h_c, for $x/2$, dislocations are generated at both the SLS/GaAs (substrate) and the GaAs (epilayer)/SLS interfaces. It follows, therefore, that in order to circumvent the shortcomings in the ternary-binary SLS system, we require a superlattice composed of two materials having equal but opposite lattice mismatches, such that the average lattice constant matches that of the GaAs substrate. A potential material candidate is $GaAs_{1-y}P_y$–$In_xGa_{1-x}As$ with $y \approx 2x$ which can be grown lattice matched to GaAs. In fact, we have previously reported that the ternary-ternary SLS buffer was very effective in blocking dislocations originating at the GaAs substrate.[9] Further, it was also reported that a very low dislocation density of defects in the GaAs epilayer was achieved.

In this present work we report on the effectiveness of using GaAsP-InGaAs SLS in reducing threading dislocations originating at the GaAs/Si interface. Indeed, we also report on the interface-quality of the heteroepitaxy GaAs-Si structure using high resolution electron microscopy. The GaAs films were grown on Si by the Kopin Corporation followed by the growth of the SLS and GaAs epilayers in our laboratory at North Carolina State University. Both growth steps employed MOCVD techniques. To study the atomic structure of the GaAs/Si interface, a JEOL 200-CX high resolution transmission electron microscope was used. The instrument has a point-to-point resolution of 2.5 Å. The morphology of the GaAs/Si interface is shown in Figure 1. The electron beam is incident along the <011> direction. In this image, the GaAs/Si interface appears as a bright band. The presence of steps at the interface are not visible due to atomic roughness in the interface plane. Two regions on the micrograph are clearly defined, namely an

Figure 1 High resolution TEM showing the the defects at the GaAs/Si interface

incoherent interface region labeled (A) and an area with an amorphous appearance denoted by (B). The interruption of crystallinity at the GaAs/Si interface may be due to the presence of residual oxides on the Si substrate surface. Similar observations have been reported for the MBE growth of GaAs on Si.[10] The micrograph also clearly shows individual misfit dislocations which can be identified as extra lattice fringes along the (111) or (111) planes on the Si side of the interface. Two types of misfit dislocations previously reported for MBE grown materials[2] have also been observed, namely, edge and mixed dislocations in the MOCVD grown samples.

Several $In_xGa_{1-x}As-GaAs_{1-y}P_y$ SLS buffer layers with $y = 2x$ have been investigated in our study. The corresponding values of x and y have been varied in the range of $x \sim 25\%$ and $16 - 40\%$, respectively. Depending on the composition of the ternary alloys the thickness of the individual layers were varied from 80 - 300 A. The intrinsic strain was maintained in the $0 - 2\%$ range. Both cross-sectional and plan view TEM were used to study the effectiveness of these SLS buffer layers in reducing threading dislocations. These results are summarized as follows.

1. The SLS is not very effective in reducing threading dislocations when then density is in the $10^8/cm^2$ range, or greater. This observation was valid for each of the SLS structures investigated in this study. It is apparent as shown in Figure 2(a), that in regions of high dislocation density, threading dislocations that start to bend at the SLS interfaces interact with each other. This mechanism will result in the dislocations threading and penetrating the SLS buffer and GaAs epilayer.

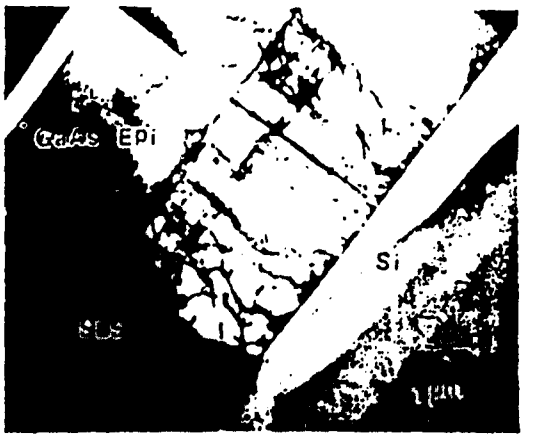

Figure 2 TEM Bright-field image illustrating:

a) Dislocations with high density, threading through the InGaAs/GaAsP SLS

2. The SLS is more effective in reducing dislocations by bending them at the SLS interface in regions were the dislocation density is approximately $10^8/cm^2$, or lower. This is clearly shown in Figure 2(b) were it is apparent that in the central region of the image, the dislocations are bent. However, at the edges the SLS is less effective due to high density of impinging dislocations.

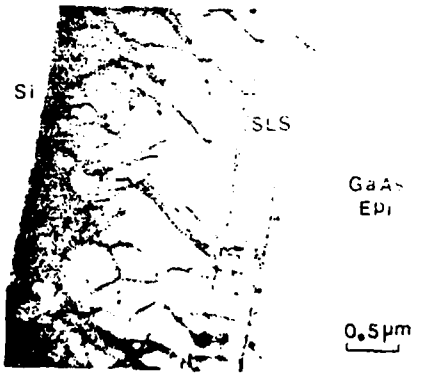

Figure 2 TEM Bright-field image illustrating:

b) A SLS effectively bending dislocation in regions where there is a low dislocation density.

3. Clearly, in order for the SLS to be made more effective the density of the impinging threading dislocations, should be reduced, within the range of $10^7/cm^2$ or lower. Two approaches were implemented to achieve this goal. The first method was to employ an in-situ anneal at 825°C for 20 minutes before the growth of the SLS. The second approach utilizes rapid thermal annealing at 900°C for 10 seconds before sample insertion in the MOCVD reactor. Both these approaches were found to be very efficient in reducing the number of dislocations to a level where the SLS behaves as an effective buffer layer. The micrograph in Figure 3 shows that the SLS is extremely efficient in bending any type of dislocation. The SLS employed in this structure is composed of five $In_{0.2}Ga_{0.8}As/GaAs_{0.78}P_{0.32}$ layers, each of 80 Å thickness with an intermediate 800 Å layer of GaAs. This structure is repeated three times and is followed by the growth of a 1 μm GaAs epilayer.

In conclusion, it is apparent that strained layer superlattices combined with rapid thermal annealing or thermal annealing of the Si/GaAs substrates, significantly reduces the number of threading dislocations in the GaAs epilayer. This work is supported by AFOSR and SERI.

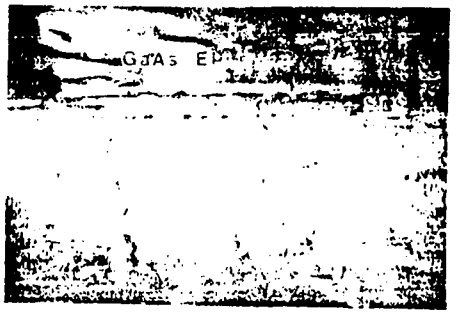

Figure 3 TEM bright-field image of a RTA sample illustrating the effectiveness of a InGaAs GaAsP SLS in both filtering and preventing threading dislocations from propagating to the sample surface.

References

1) R.D. Dupuis, J.C. Beam, J.M. Brown, A.T. Macrander, R.C. Miller and I.C. Hopkins, J. Elect. Mat., 16, 69 (1987).

2) R. Fisher, H. Morkoc, D.A. Neuman, H. Zabel, C. Choi, N. Otsuka, M. Longerbone and L.P. Erickson, J. Appl. Phys., 60, 1640 (1986).

3) T. Soga, S. Hattori, S. Sakai, M. Takayasu and M. Umeno, J. Appl. Phys., 57, 4578 (1985).

4) S.M. Bedair, J.K. Whisnant, N. Karam, M.A. Tischler and T. Katsuyama, Appl. Phys. Lett., 48, 174 (1986).

5) J.W. Lee, H. Shichijo, H.L. Tsai and R.J. Matyi, Appl. Phys. Lett., 50, 31 (1987).

6) N. Chand, R. People, F.A. Baiocchi, K.W. Wecht and A.Y. Cho, Appl. Phys. Lett., 49, 815 (1986).

7) S.M. Bedair, T.P. Humphreys, N.A. El-Masry, Y. Lo, N. Hariguchi, C.D. Lamp, D. Dreifus and P. Russell, Appl. Phys. Lett., 49, 942 (1986).

8) J.W. Matthews, A.E. Blakeslee and S. Mader, Thin Solid Films, 33, 253 (1976).

9) M.A. Tischler, T. Katsuyama, N. El-Masry and S.M. Bedair, Appl. Phys. Lett., 46, 294 (1985).

10) R. Hull, S.J. Rosner, S.M. Koch and J.S. Harris, Appl. Phys. Lett., 49, 1714 (1986).

Molecular stream epitaxy and the role of the boundary layer in chemical vapor deposition

T. Katsuyama and S. M. Bedair
North Carolina State University, Department of Electrical and Computer Engineering, Raleigh, North Carolina 27695-7911

(Received 21 September 1987; accepted for publication 22 December 1987)

Molecular stream epitaxy (MSE) is a new growth technique that modifies the nature of the metalorganic chemical vapor deposition (MOCVD) process to take advantage of molecular-beam epitaxy (MBE) growth concepts, and was used for the growth of InGaAs, GaAsP, and InGaAs/GaAsP strained-layer superlattices (SLSs). In this technique, the growth proceeds by rotating the substrate to cut into streams of reactant gases and thus eliminates gas-flow transients and provides a method to mechanically shear off the gaseous boundary layer above the substrate between successive exposures. In the growth of InGaAs and GaAsP, growth rate enhancement and compositional changes were observed in the faster rotation regime. These phenomena were attributed to the effective reduction of the diffusion boundary layer above the substrate. In the growth of InGaAs/GaAsP SLSs the individual layer thickness of these SLSs was controlled precisely down to 8 Å by simply changing the exposure time to the stream of reactant gases. The optical properties of these SLSs were comparable to those obtained for equivalent superlattices by gas source MBE.

INTRODUCTION

Metalorganic chemical vapor deposition (MOCVD) and molecular-beam epitaxy (MBE) have become the two dominant crystal-growth techniques used to synthesize sophisticated structures. However, each technique has its own advantages and disadvantages. MOCVD is a gas-phase chemical deposition process which takes place at relatively high gas pressures compared to MBE. This technique provides more flexibility than MBE, particularly for the growth of phosphorus compounds and allows uniform wide area growths. However, in the CVD process, reactant species have to diffuse through a gaseous boundary layer to reach the substrate.[1] Therefore, the abruptness of heterointerfaces will suffer from the diffusion boundary layer and gas switching transients. On the other hand, MBE is a physical deposition process that takes place in ultrahigh vacuum. No diffusion boundary layer exists, and thus, allows direct incidence of atoms or molecules in a direct line of sight onto the heated substrate. Several efforts have been made to combine the advantages of both techniques.[2–5] Recent impressive results obtained by gas source MBE (GSMBE)[6] and chemical beam epitaxy (CBE),[7] which are based on modifying the MBE growth chamber to allow the use of organometallic and hybride sources, are typical examples.

We report a new growth technique, molecular stream epitaxy (MSE), which is based on modifying the nature of the MOCVD process to take advantage of MBE growth concepts.[8,9] MSE is performed in a modified atmospheric pressure MOCVD growth system. A specially designed growth chamber and susceptor allow the substrate to cut into streams of reactant gases. This technique provides a method to mechanically shear off the gaseous boundary layer between successive exposures and the growth process occurs repetitively in the time regime where the boundary layer is not formed yet. Therefore, molecules in the stream can impinge directly onto the substrate rather than diffuse through the boundary layer. Moreover, this technique eliminates gas-flow transients and considerably reduces the dead volume and convection effects.

MSE GROWTH SYSTEM AND PROCESS

Figure 1 shows a schematic of the growth chamber and susceptor designed to allow some of the MBE features to be utilized during the MOCVD growth process. The rf-heated susceptor consists of several parts. The fixed part has two

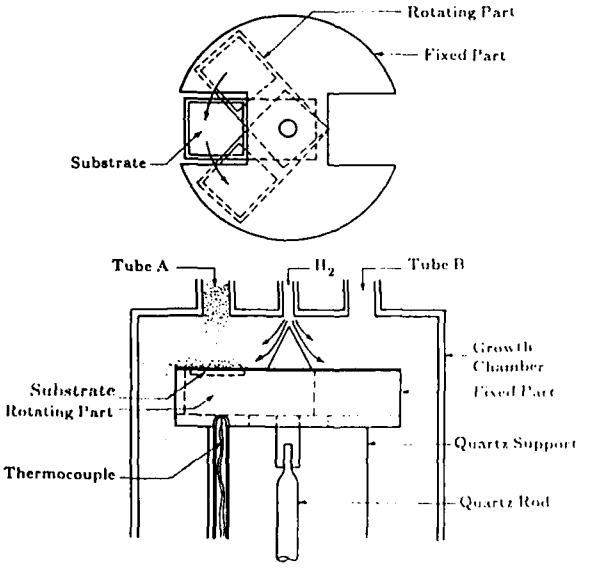

FIG. 1. Schematic of the MSE growth process. The gaseous boundary layer above the substrate is sheared off mechanically as the substrate moves out from the stream and the growth is terminated.

 0021-8979/88/105098-06$02.40

windows facing the inlet tubes A and B. The substrate sits in a recess ($1.5 \times 1.5\ cm^2$) in the rotating part of the susceptor. This part of the susceptor is driven by a computer-controlled stepping motor. The fixed part of the susceptor also acts to shear off most of the gaseous boundary layer between successive exposures. The clearance between the surface of the substrate and the top piece of the susceptor is several mils to avoid scratching of the substrate while minimizing the dead volume. Gases from the input tubes A and B flow unimpeded through the susceptor when the substrate is in position (a). This reduces the effects of convection and cross diffusion and also prevents the buildup of the gaseous boundary layer over the fixed part of the susceptor. A large flow of H_2 in the middle tube is designed to prevent mixing of the gases from tubes A and B. When the substrate is moved into the stream of reactant gases, the gas species impinge directly on the substrate due to the near absence of the diffusion boundary layer, and the deposition takes place suddenly [position (b)]. This action simulates the opening of the shutters in the MBE process. As the susceptor moves away from the stream, the gaseous boundary layer is sheared off mechanically by the top fixed part of the susceptor and the growth is terminated [position (c)]. This action simulates the closing of the shutters in the MBE process. The same process can be repeated at the other side of the susceptor and the rotation is continued until the desired thickness is obtained. The fastest transition time from one gas stream to the other is 1.5 s. The fastest rotation is 3 s per cycle corresponding to the shortest exposure time of about 0.3 s. The composition of the grown films was measured by an x-ray diffraction technique.

MSE GROWTH OF InGaAs AND GaAsP

$In_xGa_{1-x}As$ and $GaAs_{1-y}P_y$ were grown on a (100) Cr-doped GaAs substrate at atmospheric pressure by MSE to investigate the effect of the reduction of the boundary layer thickness on the composition and growth rate. Trimethylgallium (TMG), triethylindium (TEI), AsH_3 (10% in H_2), and PH_3 (5% in H_2) were used as Ga, In, As, and P sources, respectively. H_2 was used as a carrier gas with a total flowrate of 750 sccm for each of the tubes, A and B, and it was also used for the center flow with a flowrate of 4000 sccm. The substrate was cleaved to fit in the recess of the rotating part of the susceptor. The substrate position was adjusted and exposed to the stream from either tube A or B. The substrates were heated under AsH_3 at the growth temperature (550–730 °C) for about 5 min before the growth. InGaAs was grown by cutting into the stream from tube A containing TMG, TEI, and AsH_3 with various exposure times (0.3–600 s). Only carrier hydrogen (750 sccm) was passed through tube B. The rotation cycles continue until the desired thickness of InGaAs film is deposited. On the other hand, GaAsP was grown with the same manner as that of the InGaAs with the stream from tube B containing TMG, AsH_3, and PH_3 and carrier hydrogen (750 sccm) was passed through tube A.

Figure 2 shows the growth rate of InGaAs and GaAsP grown at 630 °C as a function of the exposure time per rotation and vertical bars present the thickness variations across the substrate in the radial direction. The growth rate is normalized to 1 min, e.g., the growth rate at 1-s exposure per rotation means the thickness of the epilayer with 60 rotations of 1-s exposure each. As the exposure time was decreased (rotation speed increased), the growth rate increased for both InGaAs and GaAsP. This growth rate enhancement in the faster rotation regime is probably due to the effective reduction of the gaseous diffusion boundary layer. This results in an increase in the flux density of Ga and In species at the substrate surface. Moreover, the reactant products such as CH_4 and C_2H_6 which might cause a reduction of the growth rate[10] were wiped out by the rotation of the susceptor before they build up over the substrate.

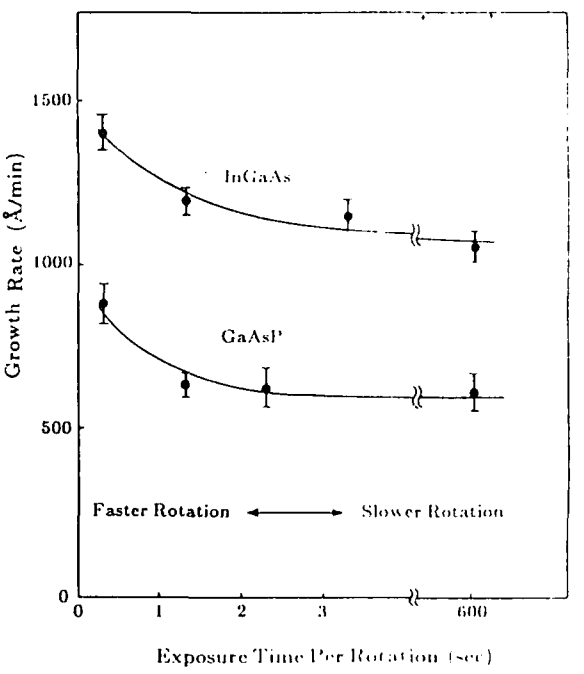

FIG. 2. Growth rate of InGaAs and GaAsP grown at 630 °C as a function of the exposure time per rotation. The growth rate enhancements for both InGaAs and GaAsP in the faster rotation regime have been observed.

The effect of the dead volume existing between the substrate surface and top part of the susceptor (< 5 mils or 127 μm) on the growth rate enhancement in the shorter exposure regime was estimated assuming that all of the TMG trapped in this dead volume ($1.5 \times 1.5 \times 0.0127\ cm^3$) contributes to the growth. The calculated extra thickness of the epilayer was 0.023 Å per growth cycle, while the observed growth rate enhancement was approximately 300 Å/min at the shortest exposure time (200 turns with 0.3 s exposure) as shown in Fig. 2. Therefore, the dead volume effect on the growth rate enhancement is approximately 1.53%, which is small enough to be negligible.

Compositional changes have also been observed for both $In_xGa_{1-x}As$ and $GaAs_{1-y}P_y$ with shorter exposure times as shown in Fig. 3. Again, the vertical bars present compositional variations across the substrate in the radial direction. For $In_xGa_{1-x}As$, this compositional enhancement may be mainly due to the variation of the flux density ratio of In and Ga (J_{In}/J_{Ga}) at the substrate surface due to

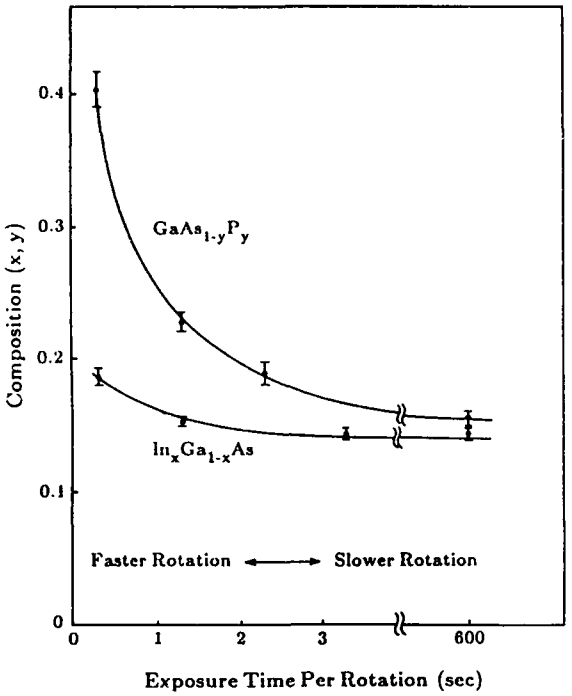

FIG. 3. Composition (x,y) of $In_xGa_{1-x}As$ and $GaAs_{1-y}P_y$ as a function of the exposure time per rotation. Compositional enhancements have been observed for both InGaAs and GaAsP in the faster rotation regime.

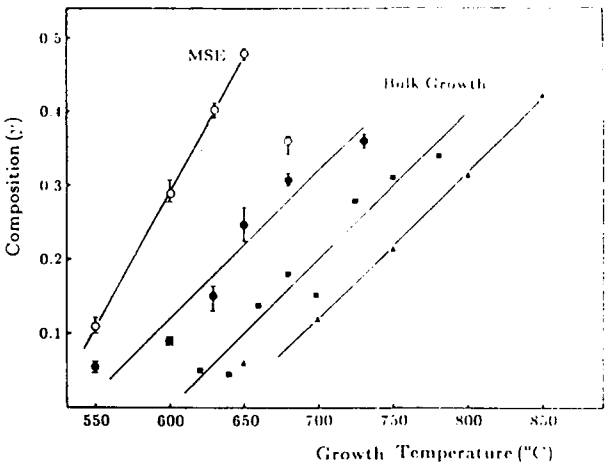

FIG. 4. GaP solid composition (y) as a function of the growth temperature for MSE and several conventional MOCVD grown GaAsP. Partial pressure ratio (PH_3/AsH_3) is unity except for in Ref. 14 where the ratio is 0.92. MSE showed a higher efficiency in incorporation of phosphorous. (◊) MSE (present work) (♦) MOCVD (present work) (■) C. R. Lewis and M. J. Ludowise (Ref. 14) (▲) L. Samuelson Omling, and Crimmeiss (Ref. 15

the reduction of the boundary layer thickness. At the growth temperature, 630 °C, both TMG and TEI molecules decompose[11,12] as they diffuse through the boundary layer toward the substrate. Since heavier molecules (TEI > TMG, In > Ga) diffuse more slowly, the flux density ratio, J_{In}/J_{Ga}, at the substrate will increase as the thickness of the boundary layer is decreased. As a result, the solid composition x is increased in the shorter exposure regime. In addition, the gas-phase reaction between TEI and AsH_3 that can take place in the gaseous diffusion boundary layer is reduced in the shorter exposure regime. The growth of InGaAs by atomic layer epitaxy (ALE) in which the TEI and AsH_3 are separated during the growth showed a similar enhancement of the solid composition (x).[13]

However, the compositional change is more significant for $GaAs_{1-y}P_y$ as shown in Fig. 3 and cannot be explained based on the molecular weight of AsH_3 and PH_3. In order to investigate this dramatic change, GaAsP films have been grown at various substrate temperatures. Figure 4 shows the solid composition (y) as a function of the growth temperature for MSE and several conventional MOCVD-grown GaAsP by us and others.[14,15] Partial pressure ratio (P_{PH_3}/P_{AsH_3}) for all the grown films is unity except for Ref. 14 where the ratio is 0.92. The three different sets of conventional MOCVD growths exhibited a similar linearity, whereas MSE-grown samples showed a larger slope than others. This indicates that the MSE has a higher efficiency for incorporating phosphorus. In MSE, the solid composition (y) reached nearly 50% at 650 °C. Since the solid composition (y) is controlled by the PH_3/AsH_3 thermal cracking ratio,[16,17] this suggests that PH_3 was nearly 100% decomposed at the substrate surface at 650 °C, assuming complete decomposition of AsH_3 at the substrate surface. Although the reasons for such a dramatic enhancement of the solid composition (y) by MSE has not been clearly understood, this effect may be related to the enhancement in the cracking efficiency of PH_3 by catalyzation at the GaAsP growing surface. This can be expected from the result of complete pyrolysis of PH_3 with powdered GaP at 600 °C.[17] Another possible mechanism for the enhancement of the solid composition (y) is the contribution of the gas phase in the overall decomposition of the AsH_3 and PH_3 molecules. Both AsH_3 and PH_3 will decompose (or partially decompose) either thermally or catalytically at the substrate surface. Based on several experimental results of the AsH_3 pyrolysis,[11,12] it is expected that AsH_3 is nearly 100% cracked in the gas phase above 600 °C in the presence of TMG. However, the thermal cracking of PH_3 in the gas phase may not be as efficient as AsH_3 at this temperature. Therefore, as the thickness of the boundary layer is decreased, the P/As ratio at the substrate surface will be increased either by allowing more PH_3 cracking due to the surface catalytic reaction or by the reduction of AsH_3 decomposition in the thermal boundary layer. A combination of both these effects is also possible. Consequently, the solid composition (y) is enhanced by allowing the surface reactions to play a more dominant role than the decomposition taking place in the gas phase. It may be also possible that at shorter exposure times the substrate surface has less time to cool in the gas stream (than at higher exposure) and therefore the average temperature is higher, allowing more P incorporation.

It should be pointed out that the enhancements in growth rate and composition were observed when the exposure time was less than 2 s. This suggests that the boundary layer is established in the MSE system within 2 s after the exposure of the substrate to the stream of reactant gases. It

should also be noted that the composition (y) of the MSE-grown samples decreased at even higher temperature (> 650 °C). This is probably due to the desorption of phosphorus from the substrate during the rotation cycle when it is covered by the fixed part of the susceptor without phosphorus overpressure. In fact, above 650 °C the MSE-grown samples showed hazy surfaces which may be attributed to loss of phosphorus.

MSE GROWTH OF InGaAs/GaAsP SLSs

The $In_xGa_{1-x}As/GaAs_{1-y}P_y$ SLS were also grown by MSE on Cr-doped (100) GaAs at 630 °C. The GaAs substrate was exposed to the tube A stream containing TMG(-13 °C) = 3 sccm, TEI(20 °C) = 65 sccm, AsH_3 = 15 sccm, and to the tube B stream containing TMG(-13 °C) = 3 sccm, AsH_3 = 15 sccm, PH_3 = 60 sccm, alternately. The mole fraction of the reactant species was adjusted to allow the growth of a SLS with $x = 12\%$ and $y = 23\%$. These values of x and y allow the lattice constants of the SLSs parallel to the grown layer to match that of the GaAs substrate. The exposure time for each reactant gas stream was varied from 0.5 to 10.3 s with equal exposure times. The mole fractions in the gas phase were adjusted, especially for short exposure times, to give $y \simeq 2x$. The transition time from one stream to the other is about 1.5 s.

The SLSs were characterized by x ray, transmission electron microscopy (TEM), and photoluminescence (PL). Table I summarizes the growth conditions and structures of the SLSs. The period of the SLSs was determined from the separation of x-ray diffraction satellite peaks (samples a, b, and c) and from high-resolution TEM images (samples c, d, and e). Figure 5 shows bright-field cross-sectional TEM images of the samples "d" and "e". Uniform periodic layered structures with layer thicknesses of 12 Å [Fig. 5 (a), 1.3-s exposure] and 8 Å [Fig. 5 (b), 0.5-s exposure] have been observed. To the best of our knowledge, the 8-Å InGaAs and GaAsP layers are among the thinnest films ever grown in a superlattice with alternating layers having As and P compounds.[18] These structures composed of both As and P are difficult structures to synthesize with an abrupt interface[19] since AsH_3 and PH_3 cracking temperatures are relatively high.

The period of the SLSs as a function of the exposure time is shown in Fig. 6. Excellent linearity has been obtained up to 25-Å periods. This demonstrates the ability of MSE to produce multilayered structures with precisely controlled thicknesses by simply changing the exposure time to the stream of reactant gases. The 16-Å period with 0.5-s exposure is slightly thicker than the value given by the extrapolation from other measurements due to the growth rate enhancement as discussed previously.

TABLE I. Growth conditions and structures of $In_{0.12}Ga_{0.88}As/GaAs_{0.77}P_{0.23}$ SLSs. TMG (-13 °C) = 3 sccm, TEI (20 °C) = 65 sccm, AsH_3 (10% in H_2) = 15 sccm, PH_3 (5% in H_2) = 60 sccm, growth temperature = 630 °C.

Run	Exposure time (s)	Number of periods	Period (Å)	PL peak energy (eV)	FWHM (meV)
a	10.3	30	183	1.40	13.4
b	5.3	120	96	1.42	15.3
c	2.8	200	52	1.48	12.0
d	1.3	400	25	1.46	24.0
e	0.5	800	16	1.49	15.6

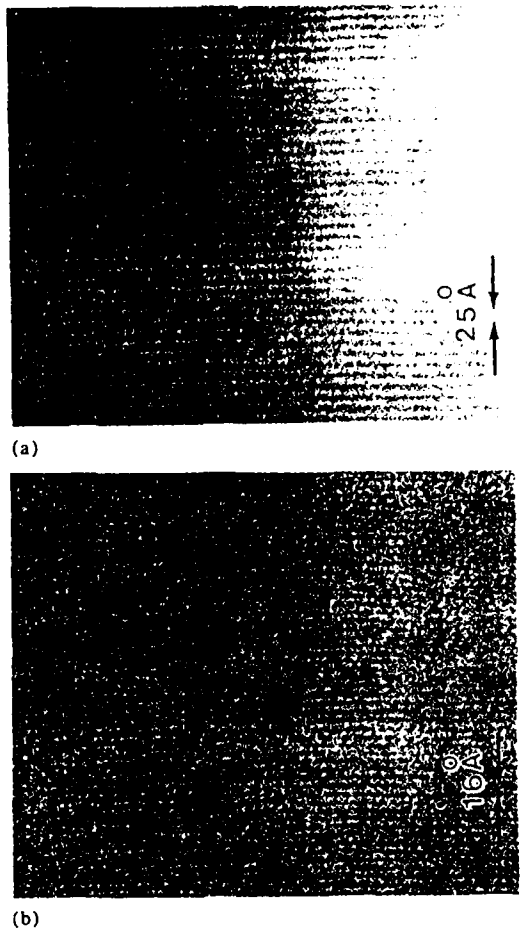

FIG. 5. High-resolution TEM images of the MSE-grown ultrathin InGaAs/GaAsP SLS. (a) 25-Å period, 1.3-s exposure. (b) 16-Å period, 0.5-s exposure.

Photoluminescence (PL) measurements were performed at 77 K. An Ar-ion laser (λ = 5145 Å) was used as an excitation source with excitation power density ranging from 100 to 500 W/cm^2. Each sample showed a strong, single, sharp peak corresponding to the transition between the first electron ($n = 1$) and heavy-hole band. Figure 7 shows the PL peak energy as a function of the period of the SLSs. As the well width (InGaAs layer thickness) was decreased, the PL peaks shifted toward the higher energy due to the quantum size effect. The solid line shows the effective band gap of the $In_{0.12}Ga_{0.85}As/GaAs_{0.77}P_{0.23}$ SLS calculated using the strain-induced band-gap shift and the modified Kronig–Penney model. The vertical bars present the variation in peak energy across the samples in the radial direction. PL results shown in Fig. 7 correspond to measurements made at the position of the substrate shown in the inset. Although the uniformity across the samples needs to be improved, full width at half-maximums (FWHMs) of the PL

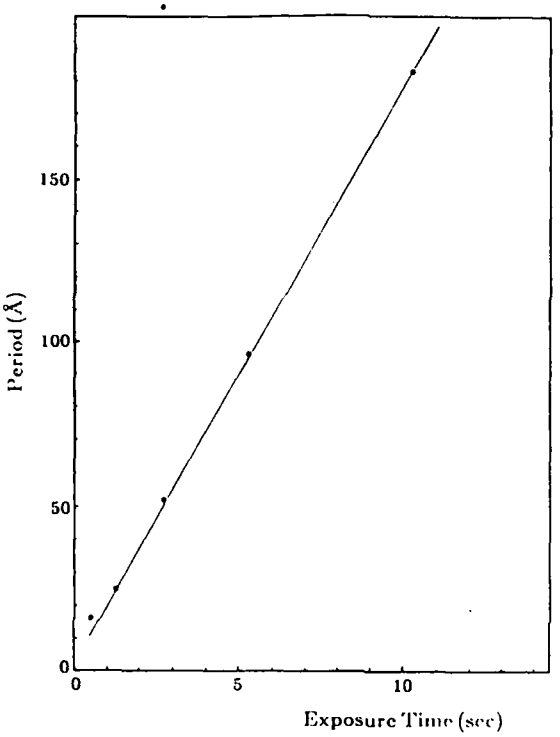

FIG. 6. Period of the SLSs as a function of the exposure time. An excellent linearity has been obtained up to 25 Å periods. Due to the growth rate enhancement in the faster rotation regime, the sample grown with 0.5-s exposure is slightly thicker than the value given by the extrapolation.

spectra (12–24 meV) indicate that these SLSs grown by MSE are of comparable optical quality to those obtained by GSMBE (Ref. 6) and CBE.[20] For example, the FWHM of InGaAs/GaAsP SLS at 77 K is about the same as that obtained by GSMBE at 6 K for the InGaAsP/InP superlattice structure with 80-Å wells.[6] Also, the 8-Å InGaAs quantum wells in the InGaAs/GaAsP SLS have comparable PL properties to those obtained by low-pressure MOCVD (Ref. 18) and CBE (Ref. 20) at 2 K for an InGaAs/InP single quantum well.

One of the main concerns of this MSE system is the diffusion of gases from one side of the growth chamber to the other. Although a large flow of hydrogen provided from the center tube of the growth chamber helps to prevent this cross diffusion, it is important to know the degree of cross diffusion taking place during the growth of the SLSs. A cross-diffusion test has been carried out by growing GaAs/GaAsP multilayer structures in the same manner as the InGaAs/GaAsP SLSs. The multilayer structures consist of ten periods of 400-Å GaAs (40-s exposure) and 100-Å GaAsP (10-s exposure). In this structure, the GaAs layers are thick enough to eliminate the quantum size effect and the GaAsP layers are thin enough to accommodate lattice mismatch. Therefore, the degree of cross diffusion can be estimated by the shift in the PL spectral energy peak from the GaAs band gap which relates to the incorporation of P in the GaAs layers. Two PH_3 flowrates (30 and 100 sccm) were used for the cross-diffusion test. The result of the cross-diffusion test indicates that approximately 2% PH_3 cross diffusion takes place in the MSE system. However, it should be noted that PH_3 creates a worst-case test because the decomposition temperature of PH_3 is higher than that of AsH_3 and other organometallic sources. Indeed, the realization of GaAs ALE in the same system has confirmed that the cross diffusion of the TMG and AsH_3 is small enough to be negligible.[21] Further improvement can be expected with a better susceptor and growth chamber design combined with operation at low pressure.

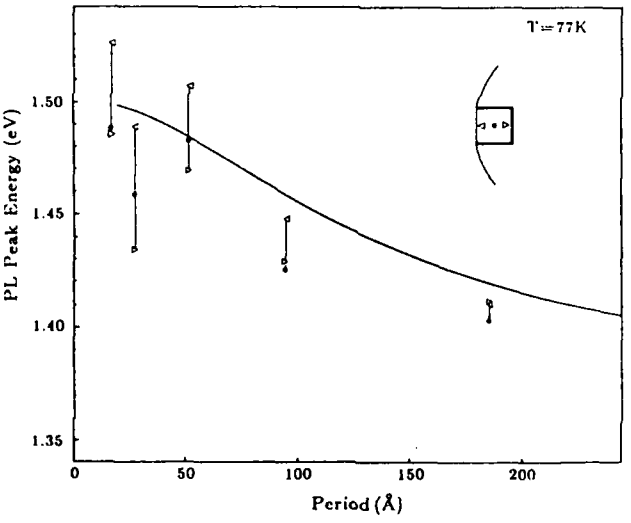

FIG. 7. Photoluminescence peak energy as a function of the period of the SLSs. PL peak shifted toward higher energy with decreasing the period of the SLSs due to the quantum size effect. Solid line shows the calculated effective band gap of $In_{0.12}Ga_{0.88}As/GaAs_{0.77}P_{0.23}$ SLS using the modified Kroning–Penney model and strain-induced band-gap shift.

SUMMARY

MSE growth has been investigated. This technique has demonstrated that the boundary layer plays an important role in the CVD growth process and also showed the ability to produce high-quality ultrathin layers with precisely controlled thicknesses. $In_xGa_{1-x}As$ and $GaAs_{1-y}P_y$ were grown on GaAs by MSE. Enhancement of the growth rate was observed for both InGaAs and GaAsP in the faster rotation regime due to the significant reduction of the boundary layer. The enhancement of the solid composition (x and y) was also observed in the faster rotation regime. These effects may be attributed to the variation of the flux density ratio (J_{In}/J_{Ga}) at the substrate surface for InGaAs and the increase of cracking efficiency of PH_3 due to the catalytic reaction at the GaAsP growing surface, or the reduction of the gas-phase reaction of AsH_3 in the thermal boundary layer. A series of InGaAs/GaAsP SLSs were also grown by MSE. An excellent linearity in the relation between the exposure time and the SLS period revealed the ability of MSE to synthesize multilayered structures with precisely controlled thicknesses without gas switching. The 8-Å InGaAs and GaAsP layers are among the thinnest films ever synthesized in a superlattice with alternating layers composed of As and P compounds. PL results indicate high optical quality and abrupt interfaces that are comparable to those obtained by GSMBE and CBE.

ACKNOWLEDGMENTS

The authors would like to acknowledge Dr. M. A. Tischler, Dr. N. H. Karam, and Dr. N. El-Masry for their assistance. This work has been supported by the National Science Foundation, the Air Force Office of Science Research, and the Solar Energy Research Institute.

[1]D. H. Reep and S. K. Ghandhi, J. Electrochem. Soc **130**, 675 (1983).
[2]F. J. Morris and H. Fukui, J. Vac Technol. **11**, 506 (1974).
[3]E. Veuhoff, W. Plestschen, P. Balk, and H. Luth, J. Cryst. Growth **55**, 30 (1981).
[4]L. M. Fraas, J. Appl. Phys. **52**, 6939 (1982).
[5]J. R. Shealy, Appl. Phys. Lett. **48**, 925 (1986).
[6]H. Temkin, M. B. Panish, P. M. Petroff, K. A. Hamm, J. M. Vandenberg, and S. Sumski, Appl. Phys. Lett. **47**, 394 (1985).
[7]W. T. Tsang, Appl. Phys. Lett. **45**, 1234 (1984).
[8]T. Katsuyama, M. A. Tischler, T. P. Humphreys, and S. M. Bedair, *Electronic Material Conference*, Amherst, MA, 1986 (The Metallurgical Society, Amherst, MA, 1986), Abstract, Technical Program, p. 70.
[9]T. Katsuyama, M. A. Tischler, N. H. Karam, N. El Masry, and S. M. Bedair, Appl. Phys. Lett. **51**, 529 (1987).
[10]V. el Jani, M. Leroux, J. C. Crenet, and P. Gilbart, J. Phys. (Paris) Colloq. C **5**, 303 (1982).
[11]J. Nishizawa and T. Kurabayashi, J. Electrochem. Soc. **130**, 413 (1983).
[12]M. R. Leys and H. Veenvliet, J. Cryst. Growth **55**, 145 (1981).
[13]M. A. Tischler and S. M. Bedair, Appl. Phys. Lett. **49**, 274 (1986).
[14]C. R. Lewis and M. J. Ludowise, J. Electron. Mater. **13**, 749 (1983).
[15]L. Samuelson, P. Omling, and H. G. Grimmeiss, J. Cryst. Growth **61**, 425 (1983).
[16]B. G. Stringfellow, J. Cryst. Growth **62**, 225 (1983).
[17]B. G. Stringfellow, J. Cryst. Growth **68**, 111 (1984).
[18]M. Razeghi and J. P. Duchemin, J. Cryst. Growth **70**, 145 (1984).
[19]J. P. Andre, E. P. Menu, M. Erman, M. H. Meynadir, and T. Ngo, J. Electron. Mater. **15**, 71 (1986).
[20]W. T. Tsang and E. F. Schubert, Appl. Phys. Lett. **49**, 220 (1986).
[21]M. A. Tischler and S. M. Bedair, Appl. Phys. Lett. **48**, 1681 (1986).

Single-crystal x-ray diffraction study of the InGaAs-GaAsP/GaAs superlattice system

B-L. Jiang,[a] F. Shimura, and G. A. Rozgonyi
Department of Material Science and Engineering, North Carolina State University, Raleigh, North Carolina 27695-7916

N. Hamaguchi and S. M. Bedair
Department of Electrical and Computer Engineering, North Carolina State University, Raleigh, North Carolina 27695-7911

(Received 14 December 1987; accepted for publication 12 February 1988)

Single-crystal x-ray rocking curve and transmission imaging topography techniques have been used for the characterization of InGaAs-GaAsP strained-layer superlattices (SLS's), which are lattice matched to GaAs substrates. The thicknesses of the SLS's and strains, $\langle\epsilon^{\perp}\rangle$ and $\langle\epsilon^{\parallel}\rangle$, were readily determined nondestructively by analyzing the rocking curves obtained with Cu $K\beta_1$ radiation. These quantitative data were combined with the qualitative defect imaging results of x-ray topography to determine the critical intrinsic SLS thickness t_{ISc} ($= P_{\mathrm{SL}}\langle\bar{\epsilon}^{\parallel}\rangle_c$) that dominates the generation of misfit dislocations. It was estimated for the InGaAs-GaAsP SLS on a GaAs substrate as 1.05×10^{-3} Å $< t_{\mathrm{ISc}} < 1.56\times10^{-3}$ Å.

Strained-layer superlattice (SLS) structures[1] have been proposed as a buffer layer that can provide a filter to provide low defect density GaAs homo- or heteroepitaxial layers. The SLS consists of alternating ternary layers whose lattice parameters are significantly different from that of the GaAs substrate. The layers can be thin enough to ensure that the lattice mismatch is entirely accommodated by elastically straining the layers without generation of misfit dislocations; however, the interfacial stress turns aside threading dislocations propagating up from the substrate.[2,3] Bedair *et al.* used a metalorganic chemical vapor deposition (MOCVD) technique to deposit $In_xGa_{1-x}As$-$GaAs_{1-y}P_y$ superlattice layers that were lattice matched to the GaAs substrate when $y = 2x$.[4] They reported that GaAs epitaxial layers grown on the InGaAs-GaAsP superlattice buffer layers showed a dislocation density lower by at least an order of magnitude than that obtained from epitaxial layers grown directly on GaAs substrates.[5] In this letter we present two single-crystal x-ray diffraction techniques that use Cu $K\beta_1$ and $K\alpha_1$ radiation sequentially to obtain the rocking curves (XRC) and topography (XRT) of SLS structures, respectively. It is demonstrated that the x-ray rocking curves can rapidly and quantitatively characterize such structural parameters as the SLS period and average layer strains, both parallel and perpendicular to the surface, generated at the SLS interfaces. Qualitative defect images are then obtained by using compositional and transmission x-ray topography to delineate dislocations separately in the substrate and SLS layers. Finally, a parameter that yields an intrinsic critical thickness of SLS for generation of misfit dislocations is proposed.

Thirty-period $In_xGa_{1-x}As$-$GaAs_{1-y}P_y$ SLS layers were grown by MOCVD at atmospheric pressure in a vertical reactor. Two different GaAs substrates grown by the horizontal Bridgman method were used: one Cr doped and the other Zn doped. The dislocation densities of these crystals were on the order of 10^3–10^4/cm^2, as determined by transmission XRT. All substrates were (100), off oriented 2° towards ⟨110⟩. Details of the growth conditions have been previously reported.[5] The nominal structural parameters for samples A–D, which were grown in different runs, are listed in Table I.

The x-ray rocking curves were obtained by using $\mathbf{g}_{400}$ symmetric diffraction vectors, and $\mathbf{g}_{422}$ and $\mathbf{g}_{511}$ asymmetric reflections by using Cu $K\beta_1$ radiation. The primary incident beam was collimated by a slit of 0.05 mm in width. In order to observe defects induced in the samples, x-ray topographs were obtained with a Lang camera with the use of Cu $K\alpha_1$ radiation under the condition of anomalous transmission with $\mu t \approx 17$. An intrinsic critical thickness of SLS for generation of misfit dislocations was estimated by the analyses of both x-ray rocking curves and x-ray topography. Moreover, compositional x-ray topography[6] clearly distinguished the defects in the SLS from those in the substrate.

The Cu $K\beta_1$ x-ray rocking curves obtained with the use of the (400), (422), and (511) reflections consist of a main peak from the GaAs substrate and periodic satellite peaks from the SLS layers. Typical x-ray rocking curve profiles obtained by using the (422) reflection for samples A, B, C, and D are shown in Figs. 1(a), 1(b), 1(c), and 1(d), respectively. The location of the SLS zeroth-order satellite peak can be identified by measuring the absolute value of the angular distance between the positive and negative first-order satellite peaks, and dividing by two. For samples A and B, the SLS zeroth-order satellite peak overlaps the substrate

TABLE I. Nominal structure parameters for the $In_xGa_{1-x}As$-$GaAs_{1-y}P_y$ superlattice samples.

Sample	In/P = x/y (%)	GaAs substrate	Period of SLS (Å)
A	7/14	Cr doped	300
B	7/14	Cr doped	300
C	7/12	Si doped	300
D	7/12	Si doped	300

[a] Visiting from Department of Material Physics, Beijing University of Iron and Steel Technology, Beijing, People's Republic of China.

 0003-6951/88/151258-03$01.00

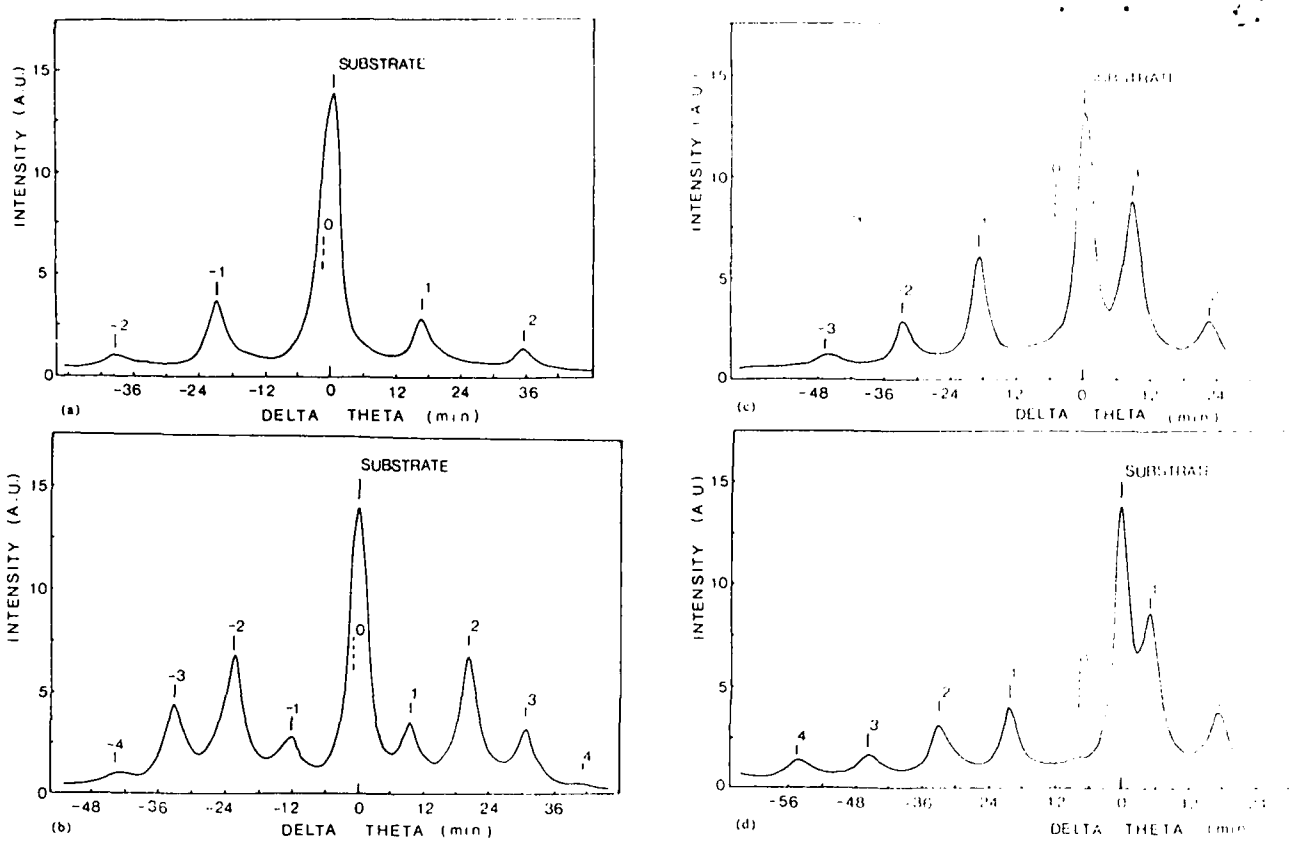

FIG. 1. X-ray rocking curves obtained with the use of Cu $K\beta_1$ (422) reflection. (a) Sample A, (b) sample B, (c) sample C, and (d) sample D.

peak; it therefore follows that the SLS, as a whole, is essentially lattice matched with the substrate. However, considerable lattice mismatch is observed in samples C and D, as shown in Figs. 1(c) and 1(d). Moreover, the difference in the number of satellite peaks and their relative intensity profiles for the different order reflections for each sample can be attributed to compositional fluctuations in the SLS.[7,8]

The angular distance $\Delta\theta$ between two neighboring satellite peaks yields the periodic thickness of superlattice, P_{SL}, as follows[9]:

$$P_{SL} = \lambda\,|\gamma_H|/\Delta\theta \sin 2\theta, \tag{1}$$

where λ is the wavelength of Cu $K\beta_1$, $|\gamma_H|$ the direction cosines of the diffracted beam, and θ the Bragg angle of the GaAs substrate. The superlattice period P_{SL} calculated by using the (400), (422), and (511) reflection and the averaged period P_{SL} for the samples are shown in Table II. The periods obtained from different reflections are in excellent agreement with each other; however, it is found that the actual SLS period deviates largely from the nominal one. This deviation is attributable to unstable SLS growth conditions.

If the SLS zeroth-order peak is displaced by an angle $\Delta\theta_0$ from the substrate peak, e.g., as in Fig. 1(c), the strain at the SLS/substrate interface normal and parallel to the surface can be calculated from the following equations[7]:

$$-\Delta\theta_0 = K_1\langle\epsilon^{\perp}\rangle + K_2\langle\epsilon^{\parallel}\rangle,$$
$$K_1 = \cos^2\psi \tan\theta + \sin\psi\cos\theta, \tag{2}$$
$$K_2 = \sin^2\psi \tan\theta - \sin\psi\cos\theta,$$

where $\langle\epsilon^{\perp}\rangle$ and $\langle\epsilon^{\parallel}\rangle$ are the strains, averaged over the superlattice period, perpendicular and parallel to the surface, respectively; ψ is the angle between the reflection planes and the wafer surface. From Eq. (2) the symmetric reflection g_{400} measures $\langle\epsilon^{\perp}\rangle$ only, while the asymmetric reflections g_{422} and g_{511} measure both $\langle\epsilon^{\perp}\rangle$ and $\langle\epsilon^{\parallel}\rangle$. The experimentally determined values of $\langle\epsilon^{\perp}\rangle$ and $\langle\epsilon^{\parallel}\rangle$ obtained are listed in Table II, in which $\langle\bar{\epsilon}^{\parallel}\rangle$ denotes the averaged strain of

TABLE II. Results of x-ray diffraction analyses.

Sample	P_{SL} (Å) (400)	(422)	(511)	$\bar{P}_{SL}$ (Å)	$\langle\epsilon^{\perp}\rangle$ ($\times 10^{-4}$)	$\langle\epsilon^{\parallel}\rangle$ ($\times 10^{-4}$) (422)	(511)	$\langle\bar{\epsilon}\rangle$ ($\times 10^{-4}$)	$P_{SL}\langle\epsilon^{\perp}\rangle$ ($\times 10^{-4}$ Å)	MD[a]
A	250	257	258	255	3.6	−1.8	−2.2	−2.0	0.51	No
B	448	431	434	437	3.7	2.3	2.5	2.4	1.05	No[b]
C	357	347	353	352	1.4	−5.6	−7.4	−6.5	2.29	Many
D	404	376	···	390	2.1	−4.0	···	−4.0	1.56	Many

[a]MD: Misfit dislocations observed by x-ray topography.
[b]Some MD's were observed locally in the SLS, but not at the SLS/substrate interface.

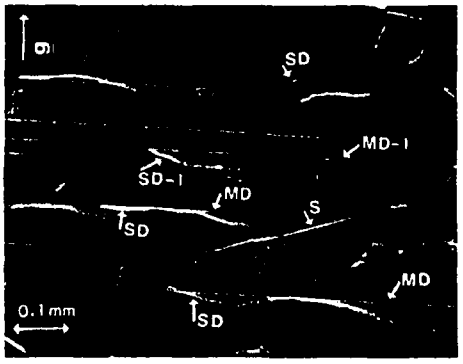

FIG. 2. X-ray topography with the use of Cu $K\alpha_1$ (220) diffraction for sample C. (MD, SD, and S denote misfit dislocations, substrate dislocations, and a mechanical scratch, respectively).

$\langle\epsilon^{\parallel}\rangle_{422}$ and $\langle\epsilon^{\parallel}\rangle_{511}$. The reason for positive $\langle\epsilon^{\parallel}\rangle$ observed in sample B is unknown.

From x-ray topography with Cu $K\alpha_1$ radiation, misfit dislocations were observed at the SLS/substrate interface of samples C and D, as shown in Fig. 2 for sample C; however, misfit dislocations were not detected in the XRT's of samples A and B. In Fig. 2 the arrows MD-1 point to misfit dislocations that lie in the SLS/substrate interface and are aligned along the ⟨110⟩ directions (the contrast feature indicated with the arrow S is due to a mechanical scratch on the surface). Note that for each MD indicated, the source of these misfit dislocations is associated with a substrate dislocation (see arrows SD in Fig. 2). As mentioned above, no extended misfit dislocations were observed at the SLS/substrate interface of samples A and B; however, transmission XRT and compositional XRT revealed some dislocations locally distributed in the SLS of sample B. Figure 3 shows the compositionally differentiated XRT for the (a) substrate and (b) SLS of sample B. These images were obtained by separately recording (422) reflections from the substrate peak and the second-order ($n = -2$) SLS satellite peak, respectively. No defect contrast, except weak contrast that is considered to be due to misfit dislocations running in the SLS very close to the interface, is observed in the substrate [Fig. 3(a)]. However, both threading and misfit dislocations are found in the SLS. These defects observed in the SLS of sample B may be related with its positive $\langle\epsilon^{\parallel}\rangle$ shown in Table II.

This sequence of bending a substrate defect into the epitaxy interfacial plane and then extending the defect to the edge of the wafer is precisely the goal of those workers who desire the elimination of substrate defects using lattice misfit. The challenge is, of course, to achieve this without introducing unwanted new dislocations, which thread up to the wafer surface.

It is recognized that an elastic force from strain energy existing at a misfit interface will act on a substrate dislocation as it passes through a heteroepitaxial interface.[1] The propagation direction of the dislocation can, therefore, be changed so that the dislocation does not enter into the epitaxial layer. Rozgonyi *et al.*[3] have verified experimentally this model by carefully controlling the layer thickness and the lattice parameter mismatch in growing heteroepitaxial layers of GaAlAsP on GaAs substrates. Mathematically, the

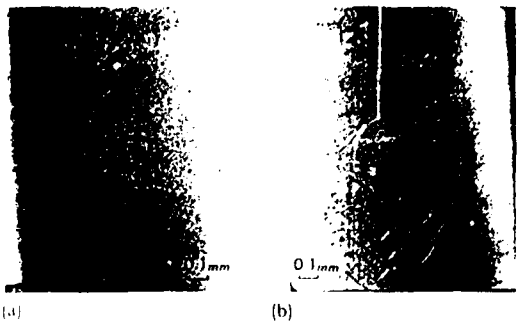

FIG. 3. Compositional x-ray topographs with the use of Cu $K\beta_1$ (422) diffraction for sample B. (a) Substrate and (b) SLS.

misfit-induced elastic force F_ϵ acting on a dislocation has been expressed for a single heteroepitaxial layer as

$$F_\epsilon = Ktf, \tag{3}$$

where t is the layer thickness, f is the layer/substrate misfit, and K is proportional to the Burgers vector.[3] For SLS the misfit-induced elastic force can be proportional to the value $P_{SL}\langle\bar{\epsilon}^{\parallel}\rangle$. The calculated value of $P_{SL}\langle\bar{\epsilon}^{\parallel}\rangle$, which is referred to as *intrinsic strained thickness* t_{IS} hereafter, is given in Table II for samples A–D.

According to the calculated values of $P_{SL}\langle\bar{\epsilon}^{\parallel}\rangle$ and the images obtained with x-ray topography, the critical intrinsic strained thickness t_{ISc} ($= P_{SL}\langle\bar{\epsilon}^{\parallel}\rangle_c$), which dominates the generation of misfit dislocation, can be estimated to be

$$1.05\times10^{-3}\ \text{Å} < t_{ISc} < 1.56\times10^{-3}\ \text{Å}. \tag{4}$$

It is important to recognize that the parameter t_{IS}, rather than the simple thickness of SLS or heteroepitaxial layers, can be the dominant factor in correlating the critical growth conditions with the application of misfit dislocation generation to the elimination of substrate defects.

In summary, single-crystal x-ray rocking curve and topography techniques using Cu $K\beta_1$ and Cu $K\alpha_1$ radiation, respectively, have been used for the characterization of InGaAs-GaAsP strained-layer superlattices on GaAs substrates. The thickness of the SLS and strains $\langle\epsilon^{\perp}\rangle$ and $\langle\epsilon^{\parallel}\rangle$ were well determined by analyzing the rocking curves. Combining the results of x-ray topography, the critical intrinsic strained thickness t_{ISc} ($= P_{SL}\langle\bar{\epsilon}^{\parallel}\rangle_c$) that dominates the generation of misfit dislocation was determined for InGaAs-GaAsP strained-layer superlattice/GaAs substrate system.

This work was supported by the Air Force Office of Scientific Research and the Solar Energy Research Institute.

[1] J. W. Matthews, A. E. Blakeslee, and S. Mader, Thin Solid Films 33, 253 (1976).
[2] J. W. Matthews, S. Mader, and T. B. Light, J. Appl. Phys. 41, 3800 (1970).
[3] G. A. Rozgonyi, P. M. Petroff, and M. B. Panish, Appl. Phys. Lett. 24, 251 (1974).
[4] S. M. Bedair, T. Katsuyama, M. Timmons, and M. A. Tischler, IEEE Electron Device Lett. EDL-5, 45 (1984).
[5] M. A. Tischler, T. Katsuyama, N. A. El-Masry, and S. M. Bedair, Appl. Phys. Lett. 46, 294 (1985).
[6] J. K. Howard and R. D. Dobrott, J. Electrochem. Soc. 113, 567 (1966).
[7] M. Quillec, L. Goldstein, G. LeRoux, J. Burgeat, and J. Primot, J. Appl. Phys. 55, 2904 (1984).
[8] M. C. Joncour, M. N. Charasse, and J. Burgeat, J. Appl. Phys. 58, 3373 (1985).
[9] V. S. Sperios and T. Vreeland, Jr., J. Appl. Phys. 56, 1591 (1984).

Defect reduction in GaAs epitaxial layers using a GaAsP-InGaAs strained-layer superlattice

M. A. Tischler, T. Katsuyama, N. A. El-Masry, and S. M. Bedair
Electrical and Computer Engineering Department, Box 7911, North Carolina State University, Raleigh, North Carolina 27695-7911

(Received 30 August 1984; accepted for publication 9 November 1984)

GaAsP-InGaAs strained-layer superlattices grown lattice matched to GaAs have been used to reduce the density of threading dislocations originating from the GaAs substrate. GaAs epitaxial layers grown on the GaAsP-InGaAs superlattice buffer layers showed a dislocation density lower by at least an order of magnitude than that obtained from epitaxial layers grown directly on GaAs substrates. Transmission electron microscopy showed that dislocations originating from the GaAs substrate do not penetrate the GaAsP-InGaAs superlattice layers.

The recent advances in GaAs device and integrated circuit technology have stimulated the need for high quality, uniform substrates. These are necessary to achieve uniform circuit parameters and respectable yields. However, compound semiconductor substrates typically have several types of defects, such as dislocations, which can degrade the operation of devices and circuits. Typical substrates have dislocation densities on the order of 10^4 cm^{-2} and greater. Additionally the dislocation density is not uniform across the wafer; for example, dislocations in liquid encapsulated Czochralski (LEC) wafers usually have a W-shaped distribution, with larger densities at the edge and center of the wafer.[1] These dislocations, as evidenced by etch pits, x-ray topography, and transmission electron microscopy (TEM) have been correlated to material parameters such as photoluminescence intensity,[2,3] sheet carrier concentration, and sheet resistance[4,5] as well as device parameters including leakage[6] and drain-source[1] currents, and threshold voltage.[7-10] Sheet carrier concentration directly tracks the dislocation density while the sheet resistance is inversely proportional to it.[4] Metal-semiconductor field-effect transistor arrays across 2-in. LEC wafers show threshold voltage variations of about 400 mV [for V_{th} (mean) $= +0.126$ V] with V_{th} becoming more negative as the dislocation density increases.[7] LEC wafers typically have dislocation networks which result in large variations in device parameters while horizontal Bridgman (HB) wafers usually have more uniform dislocation densities.[11] Defect density variations across the boule can be another source of problems for GaAs technology. Thus, it is evident that the quality of the GaAs must be improved to have a viable integrated circuit process.

One possible method for reducing defects is to improve the bulk growth of GaAs. There have recently been reports[12] of HB, silicon-doped GaAs substrates with less than 200 dislocations cm^{-2}. This low density has not yet been realized in LEC or Cr-doped material, which is required for GaAs integrated circuits. The approach we have investigated is to provide a low defect density epitaxial layer using a strained-layer superlattice. This was first proposesd by Matthews and Blakeslee[13,14] who used the strain field in a GaAsP-GaAs superlattice to turn aside dislocations propagating up from the substrate. A superlattice is constructed of layers with different lattice constants such that layers are alternately under compression and tension. The layers are thinner than a maximum thickness such that the strain is accommodated elastically, but greater than a minimum thickness required for "bending over" the dislocations.[13-15] The dislocations propagating up from the substrate encounter the strain field and are bent over and forced to move laterally towards the edge of the substrate. Note that the materials must have enough lattice mismatch to generate the required strain. The problem that arises with strained-superlattice structures such as GaAs-InGaAs and GaAs-GaAsP is that they are not, as a whole, lattice matched to the GaAs substrate or epitaxial layer. Thus more dislocations are produced at these interfaces. What is needed is a superlattice composed of two materials having equal but opposite lattice mismatches, such that the average lattice constant matches that of GaAs. We have proposed a materials system, $GaAs_{1-x}P_x$-$In_yGa_{1-y}As$, which is lattice matched to GaAs when $x = 2y$.[16] Additional potential material systems are GaAsP-GaAsSb, GaAsP-InGaAsSb,[17] and $Ga_{0.52+x}In_{0.48-x}P$-$Ga_{0.52-x}In_{0.48+x}P$. This allows a high quality GaAs layer to be grown lattice matched on top of the superlattice buffer (SLB) layer. There is also some evidence that a strained superlattice may act as a gettering site for impurities out diffusing from the substrate.[18,19]

Ten period SLB's were grown by metalorganic chemical vapor deposition at atmospheric pressure in a vertical reactor. Gallium was supplied from a trimethylgallium bubbler (0 °C) at a flow rate of 5 sccm. Indium was supplied from a triethylindium bubbler (20 °C) at a flow rate of 200 sccm. AsH_3 and PH_3 (both 5% in H_2), at flow rates of 40 and 60 sccm respectively, were used as the As and P sources. Palladium diffused H_2 flowing at a rate of 4 l/m served as the carrier gas. The growth temperature was 630 °C. Four different substrates were used; two silicon doped, one Cr-doped, and one LEC (semi-insulating). All substrates were (100), oriented 2° towards (110). Details of the calibration procedure to produce the SLB lattice matched to GaAs have been previously reported.[16] For these experiments x(% P) ~ 17% and y(% In) ~ 8%. X-ray diffraction showed that the mismatch between the SLB and the GaAs substrate is less than 0.1%. The thickness of each layer is between 100–180 Å; the minimum and maximum thicknesses mentioned above are calculated (for $GaAs_{0.83}P_{0.17}$-$In_{0.08}Ga_{0.92}As$) to be on the order of 100 and 300 Å, respectively. GaAs epitaxial layers were then simultaneously grown on the SLB and directly on

 0003-6951/85/030294-03$01.00

TABLE I. Results of etch pit density measurements.

Run	Substrate	Etch pit density (cm^{-2})		
		Substrate	GaAs epilayer	SLB plus GaAs epilayer
A	Cr	$1-2\times10^{4}$	$1-8\times10^{3}$	50
B	Si	$\sim10^{4}$	$\sim10^{3}$	20
C	Si	$\sim6\times10^{3}$	$\sim10^{3}$	400
D	SI LEC	$1-3\times10^{4}$	$\sim4\times10^{3}$	~0
E	Si	$\sim6\times10^{3}$	$\sim2\times10^{3}$	180

GaAs substrates for etch pit density (EPD) comparison. All the GaAs epitaxial layers were about 2 μm thick and they had mirrorlike surfaces with no cross hatching. This indicates the good lattice match between the SLB and GaAs.

Molten KOH at 330 °C was used to delineate the dislocations. Table I shows the etch pit density of the substrates, the GaAs epitaxial layers directly on the substrates, and the GaAs epitaxial layers on the 10 period SLB layers. The etch pit densities of the epitaxial samples were taken over an area about 0.5 cm square. In addition to the five sets of samples in Table I, EPD measurements were also made on five other samples. These had 10–35 superlattice periods and GaAs epitaxial layers 2–4 μm thick. The EPD's on these samples varied from 200 to 500 cm^{-2}. While EPD measurements are statistical in nature, and somewhat variable across a sample, we have consistently seen EPD's in epitaxial layers directly on GaAs substrates in the thousands per square cm range, while the SLB reduces the EPD to the hundreds per square cm range. It should be noted that this type of approach can only reduce dislocations threading up from the substrate. Dislocations produced by vacancies, interstitials, etc. within the epitaxial layer may still be present.

Transmission electron microscopy (TEM) was also done on several of the epitaxial layers on a SLB. The TEM samples were prepared by lapping and ion milling two pieces bonded together face to face. They are viewed in cross section, with the electron beam parallel to the ⟨110⟩ zone axis. Figure 1(a) shows a TEM cross section for a 10-period GaAsP-InGaAs SLB indicating the uniform thickness of the two ternary alloys. The period of the superlattice in Fig. 1(a) is about 230 Å. Figure 1(b) shows a threading dislocation which started in the GaAs substrate and does not penetrate the SLB. The SLB is delineated by the arrows. The diffraction conditions for these micrographs are not optimized for the simultaneous observation of the SLB layers and the dislocation lines. Additionally, the low dislocation density makes it quite difficult to find a dislocation using TEM. These micrographs are the results from several trials. Figure 1(c) shows another TEM cross section in which a threading dislocation does not penetrate the SLB. These TEM micrographs are another demonstration that threading dislocations which start in the substrate may not penetrate the SLB. It is not clear at this stage how many periods are required to eliminate these threading dislocations.

In conclusion, strained superlattice buffer layers have been grown with an average lattice constant equal to that of GaAs, as shown by the x-ray diffraction data. Epitaxial GaAs layers grown on these SLB's show significantly smaller dislocation densities than simultaneously grown layers directly on GaAs substrates. TEM studies show that threading dislocations which start in the GaAs substrate do not penetrate the SLB layer. It is expected that devices and circuits fabricated in epitaxial layers on top of SLB's will exhibit less variation in electrical parameters than those fabricated directly on a GaAs substrate.

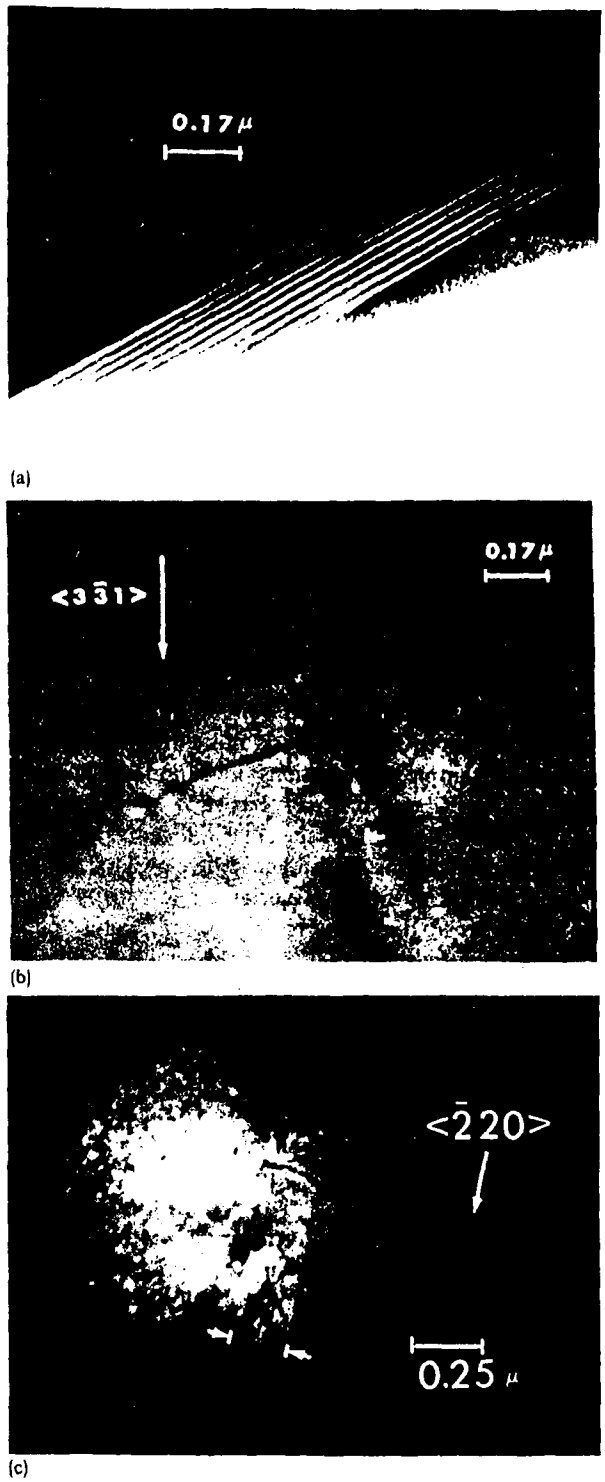

FIG. 1.(a) TEM micrograph of GaInAs-GaAsP superlattice. (b) TEM micrograph showing a threading dislocation which does not penetrate the SLB. The substrate is on the left side of the SLB. (c) TEM micrograph showing a threading dislocation which does not penetrate the SLB. The substrate is on the right side of the SLB.

This work is supported by NSF and the Army Research Office.

[1]Y. Nanishi, S. Ishida, and S. Miyazawa, Jpn. J. Appl. Phys. **22**, L 54 (1983).
[2]W. Heinke and H. J. Queisser, Phys. Rev. Lett. **33**, 1082 (1974).
[3]K. Böhm and B. Fischer, J. Appl. Phys. **50**, 5433 (1979).
[4]T. Honda, Y. Ishii, S. Miyazawa, H. Yamazaki, and Y. Nanishi, Jpn. J. Appl. Phys. **22**, L 270 (1983).
[5]H. Yamazaki, Y. Nanishi, S. Miyazawa, and Y. Ishii, GaAs Integrated Circuit Symposium, Phoenix, AZ, Oct. 25, 1983, pp. 30–33.
[6]S. Miyazawa, T. Mizutani, and H. Yamazaki, Jpn. J. Appl. Phys. **21**, L542 (1982).
[7]S. Miyazawa, Y. Ishii, IEEE Trans. Electron. Devices **ED-31**, 1057 (1984).
[8]Y. Ishii, S. Miyazawa, and S. Ishida, IEEE Trans. Electron Devices **ED-31**, 800 (1984).
[9]Y. Matsuoka, K. Ohwada, and M. Hirayama, IEEE Trans. Electron Devices **ED-31**, 1062 (1984).
[10]S. Miyazawa, Y. Ishii, S. Ishida, and Y. Nanishi, Appl. Phys. Lett. **43**, 853 (1983).
Y. Ishii, S. Miyazawa, and S. Ishida, IEEE Trans. Electron Devices **ED-31**, 1051 (1984).
[11]Solid State Technol. **27**, 12 (1984), Sumitomo Company Literature.
[12]J. W. Matthews, A. E. Blakeslee, and J. Mader, Thin Solid Films **33**, 253 (1976).
[13]J. W. Matthews and A. E. Blakeslee, J. Cryst. Growth **27**, 118 (1974); **29**, 273 (1975); **32**, 265 (1976).
[14]J. W. Matthews and A. E. Blakeslee, J. Vac. Sci. Technol. **14**, 989 (1977).
[15]S. M. Bedair, T. Katsuyama, M. Timmons, and M. A. Tischler, IEEE Electron Device Lett. **EDL-5**, 45 (1984).
[16]S. M. Bedair, T. Katsuyama, P. K. Chiang, N. A. El-Masry, M. A. Tischler, and M. Timmons, J. Cryst. Growth **68**, 477 (1984).
[17]W. J. Schaff, A. S. Brown, L. F. Eastman, B. Van Rees, B. Liles, and C. Hitzman, Electronic Materials Conference, Sec. F-3, Santa Barbara, CA, June 20–22, 1984.
[18]W. T. Read, *Dislocations in Crystals* (McGraw-Hill, NY, 1953) p. 7.

 0003-6951/85/030296-03$01.00

Atomic layer epitaxy of III-V binary compounds

S. M. Bedair, M. A. Tischler, T. Katsuyama, and N. A. El-Masry
Electrical and Computer Engineering Department, Box 7911, North Carolina State University, Raleigh, North Carolina 27695-7911

(Received 20 March 1985; accepted for publication 17 April 1985)

Atomic layer epitaxy (ALE) of III-V semiconductors is reported for the first time using metalorganic and hydride sources. This is achieved by using a new growth chamber and susceptor design which incorporates a shuttering mechanism to allow successive exposure to streams of gases from the two sources. Also, most of the gaseous boundary layer is sheared off after exposure to the gas streams. GaAs and AlAs deposited by ALE are single crystal and show good optical properties.

The recent interest in high electron mobility transistors (HEMT's), superlattices, and quantum well structures and devices has required improvements in the ability to produce thin layers and abrupt interfaces. Both molecular beam epitaxy (MBE) and, to a lesser extent, metalorganic chemical vapor deposition (MOCVD) have made impressive advances in this respect and yet both are limited by operating in a "bulk" growth regime. The ultimate control of the growth of III-V compounds would be achieved by the deposition of one monolayer of column III atoms followed by a monolayer of column V atoms. This process would then be repeated until the desired thickness has been reached. The total layer thickness could be controlled very accurately since each cycle of exposures would result in the growth of a known thickness. The interfaces, in principle, would be atomically abrupt since the reactant fluxes could be changed within one atomic layer. The atomic layer epitaxy (ALE) of III-V compounds could be achieved using either MBE or MOCVD. In the case of MBE, the shutters are assumed to allow the exposure of the substrate to either column III or V beams independently. In the case of MOCVD, an analogous shuttering mechanism would be used.

We report for the first time the successful atomic layer epitaxy of GaAs and AlAs by MOCVD. This technique can also be used to investigate the MOCVD growth mechanism and will be reported on at a later date. The growth chamber is schematically shown in Fig. 1. For the growth of GaAs, $AsH_3 + H_2$ and trimethylgallium (TMG) $+ H_2$ flow through the inlet tubes *A* and *B*, respectively. A large flow of H_2 in the middle tube (*C*) is designed to prevent mixing of the gases from tubes *A* and *B*. The rf heated susceptor is made of graphite coated with silicon carbide, and consists of several

 0003-6951/85/130051-03$01.00

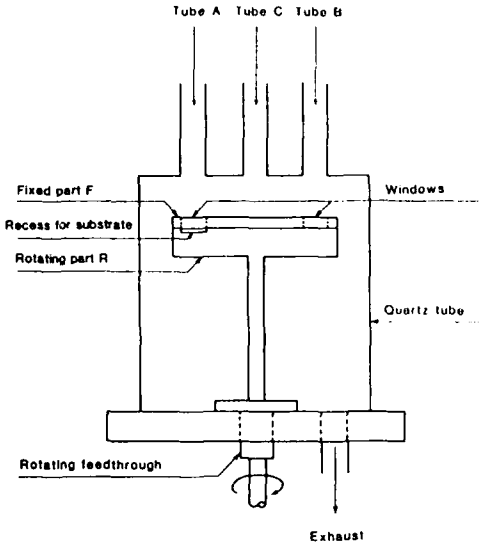

FIG. 1. Schematic diagram of the growth chamber and susceptor for ALE. The susceptor consists of a fixed part *F*, a rotating part *R*, and a recess in part *R* which holds the substrate. Inlet tubes *A* and *B* provide the reactant gases. A large H_2 flow in tube *C* helps prevent mixing of the gases from tubes *A* and *B*.

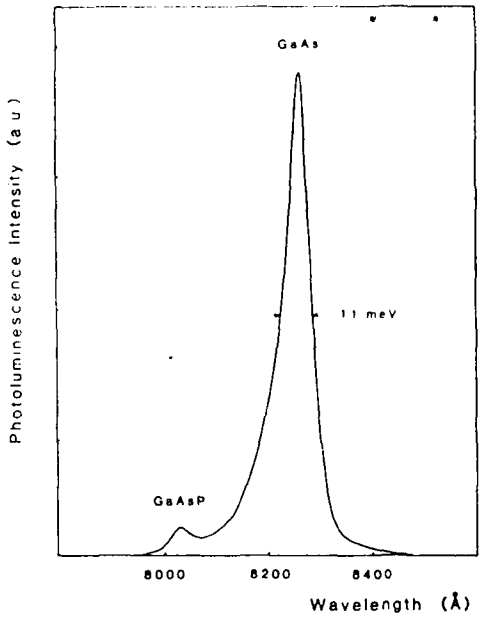

FIG. 2. Photoluminescence at 77 K of 100 cycles of GaAs grown by ALE sandwiched between layers of $GaAs_{0.97}P_{0.03}$. The full width at half-maximum is 11 meV.

parts. Fixed part *F* has two windows aligned to face the inlet tubes *A* and *B*. The substrate sits in a recess in the rotating part *R* and can be positioned under the windows of the fixed part *F*, thus facing either the column III or V input flux. The position of the substrate is controlled through a rotating feedthrough at the base of the growth chamber. The recess in part *R* and the thickness of the substrate are chosen to allow minimum clearance between the substrate surface and the fixed part of the susceptor. When the substrate is exposed to the stream of column III species from inlet *B*, a boundary layer will build up on the substrate surface. When the substrate is rotated away from this position, most of the boundary layer will be sheared off by the fixed part *F*, allowing an almost immediate termination of exposure of the substrate to the input flux. Additionally, the initial substrate exposure to the column III flux will take place almost without the presence of any gaseous boundary layer (made up of $H_2 + AsH_3$ in this case). The above arguments can also be applied when the substrate is moved under tube *A* and exposed to AsH_3. Thus, for a short exposure time, it is possible that the adsorption process is controlled by surface kinetics rather than diffusion of the reactant species through a boundary layer, as is always the case in conventional MOCVD growth.[1]

This technique was used to deposit GaAs and AlAs. In the case of GaAs, AsH_3 (5% in H_2) + 500 sccm of H_2 and trimethylgallium (TMG) + 500 sccm of H_2 flowed through tubes *A* and *B*, respectively. The flow of H_2 through the TMG bubbler and the temperature of the bubbler were set to 0.5 sccm and − 15 °C respectively which are the minimum values available in our system. The flow of AsH_3 was 10 sccm. Three liters per minute of H_2 flowed through the center tube (*C*) to prevent mixing. The substrate temperature was in the range of 560–600 °C. All substrates were *n*-type GaAs, (100), oriented 2° towards (110). The growth process starts by heating the substrate under AsH_3 (tube *A*) for a few minutes. The substrate is then exposed to the TMG (tube *B*) for 1 s and then moved back under the AsH_3 for 5 s. One complete cycle was performed in about 10 s. All growths consisted of 100 cycles. The exposure time to AsH_3 is not critical since excess As atoms will evaporate almost immediately. The sticking probability of As on GaAs covered with Ga is very close to unity.[2] After the first monolayer of As is adsorbed, its sticking probability reduces to almost zero. The growth of AlAs was carried out in an analogous manner using trimethylaluminum (TMA) at 9 °C and a flow of H_2 through the bubbler of 2.5 sccm.

The ALE samples of GaAs were characterized by photoluminescence (PL) at 77 K. Two types of samples were grown. One consisted of 100 cycles of GaAs grown by ALE on a 3-μm-thick InGaAs-GaAsP superlattice grown by conventional MOCVD.[3] The superlattice is lattice matched to GaAs and has an effective band gap of about 1.3 eV. The second type of sample consisted of a 2-μm-thick $GaAs_{0.97}P_{0.03}$ layer, 100 cycles of GaAs by ALE, and a 300–500-Å $GaAs_{0.97}P_{0.03}$ cap. The $GaAs_{0.97}P_{0.03}$ layers were grown by conventional MOCVD. This was achieved by adding a second TMG and PH^3 sources to line *A*. The superlattice and the thick $GaAs_{0.97}P_{0.03}$ layer prevented photoluminescence from the GaAs substrate from interfering with the signal from the ALE GaAs layer. The cap layer facilitated cross-sectional thickness measurements.

Figure 2 shows the PL spectra of the latter type of sample with 100 cycles of ALE GaAs. The GaAs peak is clearly evident and has a full width at half-maximum of about 11 meV indicating the good quality of the GaAs grown by ALE. The small peak is from the $GaAs_{0.97}P_{0.03}$ layer. The former type of sample also showed a GaAs peak. The AlAs samples consisted of 2 μm of GaAs, 100 cycles of AlAs, and a 1000-Å GaAs cap. The GaAs in this case was also grown by conventional MOCVD.

Figure 3 shows the surface of a GaAs layer grown by ALE. All the deposited layers had mirrorlike surfaces

FIG. 3. Photomicrograph of the surface of 100 cycles of GaAs grown by ALE.

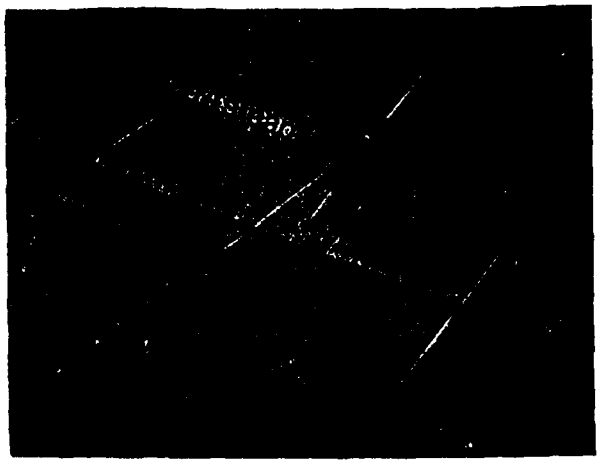

FIG. 4. Photomicrograph of 100 cycles of AlAs grown by ALE sandwiched between layers of GaAs, and angle lapped at 1/3°.

Transmission electron microscope (TEM) samples were prepared by lapping and ion milling two pieces which were bonded together face to face. They were viewed in cross section with the electron beam parallel to the ⟨002⟩ zone axis. Diffraction studies by TEM indicated that the ALE growths are single crystal. The GaAs layer is about 800 Å thick as measured by TEM. Figure 4 shows an AlAs sample angle lapped at 1/3°. The dark line is the AlAs layer grown by ALE. It is about 300 Å thick.

The difference in thicknesses between ALE GaAs and AlAs is a result of the flux of the column III species. Ideally, 100 cycles, each depositing one monolayer of column III and one monolayer of column V species, would produce a layer about 283 Å thick. However, the minimum fluxes available were system limited with the TMG flux several times larger than the TMA flux. Additionally the minimum reproducible exposure time was one second. Thus for ALE of GaAs, about two to three monolayers of Ga were deposited on the surface, whereas in the case of AlAs about one atomic layer of Al was deposited. The use of triethylgallium, with its lower vapor pressure, should allow the deposition of single layers of gallium. The deposition of more than one monolayer is not present in the ALE of II-VI compounds[4] due to the very high vapor pressure of the species.

In order to make sure that conventional MOCVD growth was not occurring from any mixing of gases in the growth chamber, the following experiment was carried out. The substrate was exposed to the TMG stream for 3 min while the AsH_3 and center H_2 lines were flowing as described above. The deposited film had a dull surface and could be wiped off by a cotton swab. PL on this layer deposited on a superlattice substrate showed only a very weak GaAs peak. The corresponding experiment with a superlattice substrate exposed only to AsH_3 with the TMG and center H_2 lines flowing showed no GaAs PL peak. Thus, the amount of mixing is quite small and is not expected to play a significant role in the ALE process.

The ALE method gives more insight into the MOCVD process. Several models for the deposition mechanism have been proposed. For example, one model proposed that the metalorganic molecule and the hydride adsorb on separate surface sites, followed by the formation of intermediate complexes and then the desorption of methane.[5] Another model showed that intermediate complex formation takes place in the gas phase.[6] It was also proposed that complete reaction in the gas phase takes place followed by the successive diffusion of small GaAs clusters towards the surface.[7] However, the result of the current experiment clearly indicates that MOCVD can also take place through independent deposition of Ga and As species.

In conclusion, ALE of GaAs and AlAs has been demonstrated by MOCVD for the first time. This has been accomplished by using a new design for the growth chamber and susceptor. The susceptor incorporates a shuttering action which allows the substrate to be sequentially exposed to different gas streams and also shears off most of the boundary layer which builds up during exposure. The current results also indicate that the growth by MOCVD takes place through the independent deposition of both Ga and As species. We believe that atomic layer epitaxy will be useful for growing structures and devices requiring very well controlled thicknesses and/or very abrupt interfaces. Additionally, ALE may provide a vehicle for investigating fundamental aspects of compound semiconductor growth.

This work was supported by Army Office of Research and Air Force Office of Scientific Research.

[1]M. R. Leys and H. Veenvliet, J. Cryst. Growth **55**, 145 (1981).
[2]J. R. Arthur, J. Appl. Phys. **39**, 4032 (1968).
[3]S. M. Bedair, T. Katsuyama, M. Timmons, and M. A. Tischler, Electron Device Lett. **5**, 45 (1984).
[4]M. Pessa, P. Huttunen, and M. A. Herman, J. Appl. Phys. **54**, 6047 (1983).
[5]D. J. Schlyer and M. A. Ring, J. Electrochem. Soc. **124**, 569 (1977).
[6]W. H. Petzke, V. Gottschalch, and E. Butter, Kristall Tech. **9**, 763 (1974).
[7]I. A. Frolov, P. B. Boldyrevskii, P. L. Druz, and E. B. Sokolov, Inorg. Mater. **13**, 632 (1977).

Self-limiting mechanism in the atomic layer epitaxy of GaAs

M. A. Tischler and S. M. Bedair
Electrical and Computer Engineering Department, North Carolina State University, Raleigh, North Carolina 27695-7911

(Received 20 May 1985; accepted for publication 18 April 1986)

A self-limiting mechanism has been observed in the atomic layer epitaxy (ALE) of GaAs deposited by alternate exposure to AsH_3 and trimethylgallium (TMG). The thickness of the deposited film was found to be independent of the mole fractions of both TMG and AsH_3 in the gas phase. These results will allow the use of ALE to deposit III-V compounds with growth rates which are insensitive to the input partial pressures of the reactive gases.

Atomic layer epitaxy (ALE) of III-V compounds offers a new approach for the synthesis of these material systems. The crystal structure of GaAs, for example, grown by ALE is built by the deposition of alternate layers of Ga and As. ALE can be used as a means to accurately control layer thickness and obtain abrupt interfaces, potentially within one atomic layer. ALE can also be a basis for studying the deposition mechanism of III-V compounds, where in this case column III and V elements are not deposited simultaneously. ALE using molecular beam epitaxy (MBE) can develop more understanding of the residence time of the species,[1] the cracking efficiency of column V molecules,[2] and the incorporation of atoms at their lattice sites. In the case of metalorganic chemical vapor deposition (MOCVD), ALE can help in understanding the cracking mechanism of alkyl and hydride molecules and the effect of the gaseous boundary layer on the growth process.[3]

ALE has been previously reported for II-VI[4] and III-V[5-7] compounds. ALE of II-VI compounds relies on the fairly high vapor pressure of the constituent elements. This will allow only one chemically adsorbed monolayer to remain on the substrate surface at the growth temperature irrespective of the number of layers that were initially deposited.[4] This self-limiting mechanism will guarantee that the epitaxial layer is built up by the deposition of a sequence of monolayers of column II and then VI elements. The conditions are quite different in the case of III-V compounds since the vapor pressure of most column III elements is fairly low at the deposition temperature. In this case the self-limiting mechanism that relies on the re-evaporation of excess atoms or molecules may not apply. ALE of III-V compounds is expected to require precise control of the column III flux, otherwise, excess amounts will deposit and ball and will result in poor surface morphology. There is no equivalent problem for the case of column V elements such as As or P because of their fairly high vapor pressures. Sb may be an exception due to its relatively lower vapor pressure. In this letter we report on our findings that a self-limiting mechanism is also taking place in the ALE of GaAs by MOCVD. This self-limiting mechanism may be related to the process of decomposition of trimethylgallium (TMG) on the substrate surface and in the thermal boundary layer.

The experimental setup for the ALE of GaAs using TMG and AsH_3 has been previously described[5] and a schematic of the growth system is shown in Fig. 1. Growth proceeds by alternately exposing the substrate to the AsH_3 and TMG fluxes from different inlet tubes as indicated. The substrate sits in a recess in the rotating part (R) of the susceptor. The gases flow through two windows in the fixed top part (F) and through two corresponding holes in the base of the susceptor as shown in Fig. 2. The fixed top part also acts to shear off most of the gaseous boundary layer between successive exposures. Thus, the gases flow unimpeded through the susceptor except when the substrate cuts through the streams. This acts to prevent the formation of a gaseous boundary layer over the rotating part of the susceptor which holds the substrate. The clearance between the surface of the substrate and the top piece is several mils to avoid scratching the substrate. The amount of TMG or AsH_3 trapped in this small volume, which could be transferred to the AsH_3 or TMG side respectively, is, in the current experiment, only enough to deposit less than 1/10 of a monolayer per cycle and thus cannot account for the observed growth. The H_2 carrier gas flows for TMG (-13 °C) and AsH_3 (5% in H_2) were 500 sccm each and the H_2 flow in the center tube was 5000 sccm. A graphite wedge just below the center inlet tube, in conjunction with the H_2 flow through that tube, acts to

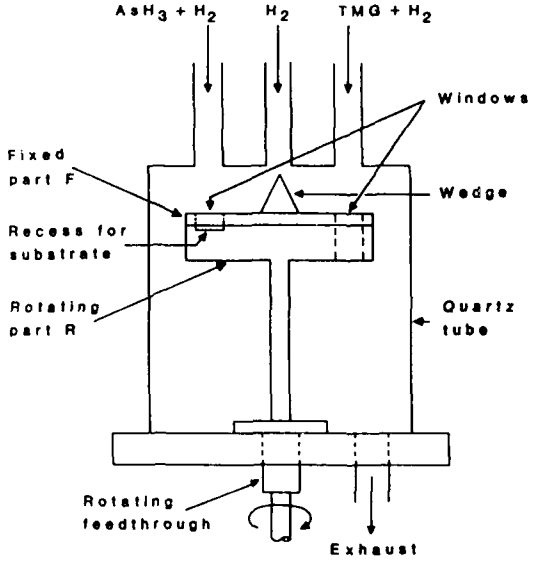

FIG. 1. Schematic diagram of the growth chamber and susceptor for ALE. The susceptor consists of a fixed part *F*, a rotating part *R*, and a recess in part *R* which holds the substrate. The left and right inlet tubes provide the AsH_3 and TMG, respectively. A graphite wedge in conjunction with a large H_2 flow from the center tube helps prevent mixing of AsH_3 and TMG.

 0003-6951/86/241681-03$01.00

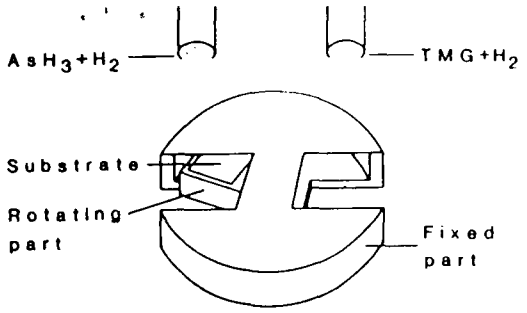

FIG. 2. Schematic diagram of the susceptor showing holes in the base of the susceptor through which the input gases flow. The rotating part of the susceptor containing the substrate cuts through these gas streams.

separate the AsH_3 and TMG gas streams. The AsH_3 flow was 25 sccm and the substrate temperature was 630 °C.

The inside diameters of the growth chamber and inlet tubes are 95 and 10 mm, respectively. The substrate is about 2 cm below the top of the growth chamber. The cross-sectional area of the gas stream at the substrate is not well known, and thus the exact flux impinging on the substrate is difficult to calculate. However, the total gas flow in each inlet tube was kept constant throughout these experiments resulting in a constant cross-sectional area at the substrate. Therefore, the flux at the substrate is proportional to the mole fraction of each species in the gas phase.

The substrate was rotated continuously using a stepping motor and one complete exposure cycle was performed in 2.6 s. This results in equal exposure times of about 0.3 s each to the AsH_3 and TMG gas streams. A standard growth run in this study consists of 1200 cycles. The thickness of the deposited ALE film was determined from cleaved cross sections using optical and transmission electron microscopy (TEM).

The as-grown GaAs has a mirrorlike surface and is single crystal as indicated from the TEM diffraction pattern shown in Fig. 3. The thicknesses of the deposited ALE films per growth cycle, for different TMG mole fractions in the

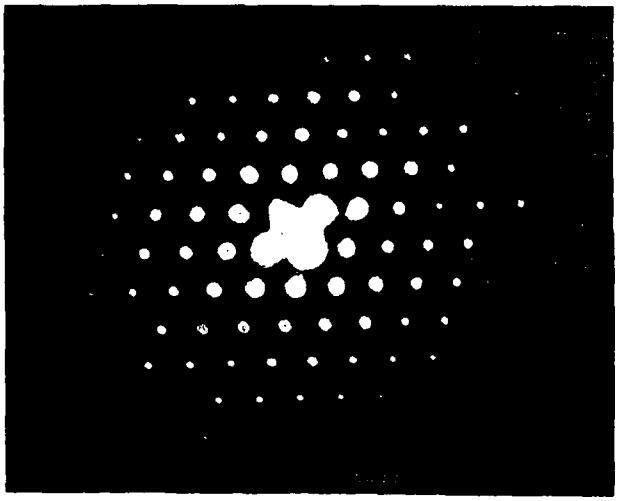

FIG. 3. Transmission electron diffraction pattern of GaAs grown by ALE.

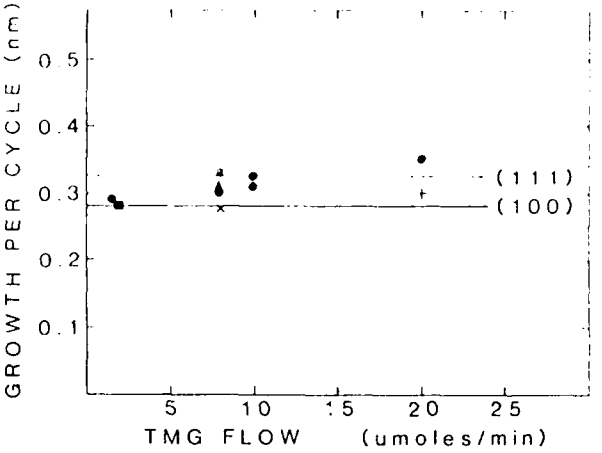

FIG. 4. Thickness per cycle of ALE GaAs vs TMG flux. The horizontal lines indicated the ideal ALE thickness per cycle for (100) and (111) orientations. (100) substrates: (●) $T_{sub} = 630$ °C, $AsH_3 = 52$ μmoles/min; (■) $T_{sub} = 450$ °C, $AsH_3 = 156$ μmoles/min; (+) $T_{sub} = 450$ °C, $AsH_3 = 410$ μmoles/min; (*) $T_{sub} = 630$ °C, $AsH_3 = 410$ μmoles/min; (×) $T_{sub} = 700$ °C, $AsH_3 = 52$ μmoles/min. (111) substrate: (▲) $T_{sub} = 630$ °C, $AsH_3 = 52$ μmoles/min.

gas phase, are shown in Fig. 4. Only about one monolayer is deposited per cycle with this being independent of the mole fraction of TMG in the gas phase. The same results were obtained for different growth temperatures in the range of 450–700 °C. Also, increasing the AsH_3 flow by about an order of magnitude still resulted in the deposition of about one atomic layer per cycle. Two GaAs substrate orientations were used in this study, (III)*B* and (100), oriented 2° towards ⟨110⟩. The deposition rate of about one monolayer per cycle was observed for both of these orientations.

This experimental result cannot be related to the volume of the trapped gas between the substrate surface and the top piece of the susceptor. If growth resulted from these trapped gases, the mole fraction of TMG in these gases and, thus, the GaAs layer thickness, should be proportional to the TMG mole fraction in the input gas phase. However, the results in Fig. 4 show that this is not the case and these results can also indicate that these trapped gases, if any, do not play a major role in the ALE process.

It might also be possible that some minor cross contamination from the AsH_3 side is responsible for the limiting process. The amount of deposited Ga and thus the ALE film thickness may be dependent on this AsH_3 flux irrespective of the TMG flux. To investigate the effect of cross contamination on the ALE process, the following experiment was carried out. The AsH_3 was switched off after every substrate exposure to the AsH_3 and enough time was allowed (20 s) to flush it out of the growth chamber before the substrate was rotated to be exposed to the TMG flux. The deposited ALE film in this case was found to be of the same quality as those obtained when AsH_3 was kept on all the time, as indicated from surface morphology and photoluminescence response. Also, the thickness of the deposited ALE was about the same as that shown in Fig. 4. Additionally, increasing the AsH_3 flow, as mentioned previously, which should also increase the amount of AsH_3 diffusing to the Ga side, resulted in a

similar growth rate. Thus, cross contamination does not seem to play any significant role in the ALE process nor can it be used to explain the above results.

The mechanism for this self-limiting action is not fully understood; however, a possible explanation can be as follows. Since the thermal boundary layer is quite thin, the TMG molecule may not decompose until it is close to, or on the substrate surface. At this point, the TMG can acquire enough thermal energy from the substrate to partially or fully decompose or to re-evaporate undissociated. The exact nature of the deposited Ga species is not known. At least a coverage of one monolayer of chemically adsorbed molecules on the GaAs substrate will take place. The cracking efficiency of TMG on the GaAs surface (630 °C) can be fairly high[7]; however, when the GaAs surface is covered with a monolayer of Ga species, the cracking efficiency or the condensation coefficient of the additional TMG molecules may then be very small. Thus, these additional TMG molecules may re-evaporate before they have a chance to decompose. This is consistent with the wide variation in the value of the condensation coefficient of given species on different substrates.[8] More work is needed to verify the above assumptions.

In conclusion, a self-limiting process for the deposition of Ga from TMG during the ALE of GaAs has been observed. This effect will make the ALE of GaAs insensitive to the mole fraction of the TMG in the gas phase, thus alleviating one of the major problems of ALE of III-V compounds by MOCVD.

This work is supported by the National Science Foundation and the Air Force Office of Scientific Research. The authors would like to thank N. A. El-Masry for performing the TEM work.

[1]J. R. Arthur, J. Appl. Phys. **39**, 4032 (1968).
[2]C. T. Foxon and B. A. Joyce, Surf. Sci. **50**, 434 (1975).
[3]M. R. Leys and H. Veenvliet, J. Cryst. Growth **55**, 145 (1981).
[4]M. Pessa, P. Huttunen, and M. A. Herman, J. Appl. Phys. **54**, 6047 (1983).
[5]S. M. Bedair, M. A. Tischler, and T. Katsuyama, Appl. Phys. Lett. **47**, 51 (1985).
[6]M. A. Tischler, N. G. Anderson, and S. M. Bedair, Electronic Materials Conference, Boulder, CO, June 1985.
[7]J. Nishizawa, H. Abe, and T. Kurabayashi, J. Electrochem. Soc. **132**, 1197 (1985).
[8]E. Kaldis, *Crystal Growth, Theory and Techniques*, edited by C. H. L. Goodman (Plenum, London, 1974), Vol. I, p. 112.

Defect reduction in GaAs grown by molecular beam epitaxy using different superlattice structures

S. M. Bedair, T. P. Humphreys, N. A. El-Masry, Y. Lo, N. Hamaguchi, C. D. Lamp, A. A. Tuttle, D. L. Dreifus, and P. Russell

Department of Electrical and Computer Engineering, North Carolina State University, Raleigh, North Carolina 27695-7911

(Received 23 June 1986; accepted for publication 12 August 1986)

Several superlattice structures, grown by molecular beam epitaxy, have been used to reduce the density of threading dislocations originating from the GaAs substrate. Results clearly indicate that compared to epitaxial layers grown directly on GaAs substrates, a GaAs-$In_xGa_{1-x}As$ superlattice ($x < 0.12$) reduces the dislocations by approximately two orders of magnitude. Transmission electron microscopy, electron beam induced current, and etch pit density have been used to characterize the effectiveness of using superlattice buffer layers for the reduction of defects in GaAs epilayers.

Compound semiconductor substrates typically have several types of defects, such as dislocations, which can degrade the operation of devices and circuits. For example, semi-insulating GaAs substrates have dislocations of the order of 10^4 cm^{-2} and greater. Moreover, the dislocation density which typically has a W-shaped distribution is nonuniform across the sample surface.[1] The presence of such defects greatly influences device parameters such as source-drain currents and threshold voltages resulting in a dramatic degradation of performance.[2] We have recently reported the use of GaAsP-InGaAs strained-layer superlattices (SLS's) to reduce threading dislocations originating from the GaAs substrate. Furthermore, the GaAs epilayers grown on this SLS buffer were found to be almost dislocation-free.[3] This SLS structure, grown by metalorganic chemical vapor deposition, was constructed from alternating layers under tension (GaAsP) and compression (InGaAs). The compositions of the two ternary alloys are adjusted such that the SLS is lattice matched to GaAs.[4]

Superlattice structures composed of phosphorus and arsenic compounds are difficult to grow using molecular beam epitaxy (MBE). Consequently, most MBE superlattice buffer layers are based on $Al_xGa_{1-x}As$-GaAs SLS structures ($0 < x < 1$).[5] Since this SLS structure is nearly lattice matched, the built-in strain is insufficient to suppress the propagation of threading dislocations originating from the substrate. However, it has been reported in the literature[5] that using $Al_{0.3}Ga_{0.7}As$-GaAs and AlAs-GaAs SL's, the dislocation density can be reduced by factors of 3 and 20, respectively. This is in contrast to the three to four orders of magnitude reduction when GaAsP-InGaAs SLS's are used.[3] In this letter we report the use of GaAs-$In_xGa_{1-x}As$ ($0 < x < 0.2$) SLS buffer layers reducing dislocations in the GaAs epilayers.

The GaAs-InGaAs SLS's were grown by MBE at 550 °C on both (100) Cr- and Si-doped substrates. For comparison, a similar structure made of $Al_{0.3}Ga_{0.7}As$-GaAs superlattice was grown at 620 °C. A 2-μm GaAs epitaxial layer was grown on the SL and directly on the substrate for etch pit density (EPD) determination and comparison. All the grown layers were Si doped to the mid $10^{16}/cm^3$ range. The superlattice has five periods, each layer being 100 Å thick. Since the individual layers are sufficiently thin, the lattice mismatch is elastically accommodated by the uniform strain. This strain can be present as a compressive strain in the $In_xGa_{1-x}As$ layers only, thus maintaining the GaAs lattice constant in the growth plane. However, the strain can also be accommodated by tensile and compressive strains in the GaAs and InGaAs films, respectively. In this case the superlattice will have a lattice constant corresponding to InGaAs with an InAs mole fraction of $x/2$. If the total thickness of the SL structure made of these five periods exceeds the critical thickness[6] h_c, misfit dislocations will be generated at the SLS-GaAs interfaces. The generation of misfit dislocations has been observed in our present study and will be discussed later. Consequently, in order to prevent the generation of dislocations at the SLS-GaAs interfaces we must limit the total thickness of the SLS to a value below the critical thickness, h_c. However, by incorporating intermediate thick layers of GaAs we can extend the number of sets of five-period GaAs-InGaAs SLS's. In Fig. 1 we illustrate a structure incorporating a 2000-Å GaAs buffer layer between

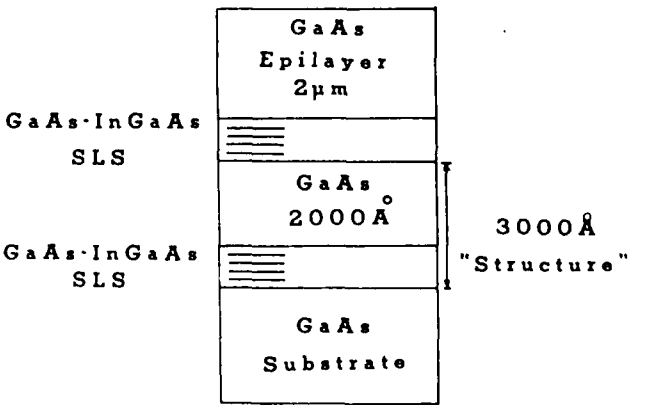

FIG. 1. Schematic of GaAs-InGaAs SLS with 2000-Å GaAs intermediate layer used to reduce defects in the GaAs epilayer.

 0003-6951/86/410942-03$01.00

TABLE I. Results of etch pit density (EPD) measurements[a]

Run	Five-period SLS structure	Number of repeat "structures" with 3000-Å period	EPD (cm^{-2})
A	GaAs-$Al_{0.3}Ga_{0.7}As$	2	1.5×10^4
B	GaAs-$In_{0.06}Ga_{0.94}As$	2	$\sim 5 \times 10^3$
C	GaAs-$In_{0.1}Ga_{0.9}As$	2	9×10^2–5×10^3
D	GaAs-$In_{0.06}Ga_{0.94}As$	5	$\sim 5 \times 10^2$
E[b]	GaAs-$In_{0.06}Ga_{0.94}As$	5	less than 10^2
F[c]	GaAs-$In_{0.14}Ga_{0.86}As$	2	$\sim 2 \times 10^4$

[a] Substrate EPD for both Si- and Cr-doped samples are of the order of 10^4 cm^{-2}. EPD for epilayers grown directly on the substrate are in the 10^4/cm^{-2} range.
[b] Si-doped substrates.
[c] The total thickness of the SLS is 1200 Å, which exceeds the critical thickness.

two successive GaAs-InGaAs SLS's. This structure, with a 3000-Å period, can be repeated to any desired number. Consequently, this will introduce more strained interfaces thereby blocking the threading dislocations originating from the substrate. In our study we have investigated samples composed of a 3000-Å period "structure," repeated two and five times with an InAs percentage of 6 and 10%.

Molten KOH was employed to reveal the dislocation density on the GaAs substrates and on the epitaxially grown layers. The etching time for each sample was 2–3 min. Etch pit densities for the substrates and the epitaxially grown GaAs cap layer on the $Al_{0.3}Ga_{0.7}As$-GaAs and $In_xGa_{1-x}As$-GaAs ($x = 0.06$ and 0.14) superlattices are compiled in Table I. The $Al_{0.3}Ga_{0.7}As$-GaAs SL reduces the EPD by one-third to one-fifth of that of the substrate. Similar studies on the GaAs-$In_xGa_{1-x}As$ SLS indicate a two to three orders of magnitude reduction. This trend is clearly illustrated in Table I for both semi-insulating and n-type GaAs substrates. Increasing the number of five-period SLS and GaAs intermediate layers reduces the EPD, as shown for samples D and E in Table I. Samples D and E correspond to a 3000-Å period structure repeated five times.

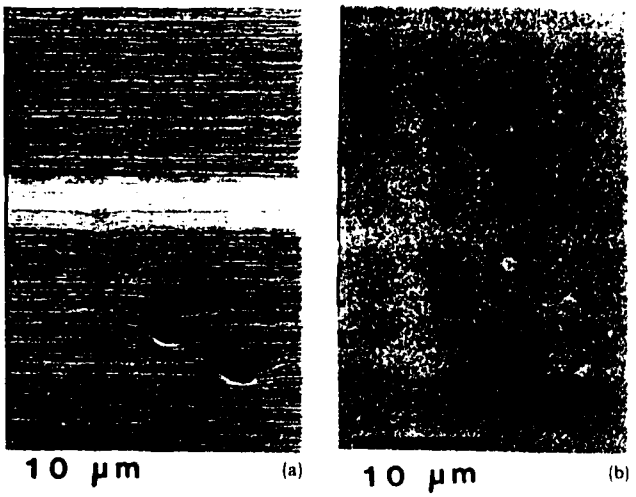

FIG. 2. (a) Y-modulation EBIC micrograph of recombination sites detected by surveying a 1-mm^2 device area. No other electrically active defects were observed in this device. The Y-modulation mode is used for enhancement of the contrast from small defects to facilitate survey scanning when covering large device areas. (b) Conventional (Z modulation) EBIC micrograph of the same area as above. Here dark areas represent lower induced current or higher recombination.

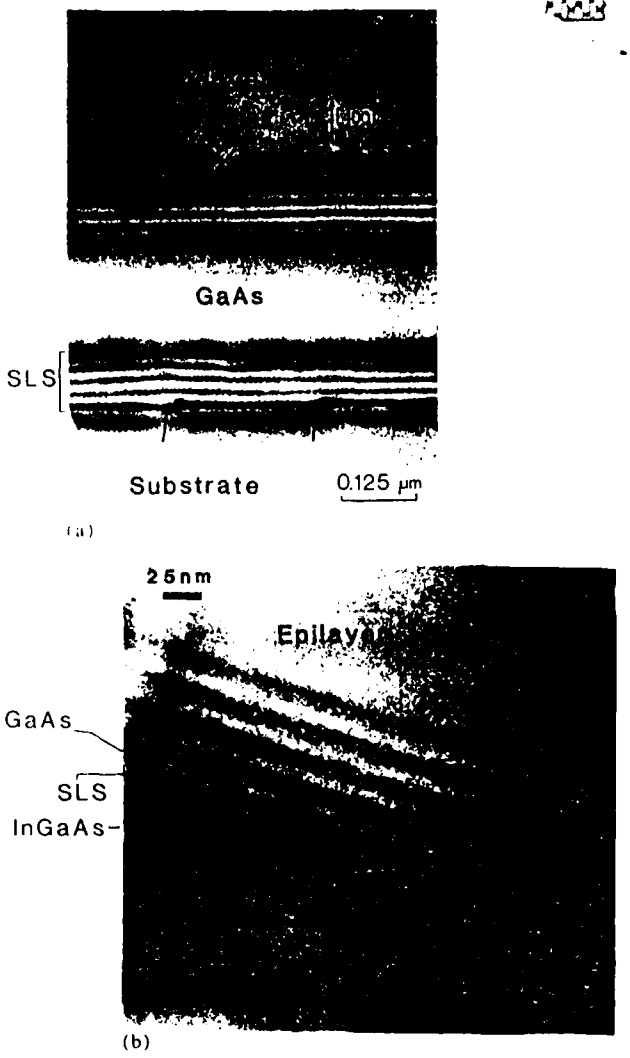

FIG. 3. TEM micrograph of GaAs-InGaAs superlattice. (a) Total thickness of the GaAs-$In_{0.16}Ga_{0.84}As$ five-period SLS exceeds the critical thickness resulting in the generation of dislocations shown by arrows. (b) GaAs-$In_{0.08}Ga_{0.92}As$ SLS composed of five periods of the 3000-Å "structures." Threading dislocations, shown by arrows, do not penetrate the SLS structure.

Dislocation densities were also characterized using the electron beam induced current (EBIC) technique. 300-Å-thick gold Schottky diodes with an area of approximately 2×10^{-2} cm^2 were evaporated on the GaAs epilayers. An electron beam with an energy in the range 10–20 keV was injected through these gold Schottky diodes. Dislocations appear as dark images in the EBIC mode since they act as nonradiative recombination centers which reduce the electric current compared to the surrounding area. Figure 2 shows the EBIC image of sample D. Over the entire metalized area ($\sim 10^{-2}$ cm^2) only four dark spots were observed. The corresponding dislocation density was approximately $4 \times 10^2/cm^2$. This result compares favorably with the average value obtained from EPD data using a KOH etch (Table I).

Transmission electron microscopy (TEM) was also used to investigate threading dislocations for several SLS samples. The TEM samples were prepared by lapping and ion milling two wafers bonded face to face. They are viewed in cross section with the electron beam parallel to the ⟨110⟩ axis. Figure 3(a) shows a TEM cross section of the GaAs-$In_{0.14}Ga_{0.86}As$ five-period SLS, with a total thickness of 1200 Å, which is larger than h_c. Misfit dislocations are generated at the SLS-GaAs interfaces as shown in Fig. 3(a). The presence of threading dislocations is consistent with the results shown in Table I for sample F, where the EPD is approximately one order of magnitude higher than those of samples B and C whose values of x are in the range of 6–10% and whose total thickness is less than 1000 Å. The GaAs and $In_{0.14}Ga_{0.86}As$ layers in Fig. 3(a) do not appear to be strained. The strain and associated defects appear to be localized at the SLS and GaAs interfaces. This result is consistent with previous observations obtained from Raman spectroscopy[7] for the accommodation of strain between GaAs-InGaAs SLS and the GaAs substrate. Figure 3(b) shows a GaAs-$In_{0.06}Ga_{0.94}As$ SLS, with the 3000-Å structure, repeated five times. Dislocations originated from the substrate are stopped by the SLS structure.

In conclusion, GaAs-InGaAs SLS's have been successfully used as buffer layers to reduce dislocations originating from GaAs substrates. Employing EPD and EBIC a reproducible set of defect densities has been recorded. An analysis of the propagation of these defects has been investigated using TEM. It is therefore expected that devices on these low defect density epilayers will exhibit less variation in electrical parameters than those fabricated directly on GaAs substrates.

The authors are grateful to M. Tischler for helpful discussions and assistance. This work is supported by the Air Force Office of Research.

[1] Y. Nanishi, S. Ishida, and S. Miyazawa, Jpn. J. Appl. Phys. **22**, L54 (1983).
[2] S. Miyazawa and Y. Ishii, IEEE Trans. Electron Devices **ED-31**, 1057 (1984).
[3] M. A. Tischler, T. Katsuyama, N. A. El-Masry, and S. M. Bedair, Appl. Phys. Lett. **46**, 294 (1985).
[4] S. M. Bedair, T. Katsuyama, F. K. Chiang, N. A. El-Masry, M. A. Tischler, and M. Timmons, J. Cryst. Growth **68**, 477 (1984).
[5] Masanari Shinohara, Tomonori Ito, and Yoshihira Imamura, J. Appl. Phys. **58**, 3449 (1985).
[6] J. W. Matthews and A. E. Blakeslee, J. Cryst. Growth **27**, 118 (1974).
[7] M. Nakayama, K. Kubota, H. Kato, S. Chika, and N. Sano, Appl. Phys. Lett. **48**, 281 (1986).